The Changing Mean Field in Exotic Nuclei: A Shell Model Study of Neutron Rich Nuclei

A Thesis Submitted
to the

University of Allahabad
for the degree of

Doctor of Philosophy
in Science

by

Kamalesh Maurya

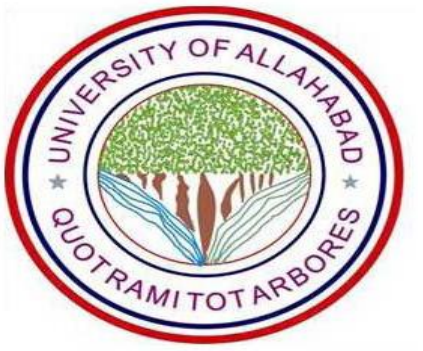

Under the Supervision of
Prof. (Mrs.) Indira Mehrotra
Department of Physics
University of Allahabad
Allahabad -211002
Year 2013

इलाहाबाद विश्वविद्यालय
UNIVERSITY OF ALLAHABAD

इलाहाबाद - 211 002 (भारत)
Allahabad - 211 002 (INDIA)

भौतिकी विभाग
Physics Department

Tel./Fax : +91(532) 2460993
e-mail : physdept@sancharnet.in

Certificate

Certified that the candidate **Mrs. Kamalesh Maurya** has fulfilled all the requirements for the degree of Doctor of Philosophy in Science of the University of Allahabad, Allahabad, India.

Prof. (Mrs.) Indira Mehrotra
Thesis Supervisor
Department of Physics
University of Allahabad
Allahabad-211002, India

Prof. M. C. Sharma
Head,
Department of Physics
University of Allahabad
Allahabad-211002, India

Prof. M. A. Tiwari
Dean Faculty of Science
University of Allahabad
Allahabad-211002, India

Declaration by the Candidate

I hereby declare that this thesis entitled "**The Changing Mean Field in Exotic Nuclei: A Shell Model Study of Neutron Rich Nuclei"** contains fully original research work carried out by me under the supervision of ***Prof. (Mrs.) Indira Mehrotra*** at ***Department of Physics, University of Allahabad, Allahabad, India***. This work has not been submitted for any other degree or diploma of this or any other university. Whenever reference has been made to the previous works of others, it has been clearly indicated as such and included in the References.

Date: (Kamalesh Maurya)

Place: Allahabad (India) D.Phil. Student

Acknowledgements

The words seem to be out of the globe to encircle the amount of gratitude and respect I have for my venerable supervisor- Prof. Indira Mehrotra, whose unlimited continuous support and guidance made this thesis possible. She, not only groomed me as a researcher, but also imparted wisdom that transformed me in to a confident human being. Her insight, quest for perfection, and passion for science has always inspired me.

My deepest gratitude goes to my mother Jarawati Maurya for her support and encouragement. You wanted credit for a small piece of this work, but you deserve so much more than that. I take a moment to express my deep sense of gratitude to the fond memories of my Late father Shri Bhumi Dhar Maurya, whose love and support, I will miss forever. He has always dreamt to see me a "Doctor" since my childhood and its unfortunate not to find him with me to share the moments of this achievement.

I express my gratitude to my brother Bal Krishna and my sister Pratima, who always understand me at every stage of my academic and non-academic life, and my cousins Geetanjali, Maneesha and Shikha for their moral support and encouragement.

Vocabulary fails me to put proper words expressing my sentiments for my father-in-law Mr. S. R. Kushwaha and mother-in-law Mrs. Manju Kushwaha for their unconditional support, love and encouragement. I wish to convey my feelings of deep affection and love to my husband Mr. Ravindra Kushwaha who has been caring of me in all those days of my busy schedules and always saying " you concentrate on your studies...I will handle...". I would also like to thank for the love and support, I have been having from my sister-in-laws Sushama, Reena and Neelam .

I would like to thank Dr. Vivek Kumar Tiwari for his fatherly affection and blessings. I take the opportunity to thank Prof. M. C. Sharma, Head, Department

of Physics, University of Allahabad and all the faculty members of the department of physics for enhancing my knowledge which make successful my research work. I also thank to the my senior research scholar Dr. Pramila Gupta, Dr. Tarkeshwar Trivedi, Dr. Arati Devi for their valuable help and specially to Dr. Praveen Chandra Srivastava and Dr. Uma shankar Gupta for very informative discussion in the learning of Nushell code, Latex and computer software system from time to time during my research work.

The support, cooperation and patience which I have received from my classmate friends are beyond the scope of any acknowledgement, yet I would like to express my heartfelt thank to Atul, Rajani, Nazia, Sangeeta, Monika and specially to Nivedita, Nidhi and my roommate Mitra for the quality time that I spent with them and to give me much more moral support during my research works. Thank you for always listening and for your blind faith in me.

In my five years here, I've made friends I'll have for life, better friends than I deserve. Thank you my all junior research scholar "CHAY PARTY GROUP" Ajay Yadav, Ajay Maurya, Vikram Verma, Harish Yadav, Ram Pratap, Vineet Singh, Arti Drivedi and Archana Maurya for all of the happy hours .Thank you for believing in me when I wouldn't seem to believe in myself. You cannot know what your friendship and support has meant to me. My friends are my rocks,

Finally, I have to thank my almighty God, who has given me such families and friends to make a good environment for me to pursue the D. Phil. Degree.

Date: (Kamalesh Maurya)

Dedicated
to
My Late Father

Shri Bhumi Dhar Maurya

Contents

List of Tables

List of Figures

Chapter 1

Introduction

The atomic nucleus, which consists of a few upto nearly two hundreds nucleons, governed by the nucleon-nucleon interaction active inside the nucleus, is a complicated interacting many body system. Strong interaction that acts between nucleons is responsible for most of the observed characteristic of the atomic nucleus. In order to know how various nuclear properties change from nucleus to nucleus and how nucleons interact with each other in a nuclear medium several theoretical models have been constructed. The best known model that provides a framework of an understanding of nuclear structure is Nuclear Shell Model, developed in large part by Maria Goeppert-Mayer. Nuclei with certain numbers of neutrons and protons (the magic numbers 2, 8, 20, 28, 50, 82, 126, ...) are particularly stable, because their shells are filled. It describes nuclear properties as originating from the motion of independent particles each with independent spin and energy levels moving in an average potential well produced by rest of the particles inside the nucleus. This is the basis of the shell model in which the interaction energy between individual nucleons is negligible compared to the energy of the central nuclear potential. The other model is collective model that describes properties originating from the collective behavior of nucleons. Other more complicated models for the nucleus have also been proposed, such as the interacting boson model, in which pairs of

neutrons and protons interact as bosons, analogously to Cooper pairs of electrons.

The above models are quite successful for understanding the properties of nuclei close to the stability but how well these models are applicable to the nuclei at the far-out regions of the nuclear chart, where experimental data is scarce or non-existing is however quite unclear. So to gain further insight, it is necessary to gather experimental data in these unexplored regions and to test the various models by comparing them with the obtained data.

Much of current research in nuclear physics relates to the study of nuclei under extreme conditions such as high spin and excitation energy. Nuclei may also have extreme shapes (similar to that of Rugby balls) or extreme neutron-to-proton ratios. Experimenters can create such nuclei using artificially induced fusion or nucleon transfer reactions, employing ion beams from an accelerator. Beams with even higher energies can be used to create nuclei at very high temperatures, and there are signs that these experiments have produced a phase transition from normal nuclear matter to a new state, the quark-gluon plasma, in which the quarks mingle with one another, rather than being segregated in triplets as they are in neutrons and protons.

1.1 Exotic Nuclei

The stable nuclei in equilibrium have cohesion such that no radioactive transmutation is possible. For a given mass, the proportion of neutrons and protons correspond to structures strongly bound by the combined action of the various interactions: strong interaction, the pairing, the spin orbit and the Coulomb repulsion. Now with the advent of accelerator facilities allover the world it has become possible to produce the nuclei outside this equilibrium. These unstable nuclei do not exist naturally on the Earth and have ratios of neutron to proton much larger or much smaller than those of nuclei found in nature. Stable nuclei lie in the so-called valley of beta stability. As the N/Z ratio decreases (proton rich nuclei) or increases (neutron rich nuclei) compared to that of the stable nuclei, there is energy for a proton or neutron in the nucleus to undergo beta (β^+, β^-) decay to move the nucleus back towards the stability. So exotic nuclei refer to β-unstable nuclei with extreme ratios of neutron to proton number on both the neutron and proton rich sides of stability. Exotic nuclei exhibit decay modes not seen near stability , such as proton radioactivity and beta-delayed particle emission. There is also maximum limit to neutron and proton numbers in these exotic nuclei, out of which they become unbound. These limits respectively define neutron and proton drip-lines. On the Earth 277 nuclei exist in equilibrium with different combinations of neutron and proton and 26 (half life $\geq 10^{12}$) nuclei with quasi-stable configuration. Quasi-stable nuclei are those

whose half-life is comparable to the age of the Earth or longer, so they are still present on the Earth. In the chart of nuclides, the terra incognita region have between 4000 to 7000 unbound nuclei predicted by different models but only 3063 of them have been observed till now. At present 9 doubly magic nuclei are known, of which 5 are stable nuclei namely ^{4}He, ^{16}O, ^{40}Ca, ^{48}Ca and ^{208}Pb and 4 unstable nuclei are ^{56}Ni, ^{78}Ni, ^{100}Sn and ^{132}Sn.

1.2 Drip-lines

As N/Z decreases or increases from the stable values, a point is reached for a given Z where, if one more neutron is pulled out, a proton becomes unbound (an isotope of that element cannot exist with that number of neutrons), or if one more neutron is added, that neutron is not bound to the nucleus. These limits define, the proton and neutron drip-lines respectively. The drip line is demarcation line between the last bound nuclei and its neighbor and each element has a lightest (proton drip line) and a heaviest (neutron drip line) nucleus. The location of the drip line constraints the path of the nucleosynthesis in explosive astrophysics scenarios such as novae x-ray bursters and consequently controls the rate of energy generation. One of the most challenging topics of research in experimental nuclear physics is the creations of exotic nuclei in the lab with proton or neutron excess and reaching the limits of stability of matter beyond which a nucleon is no more bound.

The proton drip line has been studied since the beginning of nuclear reactions because it is much closer to the valley of β-stability than the neutron drip line. Whereas most of the neutron drip line will be unreachable for some time, since it is still impossible to produce in the laboratory heavy fragments that could fuse to produce heavier ones, or even use neutron transfer to reach the limits of neutron excess. The proton drip line lies closer to the stability region because Coulomb repulsion restricts the number of protons that can be added to the nucleus. On the other hand, the neutron binding energy gradually approaches to zero as neutron number increases. Low Z nuclei lying beyond the drip line only exist as short-lived resonances and cannot be detected directly. In higher Z region of the drip line, the potential energy barrier resulting from the mutual electrostatic interaction between the unbound proton and core can cause nuclei to survive long enough to be detected.

Fusion evaporation reactions always populate proton rich nuclei making the proton drip line more accessible than the neutron drip line. Proton drip line has been mapped extensively in the region of low and intermediate nuclei and most recently [1,2] for nuclei within $50<Z<83$. Till 1987, stable nuclei up to Z=23 were discovered. The drip line has reached for odd Z nuclei up to Z=91 yet while bound nuclei that have yet to be discovered are limited to even Z nuclei in the region Z=32 to Z=64 and for $Z\geq82$. Drip line for two proton the limit of proton rich even Z nuclei has been reached only up to Zinc(Z=30). The situation is more

dramatic on the neutron rich side of the valley of the stability where except for the lightest nuclei we are still far from reaching the neutron drip line. Indeed, the neutron drip line is at present known only for elements up to fluorine(Z=9). The only method available to produce nuclei at, or near the neutron drip line is through the fragmentation of stable nuclei followed by the separation and identification of the products in less than a microsecond. First heaviest bound Oxygen isotope ^{24}O had been observed in 1970. However it was much later before experiment showed that the nuclei ^{25}O and ^{28}O are unbound with respect to prompt neutron emission. In 1997, the drip line for Oxygen had been established. Subsequently, the isotope ^{31}F, ^{34}Ne and ^{37}Na have been observed. Although no experiment has established that ^{33}F, ^{36}Ne and ^{39}Na are unbound, these heavier isotopes probably do lie beyond the neutron drip line. In NSCL at MSU newly discovered several neutron rich isotopes ^{44}Si, ^{40}Mg, ^{42}Al and ^{43}Al [3,4] are at the neutron drip line.

The physics at drip line will be the main motivation to develop new high performance nuclear physics facilities. With these experimental efforts to approach the drip line for heavier elements, theoretical studies are also needed which provide satisfactory description of the structure of the nuclei at or beyond the drip line.

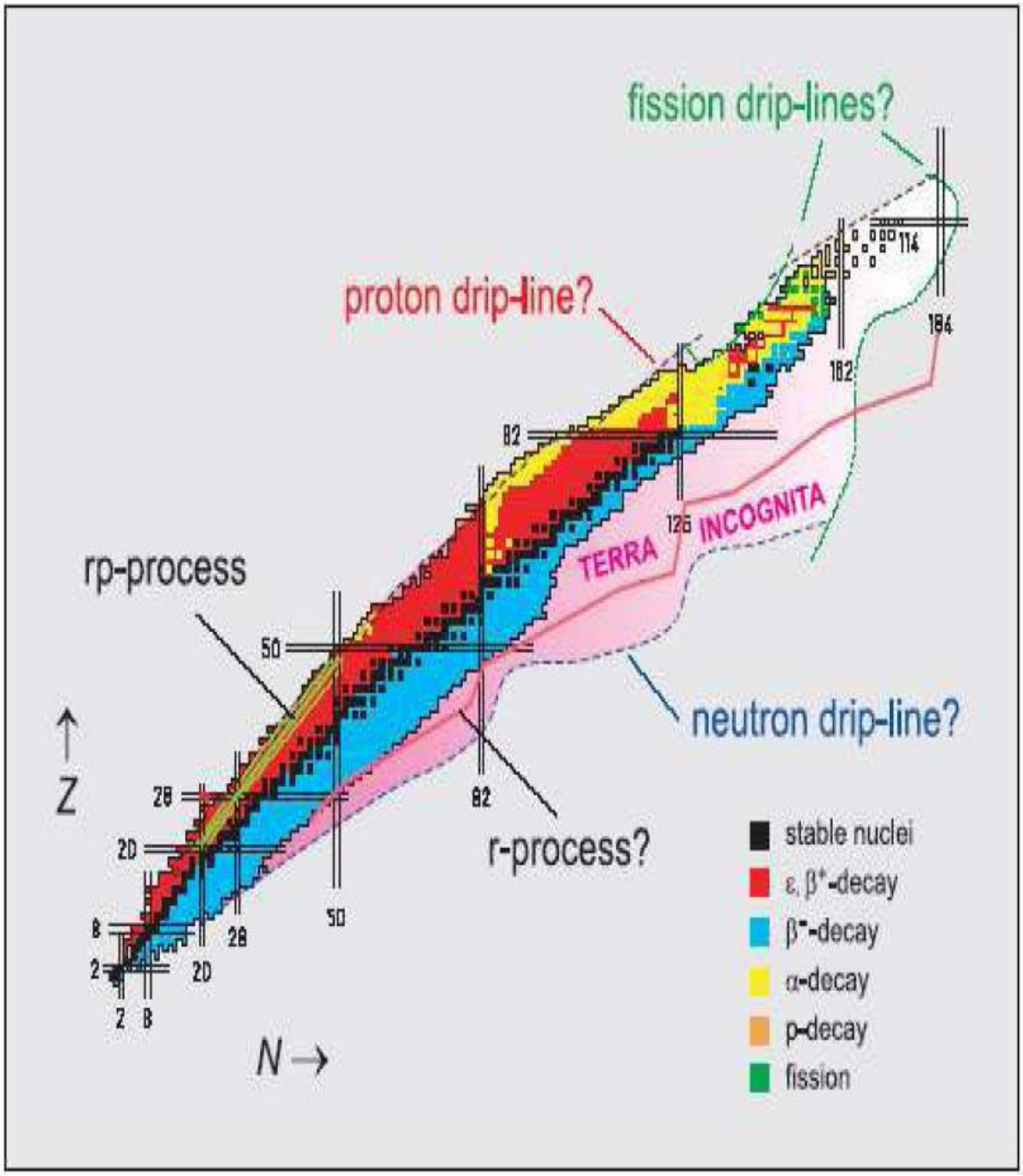

Figure 1.1: Figure of the nuclear chart, the valley of β-stability is indicated by the black squares. A number of important nuclei mentioned in the text and the N=Z line are marked. The horizontal and vertical lines correspond to the magic particle numbers.

1.3 Experimental techniques to produce exotic nuclei

From the technical point view, two methods are used to produce exotic nuclei: in flight method and the on-line method or ISOL. Beam of exotic nuclei produced in flight are used directly for experiments following a fast filtering while in ISOL these are first ionized and then accelerated for experiments. After production, the nuclei of interest are usually separated electromagnetically from other reaction products before they can be studied. These two methods have their advantages and their drawbacks but are perfectly complementary.

1.3.1 In-flight method:

Exotic nuclei with half-lives of order of 100 ns to 100 ms are studies in In-flight method. In this method a sufficiently high energy primary beam or a projectile having mass larger than the mass of the target nuclei induces a nuclear reaction. This method can be applied to energy range from Coulomb barrier(~5 MeV) using inverse fusion-evaporation reactions to very high energy using projectile fragmentation reactions(50-500 MeV). In range 5-10 MeV mainly exotic nuclei on the neutron deficient side are produced. The reaction products are subsequently transported to a secondary target after mass, charge and

momentum selection in a fragment separator and no post acceleration is required. This method is most favorable for high energy beam (above about 50 MeV) of very short lived nuclei. Two in-flight RNB facilities are operational one at GANIL and other is FRS at GSI. Flerov Laboratory at Dubna, Russia, operates two cyclotrons, U400 and U400M, whose beams can be fragmented. The resulting nuclei are studied at the separators ACCULINNA and COMBAS. In North America, the NSCL at East Lansing, USA, operates the K1200 superconducting cyclotron which produces heavy ion beams in the 100 to 200 MeV/u energy range. In Japan, the RIKEN laboratory at Saitama includes a heavy ion ring cyclotron, RRC producing beams at energies up to 135 MeV/u and a new fragment separator BigRIPS.

1.3.2 ISOL Method:

In ISOL method radioactive nuclei are produced by low energy beam (<100 KeV) at rest in thick target, a catcher or a gas cell bombarded with particles from a primary source or driver accelerator. Electromagnetic devices are used to ionize it and to select a specific mass after which these nuclei are accelerated in a post accelerator to the energy desired. In this way a relatively pure beam of one particular mass with high intensity and high quality at energies up to 25 MeV are obtained. The life time of the accelerated radioisotopes are limited downwards by their extraction time from target and their transfer time to

the ion source. A large number of radioactive nuclei with life times of the order of several milliseconds are obtained by ISOLDE CERN facility. For the production of short-lived isotopes, faster reaction mechanism are used such as fusion-evaporation reaction or reaction induced fission on thin target. In practice, the ISOL method is mostly limited to nuclei of span of the order of 0.1 to 1 second. In Europe, a broad range of the first generation ISOL RNB facilities have been developed like SPIRAL facility at GANIL Caen, ISOLDE and REX-ISOLDE at CERN's in Geneva, EXCYT facility at LNS, Catania. In North America, ISOL RNB facilities exist at TRIUMF, Vancouver, Canada, ORNL, Oak Ridge, USA and ANL, Argonne, USA.

1.4 Mechanism for production of exotic nuclei

Nuclear reactions are the tools to produce exotic nuclei in the laboratory. Various mechanism for the reactions are used, depending on the nature of primary beam and its energy , and nuclei to be produced. These are:

Fusion evaporation reaction : In this reaction heavy ions having energy slightly above the coulomb barrier (5MeV) are bombarded on a target and then they are fused together form a compound nucleus. With large excitation energy and high angular momentum, the compound nucleus cools down rapidly by evaporating a few neutrons, protons and sometimes in addition light fragment depending on the amount of energy

it contains. When it cools down below the separation energy of a neutron, then further cooling is followed by emission of a few high energy 'statistical' gamma rays. Proton rich nuclei are mostly produced in these reactions e.g. ^{96}Ru(^{16}O, 4n)^{108}Te and ^{96}Ru(^{16}O, 5n)^{107}Te [5].

Multinucleon transfer reaction : In these reactions two or more nucleons are transferred from projectile to the target nucleus while target nucleus losing neutrons tends to gain some charges. Heavy neutron rich nuclei are produced by these reactions e.g. ^{48}Ca(^{6}Li, ^{8}B)^{46}Ar [6] and ^{48}Ca(^{3}He, ^{8}B)^{43}Cl [7]. The use of multi particle transfer reactions led to the first observation of the proton drip line ^{9}C, ^{20}Mg and ^{22}Al [8].

Target fragmentation reaction : This process is used to produce neutron rich nuclei having medium mass where fragmentation reactions can be induced by neutron, energetic proton or heavy ions. In 1965 Poskanzer et. al.[9] bombarded a ^{17}N target with protons and ^{12}Be was produced by the (p, 4p) reaction. Other nuclei are ^{17}C[10], ^{17}N and ^{21}O[11] which were produced by using this technique.

Deep inelastic reaction : In this reaction target and projectile exchange a certain number of nucleons. Beam energy required for this reaction to take place is typically 5-10 MeV/nucleon. This reaction were first successfully used to explore neutron rich nuclei from carbon to chlorine

[12,13]. By bombardment of ^{64}Ni on heavy target nuclei the energy states in ^{68}Ni have been observed.

Projectile fragmentation reaction : At high beam energies, interaction between a heavy projectile and a target induces the breakup of the fast projectile into a variety of ion lighter than the beam with unusual neutron to proton ratio. This method is used to predominantly populate the area between the stable isotopes and proton drip line from the atomic number of projectile down to the atomic number of lightest element[14]. At the energies above the Fermi level this method is used to produce exotic nuclei over entire range of periodic table up to the heaviest projectile beam.

Pion double charge exchange reaction : The pion double charge exchange reaction on nuclear targets has been extensively studied, both experimentally and theoretically, throughout the last two decades. At least two nucleons must be involved in this process and therefore the study of double charge exchange is a natural tool for exploring the N-N correlation (a means of probing the short-range part of the nucleon-nucleon correlations in the nucleus). ^{28}S nad ^{40}Ti were populated by the reaction ^{28}Si(π^+, π^-)^{28}S and ^{40}C(π^+, π^-)^{40}Ti [15]. States of unbound ^{4}He [16] and ^{6}H [17] were observed with this technique.

Induced fission by thermal neutron capture : In this reaction the proton or neutron beam from a high intensity accelerator is bombarded on a fissile target. The secondary beam of selected heavy fission fragments can be further accelerated and bombarded on suitable targets for production of super heavy nuclei.

1.5 Special Features of Exotic Nuclei :

Halo : Atomic nucleus are usually uniformly dense objects with surfaces that are nearly well defined having only a modest amount of diffuseness. As binding energy becomes smaller in the vicinity of the drip line, the valence nucleons tunnel out of the central potential and form a halo nuclei with more diffuseness of the nuclear surface. Halo nuclei are weakly bound exotic states of nuclear matter in which outer one or two valence nucleons are spatially decoupled from a tightly bound core. Their wave functions extend far outside the nucleus so that the matter distribution has a long tail. The first halo nuclei observed was ^{11}Li [18], which has two correlated neutrons in its halo[19]. This phenomena also has been observed in ^{11}Be. In the limit of vanishing binding, extremely large neutron halo occurs. Halo nuclei ^{11}Be, ^{19}C for one neutron halo and ^{6}He, ^{11}Li, ^{17}B for two neutron halo and ^{8}He, ^{14}Be for four neutron halo have been observed. Recently ^{22}C has been observed as two proton halo[20]. No proton halo nuclei have yet been discovered but it has been assumed that the proton halo may only exist for loosely bound nuclei

with $Z \leq 10$ in either an s or a p state. Initially ^{8}B [21,22] and ^{17}Ne[23] are expected to be a one proton and two proton halo. Other expected one proton and two proton halo nuclei is ^{26}P and ^{27}S. Conditions for the formation of the halo have been studied by Jensen and Riisage[24].

The existence of a genuine halo depends on the predominance of only two halo particle motion in s or\and p orbital. When one neutron is bound weakly to a core, an rms radii of the density distribution of this neutron diverges to the infinity as the separation energy goes to zero if it is in s- or p- orbital. A neutron in a higher orbital does not show this divergence because of the centrifugal barrier. A neutron with a small orbital angular momentum extend the tail of the wave function much more than a neutron with a large orbital angular momentum. Experimentally it is identified by a large interaction or reaction cross section and a narrow momentum distribution of the core fragment of the nucleons.

Skin : For a large neutron excess, the bulk of the neutron density is predicted to extend beyond the proton density creating a sort of "neutron skin". Similar effect may appear for a large proton excess. These skin might change nuclear properties e.g. one could imagine different deformations of the neutron and proton distribution. It helps to study the behavior of abnormal nuclear matter with large T_z[25] and also in improving the reliability of calculations of the properties of the neutron stars.

Halo and skin can be differentiated by slop factor in the density tail that is related to the separation energy [26]. The density of halo state is more diffused than that of a skin. Only a small number of neutron can be included in the last orbit of neutron halo but a neutron skin can include a considerable number of neutron.

In neutron halo, the last neutron have extremely small separation energy than skin. One neutron separation energy is 0.7 MeV for ^{11}Li and 0.5 MeV for ^{11}Be. Two neutron separation energy are 0.97 MeV for ^{6}He which is arbitrarily called halo or skin while ^{8}He is a neutron skin have a separation energy of 2.13 MeV. Neutron and proton skin are common phenomena in unstable nuclei but do not exist in stable nuclei.

Vanishing of shell closure : Theory and experiment are now indicating that shell closure may change far from stability. A well known example is the disappearance of N=20 a neutron magic number in the Ne, Mg and Na isotopes. But physical mechanism which is responsible for this disappearance of the shell gaps, allowing many-particle, many-hole excitations to become more favored in energy, leading to shape changes and shape coexistence. In the study of exotic nuclei it has been shown that new magic number appear (N=14, 16, 34….) like in ^{24}O, ^{54}Ca… and some other disappear (N=8, 20, 28, 40….) like in ^{11}Li, ^{32}Mg, ^{42}Si, ^{68}Ni, ^{40}Zr… in moving from stable to exotic nuclei in a rather novel manner due to the monopole part of the nucleon-nucleon interaction. The N=20

magic structure is evident for ^{34}Si which is a stable nuclei with 6 proton in $0d_{5/2}$ state, whereas the N=16 magic number arises in ^{24}O, a exotic nuclei with proton shell closure at Z=8. In ^{24}O, N=16 magic number arises due to the large gap (~6MeV) between $0d_{3/2}$ and $1s_{1/2}$ [27] . On the other hand in ^{34}Si, N=20 gap (~4MeV) is created between the $0d_{3/2}$ and fp shell.

Nuclei with N=Z : Nuclei with equal or almost equal number of neutrons and protons are of particular, multidisciplinary interest:

- nuclear physics structure, in particular effects related to the vicinity of the proton drip line and to the occupation of identical orbits by neutrons and protons
- fundamental physics e.g. tests of the standard model of weak interaction
- astrophysics e.g. the electron capture cooling of supernovae or the astrophysical rp-process etc.

Nuclei with equal neutron and proton, occupy same orbitals, the mutual reinforcement of the shell gaps may lead to a stabilization of exotic nuclei in ground state. N=Z nuclei is also the unique system to study proton neutron pair correlations, isospin symmetry and shape coexistence. Example of stable N=Z nuclei are ^{4}He, ^{16}O, ^{40}Ca and unstable nuclei are ^{56}Ni and ^{100}Sn [28].

For medium heavy nuclei, the N=Z line coincides with proton drip line, and proton decay from discrete excited state is possible, as observed in

^{58}Cu. Clustering and large deformation are observed as general phenomena at low excitation energy in light N=Z nuclei.

Super deformation and Hyper deformation :

Hyper deformation is theoretically predicted states of an atomic nucleus with extremely elongated shape. Less elongated states super deformation has been well observed, but experiment evidence for hyper deformation is limited. Super deformed nucleus is very far from spherical nucleus, forming an ellipsoid with axes in ratio of 2:1 and hyper deformed state correspond to an axes ratio of 3:1. They would be caused by a third minimum in the potential energy surface, the second causing super deformation and the first minimum being normal deformation. Far from β-stability line medium heavy nuclei may exhibit these type of large deformation, even at low energies. Only some nuclei can exist in super deformed state. The first super deformed states to be observed were the fission isomers, low spin states of elements in the Actinide and Lanthanide series. The super deformed states are formed only when both of largely deformed proton and neutron orbital have large energy gap between the next orbitals. ^{76}Sr, ^{80}Zr and ^{100}Zr are amongst the most deformed nuclei known in their ground state. A sequence of super deformed have been observed in ^{80}Sr and it is predicted that hyper deformed states exist in nuclei in this region as well. The hyper deformed configuration are predicted to exist at the very high spin only, in contrast

to the super deformed ones. The existence of super deformed states occurs because of a combination of macroscopic and microscopic factors, which together lower their energies, and make them stable minima of energy as a function of deformation.

1.6 Region of interest in the nuclear chart and motivation

The exotic regions of the chart of nuclides have been expanded during the last few years with discovery of a large number of exotic nuclei. Present-day experimental research in nuclear structure has made extensive use of radioactive beams (RIB - Radioactive Ion Beams) in order to study nuclear properties further away from the region of β-stability. In particular, at a number of facilities such as ISOLDE at CERN [29], GSI in Darmstadt [30], GANIL in Caen [31], NSCL at Michigan State University [32], RIBF at RIKEN in Japan [33], HRIBF at Oak Ridge [34], ISAC at TRIUMF, Vancouver [35], researchers have obtained detailed information on the low lying excited states in very unstable nuclei with an extreme N=Z ratio (proton-rich or neutron-rich nuclei) in different regions.

In the present work we have carried out nuclear structure studies in following three regions in the nuclear chart

(i) Neutron rich N=51 isotone in dsgh shell from Z=32 to 40.

(ii) Ca isotopes in fp shell from N=42 to 58.

(iii) N=50 isotone in fpg shell from Z=30 to 46.

Single particle like states in some N=51 isotones (Kr, Sr, Zr) are already known. Recently single neutron transfer reaction have been measured on two N=50 isotones at HRIBE[36,37], in which single particle like states in two more N=51 isotones viz Ge and Se have been populated. These reactions used radioactive ion beam of ^{82}Ge and ^{84}Se and the (d,p) reaction in inverse kinematics. This experiment have provided data on the level structure of ^{83}Ge, ^{85}Se, ^{87}Kr, ^{89}Sr and ^{91}Zr.

In the present work we have also studied the evolution of shell closure along the neutron rich even mass Ca isotopic chain up to N=38 in full fp shell. Since the size of Z=20 gap remains large and almost constant along the whole Ca isotopic chain, core excitation of the Ca isotopes should remain relatively weak at low excitation energy. This isotopic chain is therefore an ideal test bench for exploring the spherical neutron shell closure and subshell closures at N=28, 32 and 34, as their existence would be decoupled from the proton core excitations. In the ^{52}Ca nucleus subshell closure has been evidenced at N=32 through the observation of the first 2^+ state at 2.52 MeV. This state was populated through the β-decay of ^{52}K at the CERN/ISOLDE facility [38]. Large N=34 subshell gap has also been predicted by Honma et. al. theoretically [39].

The structure of odd and even Z, N=50 isotones between the neutron rich ^{78}Ni nuclei to proton rich ^{100}Sn nuclei have been studied in fpg shell. As N=50 is a well established shell closure, the low lying states of N=50

isotones should involve only proton excitation and the effective N-N interaction is most easily studied in the nuclei in the neighborhood of doubly magic nuclei. One interesting thing about these isotones is that the shell model orbital for neutron in nuclei with Z=28 and N=28-50 are same as those for protons in nuclei with N=50 and Z=28-50. Many experimental [40,41] and theoretical [42,43] data between two doubly magic nucleus ^{78}Ni and ^{100}Sn with Z=30-46 has been provided in the last few years. ^{78}Ni is an important waiting point nucleus in the r- process synthesis of Steller evolution.

1.7 Present Work :

In the present work we have studied the structure of certain mass exotic nuclei in the framework of nuclear shell model. In particular we have studied the following nuclei :

(i) N=51 isotones in the mass region A=83-91

For N=51 isotones calculation have been performed in the valence space comprising of ν(0g7/2, 1d5/2, 1d3/2, 2s1/2, 0h11/2) orbitals for neutrons and π(0f5/2, 1p3/2, 1p1/2, 0g9/2) orbitals for proton with ^{78}Ni taken as core. The effective interaction have been used, is based on CD-Bonn N-N potential [44,45] which is adopted to the model space based on the ^{78}Ni core.

(ii) Calcium isotopes in mass region A=42-58

The valence space chosen for Ca isotopes is full fp shell π(0f7/2, 1p3/2, 0f5/2, 1p1/2) with ^{40}Ca core and KB3G interaction. This interaction is mass dependent version of KB3 [46] which is a (mostly) monopole modification of original Kuo-Brown interaction[47,48,49].

(iii) Odd and even N=50 isotones in the mass region A=80-96

The calculation (for N=50 isotones) for the odd and even nuclei between ^{78}Ni and ^{100}Si, have been carried out in the valence space π(0f5/2, 1p3/2, 1p1/2, 0g9/2) taking ^{78}Ni as inert core and with jj44b interaction. This interaction was obtained from a fit to experimental data of about 600 binding energies and excitation energies of nuclei with Z=28-30 and N=48-50 [50].

Shell model in one of the pioneer models of nuclear physics and has been highly successful in explaining the properties of nuclei with closed shell and closed shell ± few nucleons. The energy levels of nuclei with few nucleons outside the closed core can be calculated by performing configuration mixing calculations. The three main ingredient of any shell model calculation are effective interaction, model space and suitable code. One must perform the shell model calculations either with bare N-N interaction and unlimited configuration space or with effective N-N interaction in a limited configuration space. The neglected configuration tend to renormalize the bare N-N interaction. Several effective interaction have been developed in the literature suitable for use in a

particular model space. These interaction have been tested against the prediction of experimental properties of stable nuclei. Whether the same methodology, model space and effective interaction will also be able to account for the properties of exotic nuclei, is an open question. The aim of the present work is (i) to test the suitability of effective interactions in the chosen model space in explaining the experimental data (ii) to predict for the unknown values of nuclear properties which can serve as basis for future experiments (iii) to study the shell evolution with changing proton/neutron number in going through isotonic chain/isotopic chain (iv) to study the structure of the wave function.

We have also explored the mechanisms behind these changes in single-particle structure, and make predictions for nuclei further towards instability.

References:

[1] P. J. Woods et. al., Annu. Rev. Nucl. Part Sci. 47, 541 (1997).

[2] A. A. Sonzogni : Nuclear data sheets 95, 1 (2002).

[3] Tarasov et. al., 2007

[4] Baumann et. al. 2007

[5] R. D. Macfarlane et. al., Phys. Rev. Lett. 14 (1965) 114.

[6] N. A. Jelley et. al., Phys. Rev. C 9, (1974) 2067.

[7] E. Kashy et. al., Phys. Rev. C 14 (1976) 1773.

[8] J. Cerny et. al., Phys. Rev. Lett. 13 (1964) 726.

[9] A. M. Poskanzer et. al., Phys. Rev. B 18 (1965) 138.

[10] A. M. Poskanzer et. al., Phys. Lett. B 27 (1968) 414.

[11] T. D. Thomas et. al., Phys. Lett. B 27 (1968) 504.

[12] A. G. Artukh et. al., Nucl. Phys. A 137 (1969) 348.

[13] P. Auger et. al., Z. Phys. A 289 (1979) 255.

[14] C. Scheidenberger, Eur. Organization of nuclear research

CERN-EP/99-165, 19 Nov. 1999

[15] C. L. Morris et. al., Phys. Rev. C 25 (1982) 3218.

[16] K. K. Seth et. al., Phys. Rev. Lett. 58 (1987) 1930.

[17] Gurov et. al., JETP Lett. 28 (2003) 183.

[18] I. Tanihata et. al., Phys. Rev. Lett. 55 (1985) 2676.

[19] P. G. Hansen et. al., Euro. Phys. Lett. 4, (1987) 409.

[20] K. Tanaka et. al., Phys. Rev. Lett. 104, (2010) 062701.

[21] W. Shwab et. al., Z. Phys. A 350 (1995) 283.

[22] T. Minamisono et. al., Phys. Rev. Lett. 66, (1992) 1571.

[23] A. Ozawa et. al., Phys. Lett. B 834 (1994) 18.

[24] K. Riisager et. al., Euro. Phys. Lett. 49 (2000) 547.

[25] A. A. Korsheninni Kov et. al., Nucl. Phys. A 617 (1997) 45.

[26] I. Tanihata et. al., Phys. Lett. B 289 (1992) 261.

[27] B. A. Brown, Phys. Rev. C 43 (1991) (R) 1513.

[28] Ernst Roeckl, Lect. Notes Phys. 651, 223-261 (2004).

[29] ISOLDE Radioactive Ion Beam Facility, http://isolde.web.cern.ch/isolde/.

[30] Gesellschaft für Schwerionenforschung mbH, http://www.gsi.de/.

[31] Grand Accélérateur National d'Ions Lourds, http://www.ganil.fr/.

[32] National Superconducting Cyclotron Laboratory, http://www.nscl.msu.edu/.

[33] RIKEN Radioactive Ion Beam Factory, http://ribfweb1.riken.go.jp/.

[34] Holifield Radioactive Ion Beam Facility, http://www.phy.ornl.gov/hribf/hribf.html/.

[35] Isotope Separator and Accelerator, http://www.triumf.ca/people/baartman/ISAC/.

[36] J. S. Thomas et. al., Euro. Phys. J. A 25, s01, 371 (2005).

[37] O. Perru et. al., Euro. Phys. J. A 28, 307 (2006).

[38] A. Huck et. al., Phys. Rev. C 31 (1985) 2226.

[39] M. Honma et. al., Phys. Rev. C 65 (2002) 061301.

[40] D. Verney et. al., Phys. Rev. C 76, 054312 (2007).

[41] M. Gorska et. al., Phys. Rev Lett. 79, No. 13 (1997).

[42] J Sinatkas et. al., J. Phys. G : Nucl. Part. Phys. 18 (1992) 1377-1400.

[43] X. Ji and B. H. Wildenthal, Phys. Rev. C 40, 2415, No.1 (July 1989).

[44] R. Machleidt, Phys. Rev. C 63, 024001 (2001).

[45] L. Coraggio et. al., Prog. in Part. and Nucl. Phys. 62, 135 (2009).

[46] A. Poves et. al. Nucl. Phys. A 694 (2001) 157-198.

[47] Kuo and Brown, Nucl. Phys. A 114 (1968) 241.

[48] A. Poves and A. P. Zuker, Phys. Rep. 70 (1981) 235

[49] G. Martinez-Pinedo et. al.,Phys. Rev. C 55 (1997) 187

[50] Lisetskiy and Brown (unpublished)

.

Chapter 2

Shell Model and Techniques

2.1 Nucleus: A many body system

Nucleons in nucleus, feel many body forces, interact through meson exchange. This interaction could be described by non-relativistic potential and can be solve by Schrodinger equation. The many body forces (strong or also called nuclear force) act between nucleons is responsible for most of the observed characteristics of the nucleus. The main properties of the strong nucleon-nucleon interaction are known[1], still this does not allow us to answer various simple questions that arise from nuclear physics observations (e.g. the evolution of first excited states in nuclei with even proton and neutron numbers). Several theories and models have been constructed in order to answer these questions. Study of these complex nuclei has been carried out mainly by two methods: nuclear models and microscopic theories.

2.2 Nuclear models

There are two main categories of these models: Independent particle model and collective model. The former gives the formal framework for a description of nuclei in terms of interacting neutrons and protons. The latter provides a very physical but phenomenological framework for interpreting the observed properties of nuclei.

2.2.1 Independent particle model:

In this categories there are several models which differ from one another due to a number of additional assumptions made to explain certain nuclear properties. The best known example is the nuclear shell model. It describes nuclear properties as originating from the motion of independent particles moving in a potential. The nuclear shell model is a model of the atomic nucleus which uses the Pauli exclusion principle to describe the structure of the nucleus in terms of energy levels. The strong analogy of magic numbers found in atomic physics led to the development of the nuclear shell model.

2.2.2 Collective model:

In addition to individual nucleons changing orbits to create excited states of the nucleus as described by the Shell Model, there are nuclear transitions that involve many (if not all) of the nucleons. Since these nucleons are acting together, their properties are called collective, and their transitions are described by a Collective Model of nuclear structure. High-mass nuclei have low-lying excited states that are described as vibrations or rotations of nonspherical nuclei. Many of these collective properties are similar to those of a rotating or vibrating drop of liquid, and in its early development the Collective Model was called the Liquid-Drop Model.

In the shell model, nuclear energy levels are calculated on the basis of a single nucleon (proton or neutron) moving in a potential field produced by all the other nucleons. Nuclear structure and behaviour are then explained by considering single nucleons beyond a passive nuclear core composed of paired protons and paired neutrons that fill groups of energy levels, or shells. In the liquid-drop model, nuclear structure and behaviour are explained on the basis of statistical contributions of all the nucleons (much as the molecules of a spherical drop of water contribute to the overall energy and surface tension). In the collective model, high-energy states of the nucleus and certain magnetic and electric properties are explained by the motion of the nucleons outside the closed shells (full energy levels) combined with the motion of the paired nucleons in the core. Roughly speaking, the nuclear core may be thought of as a liquid drop on whose surface circulates a stable tidal bulge directed toward the rotating unpaired nucleons outside the bulge. The tide of positively charged protons constitutes a current that in turn contributes to the magnetic properties of the nucleus. The increase in nuclear deformation that occurs with the increase in the number of unpaired nucleons accounts for the measured electric quadrupole moment, which may be considered a measure of how much the distribution of electric charge in the nucleus departs from spherical symmetry.

2.3 Microscopic theories

The nuclear mean field potential U(K) have a phenomenological shape in original shell model, i.e. the modified harmonic oscillator potential. One can obtain a nuclear mean field in a microscopic approach starting from the nucleon nucleon force, which is short-ranged and charge independent, and gives rise to the observed saturation properties like BE α A and the nuclear radius varying as $R=R_0A^{1/3}$. A more microscopic approach for the mean field U(K) is Hartree –Fock theory which essentially derives a one body potential starting from a given nucleon-nucleon two body potential $V(\bar{r},\bar{r'})$. An optimized $U_{HF}(\bar{r})$ is iteratively calculated based on a minimization of the total nuclear energy. This HF potential is given by:

$$U_{HF}(\bar{r}) = \int \rho(\bar{r}) V(\bar{r}, \bar{r'}) dr' \qquad (2.1)$$

With

$$\rho(\bar{r'}) = \sum j_{(OCP)} |\psi_j(\bar{r'})|^2 \qquad (2.2)$$

where the sum runs over all occupied orbitals j inside the atomic nucleus. One start from a good guess for density and the two body interaction, computes the mean field potential, derives the wave functions, and uses these wave functions to obtain a better approximation for the density. A two body interaction which is widely used in "self-consistent" HF calculation is the Gogny and the Skyrme interactions [2]. Similar

Relativistic Mean Field (RMF) models are based on forces originating from the exchange of effective mesons between the nucleons [3]. These are three “standard models” for the nuclear mean field which are widely used.

But using effective two-body forces that allow to determine the nuclear average potential through HF(B) theory, one runs into problems when moving far away from the region of stable nuclei.

2.4 Basic Description of the Shell Model

The Nuclear Shell Model accounts for many features of the nuclear properties. According to this model, the motion of each nucleon is governed by the average attractive force of all the other nucleons[4,5]. The resulting orbits form "shells," just as the orbits of electrons in atoms do. As nucleons are added to the nucleus, they drop into the lowest-energy shells permitted by the Pauli Principle which requires that each nucleon has a unique set of quantum numbers to describe its motion. When a shell is full (that is, when the nucleons have used up all of the possible sets of quantum number assignments), a nucleus of unusual stability forms. This concept is similar to that found in an atom where a filled set of electron quantum numbers results in an atom with unusual stability–an inert gas. When all the protons or neutrons in a nucleus are in filled shells, the number of protons or neutrons is called a "magic number." Some of the magic numbers are 2, 8, 20, 28, 50, 82, and 126. Some nuclei, for

example ^{40}Ca and ^{208}Pb, have magic numbers of both protons and neutrons; these nuclei have exceptional stability and are called "doubly magic." Magic numbers are indicated on the chart of the nuclides.

Filled shells have a total angular momentum, *J*, equal to zero. The next added nucleon (a valence nucleon) determines the *J* of the new ground state. When nucleons (singly or in pairs) are excited out of the ground state they change the angular momentum of the nucleus as well as its parity and isospin projection quantum numbers. The shell model describes how much energy is required to move nucleons from one orbit to another and how the quantum numbers change. Promotion of a nucleon or a pair of nucleons to an unfilled shell puts the nucleus into one of the excited states.Excited nuclear states decay to more stable states, *i.e.*, more stable nucleon orbitals.

Nuclear is a many body quantal system-in non relativistic framework it is described by the Schrodinger equation. Taking only two-body forces into account, the Schrodinger equation for A nucleons is,

$$\overline{H}\psi(1,2,.....A) = \left[\sum_{K=1}^{A}\overline{T}(K) + \sum_{1=K<l}^{A}\overline{V}(K,l)\right]\psi(1,2,.....A) = E\psi(1,2,.....A) \quad (2.3)$$

An exact solution of such a many-body problem can be rarely obtained except for the lightest masses. Therefore the first step towards an

approximate solution is to introduce a single-particle potential $\overline{U}(K)$ by writing the Hamiltonian as:

$$\overline{H} = \sum_{K=1}^{A}\left[\overline{T}(K) + \overline{U}(K)\right] + \left[\sum_{1=K<l}^{A}\overline{V}(K,l) - \sum_{1=K<l}^{A}\overline{U}(K)\right] = \overline{H}^{(0)} + \overline{H}^{(1)} \tag{2.4}$$

Here $\overline{H}^{(0)}$ represents the mean field produced by the closed core of the nucleus. In shell model the mean single-particle potential field is taken as a phenomenological potential usually given by a harmonic oscillator form and contains only terms related to one particle. It defines the independent-particle motion and its eigen functions are obtained as products of single-particle wave functions. The latter can be calculated much more easily for any given central potential since the equations are now uncoupled. In order to obtain good agreement with the experimental data along with harmonic oscillator potential, Mayer and Jensen[6.7] have introduced a harmonic oscillator plus a spin-orbit interaction $\alpha.\bar{l}.\bar{s}$ and a term proportional to $\beta.\bar{l}.\bar{l}$ which provides residual energy causing lowering of the $l \neq 0$ orbitals. The resulting single particle Hamiltonian has the form:

$$\overline{H} = \frac{P^2}{2m} + \frac{m\omega^2 r^2}{2} + \alpha\left(\bar{l}.\bar{s}\right) + \beta\left(\bar{l}.\bar{l}\right) \tag{2.5}$$

Where $$\alpha(r) = U_{ls}\frac{1}{r}\frac{dU(r)}{dr} \tag{2.6}$$

and $$U_r = \frac{U_0}{1+e(r-R_0)/a} \qquad (2.7)$$

with $R=R_0A^{1/3}$(R_0=1.27 fm) and a=0.67 fm. And the last term $\beta.\bar{l}.\bar{l}$ breaks the remaining *l*-degeneracy within a given major harmonic oscillator shell. This breaking appears automatically in square well or Wood-Saxon type of central potential.

The second part, $\overline{H}^{(1)}$, is called the residual interaction. It shows that the particles do not move completely independently and is responsible for collective effects like vibrations and deformations. $\overline{H}^{(1)}$ describing the residual interaction between valence nucleons outside a closed shell has two parts monopole ($\overline{H}_{\text{mono}}$) and multipole ($\overline{H}_{\text{multi}}$) : $\overline{H}_{\text{mono}}$ is related to the evolution of the spherical mean field and determines the position of single particle energy levels. The higher-order multipoles determine correlations which are not present in the spherical mean field and are responsible for configuration mixing between levels and the relative energy splitting between different angular momentum states.

With the assumption of a specific form of the residual interaction $\overline{H}^{(1)}$, solutions of the full problem are found by diagonalizing the full Hamiltonian $\overline{H} = \overline{H}^{(0)} + \overline{H}^{(1)}$. Since dimensions of the Hamiltonian matrix increase rapidly with the number of nucleons and their coupling possibilities to a given spin and isospin, the diagonalization becomes

unworkable and therefore some codes are used to diagonalize the matrix. The most widely used codes are Nushell, Antoine and Nathan. Configuration mixing between all valence nucleons outside the core- interacting through the $\overline{H}^{(1)}$ part are taken into account for describing nuclei in a given model space.

By the shell model approach we can focus on the properties of the residual interaction between valence nucleons outside the closed core. The effect of the underlying core can be incorporated by modifying the residual interaction resulting in effective residual interaction. The best choices for such core nuclei are those with closed proton and/or neutron shells, the so-called doubly- (and) and semi-magic (or) nuclei. Hence, the shell-model is best suited for nuclei composed of a closed-shell nucleus plus a few valence nucleons. This brings us to a more specific motivation of this work, namely testing the shell-model for nuclei in the vicinity of closed-shell nuclei but far from stability.

With appropriate strengths, such an independent particle model explains the known shell gaps that give rise to additional stability at N, Z=2,8,20,28,(40),50,82,126 and the spin and parity assignments of ground states and energy spectra of most stable odd-A nuclei and almost all spherical nuclei. However the shell structure of the single particle energy spectra will change for nuclei situated far from the region of β-stability (neutron or proton rich nuclei).

The resulting shell model orbits are shown in fig. 2.1 and characterized by the set of quantum numbers (*n; l; j; N*) where *n* is the radial quantum number, *l* is the orbital quantum number and *j* is the total angular momentum and *N* is the major oscillator quantum number. The single particle orbitals obtained in shell model are (2*j* +1) fold degenerate.

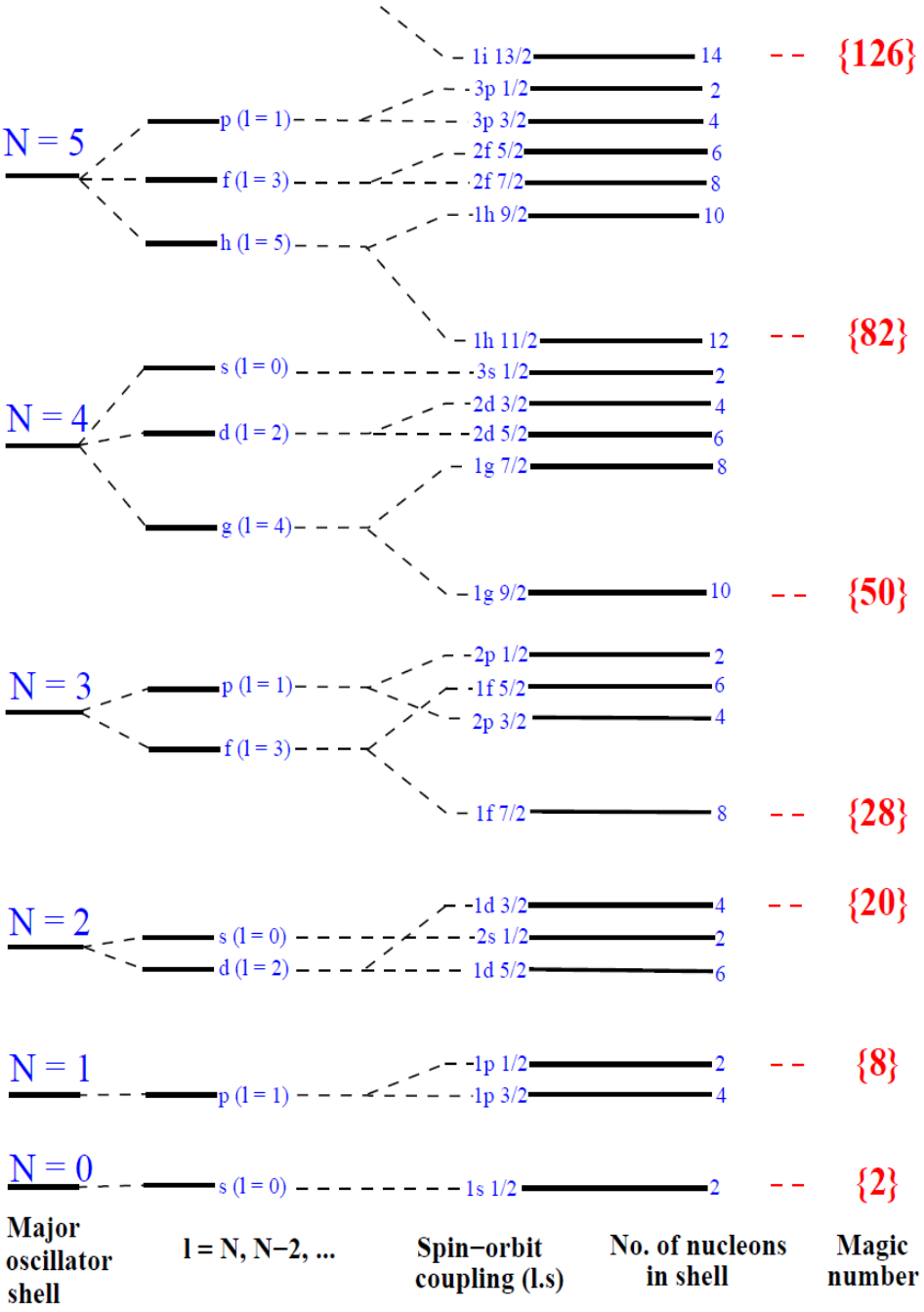

Figure 2.1: Shell Model Single Particle Levels

2.5 Nuclear Spectroscopy

On the basis of Nuclear shell model it is possible to describe the nuclear configuration and the spin in the ground state and a few low lying excited state of the nucleus. All closed shell nuclei with completely filled j-shell in protons and neutrons have spin zero in the ground state. The shell model excited states of closed shell nuclei are caused by excitation of the particle from the core across the shell gap between the major shells. Such excitated states lie high in energy. For nuclei having the closed shells with one particle or closed shells with one hole (one particle missing from the core), the ground state spin of the nucleus corresponds to the angular momentum of the valence nucleon (hole). The low lying excited states are caused by excitation of the valence nucleon (hole) to the higher single particle states of the same major shell. In the shell model approach the nucleus inside the closed core are considered inactive or inert. The nucleons outside the closed core are active or valence particle.

2.5.1 Nuclei with two particles outside the closed core: Configuration mixing

If the number of nucleons outside the closed core are more than one then these valence particle interact not only with the core with the common potential but also there is effective residual two body interaction between nucleons.

A configuration is defined by a set of quantum numbers describing all the states that are occupied by the nucleons but a practical way of defining a configuration space is by the states of 'active nucleon' outside the inert core. These active or valence particles interact with core through a common potential $V_0(r)$ and there is an effective residual two-body interaction between these valence nucleons. In the shell model, not only that the residual interaction splits the levels with different J values but also mixes configurations with same J value of active nucleons.

The shell model Hamiltonian for two nucleons outside the closed shell is written as

$$H = H_0 + V_{ij} \tag{2.8}$$

or

$$\overline{H} = \overline{T}(1) + \overline{T}(2) + \overline{V}(1,2) \tag{2.9}$$

where $\overline{V}(1,2)$ is the residual nucleon-nucleon potential. As shown in equation (2.4) the residual interaction is the difference between the cumulated nucleon-nucleon interaction and the central potential. If two particles are in the same orbit ($j_1=j_2=j$); then an allowable (antisymmetric) state of two neutron system would be:

$$\psi_{JM}(jj) = 2^{-1/2} B \sum_{m_1 m_2} \langle jjm_1m_2 \,|\, JM \rangle \times \{\phi_{jm_1}(1)\phi_{jm_2}(2) - \phi_{jm_1}(2)\phi_{jm_2}(1)\} \tag{2.10}$$

B is the normalization condition.

$|0\rangle$ corresponds to the ground state belonging to even-even core, and

$$(jjm_1 = m_2 \mid JM) \qquad (2.11)$$

are Clebsh-Gorden coefficients. The expectation values of H for the various states in a two-nucleon system outside the closed shell can be written as

$$\langle \psi_{JM}(jj)|\vec{H}|\psi_{JM}(jj)\rangle = 2\varepsilon_j + \langle \psi_{JM}(jj)|\vec{V}_{ij}|\psi_{JM}(jj)\rangle = 2\varepsilon_j + E_f(jj, jj) \qquad (2.12)$$

If two different combinations(j_1,j_2) and (j_3,j_4) give same J, then

$$\vec{H}(\alpha_1\psi_{JM}(j_1j_2) + \alpha_2\psi_{JM}(j_3j_4) = \tilde{\mathrm{E}}[\alpha_1\psi_{JM}(j_1j_2) + \alpha_2\psi_{JM}(j_3j_4)] \qquad (2.13)$$

where α_1 and α_2 are normalizing constants.

Integrating over all the space after multiplying both side by $\psi_{JM}(j_1j_2)$, we get

$$\alpha_1\{(\varepsilon_{j_1} + \varepsilon_{j_2} + \mathrm{E}_1(j_1j_2, j_1j_2))\} + \alpha_2\mathrm{E}_1(j_1j_2, j_3j_4) = \alpha_1\tilde{\mathrm{E}} \qquad (2.14)$$

Similarly integrating over all the space after multiplying both side by $\psi_{JM}(j_3j_4)$,

we get

$$\alpha_1\mathrm{E}_1(j_3j_4, j_1j_2) + \alpha\{\varepsilon_{j_3} + \varepsilon_{j_4} + \mathrm{E}_1(j_3j_4, j_3j_4)\} = \alpha_2\tilde{\mathrm{E}} \qquad (2.15)$$

These two equation can be written as;

$$\sum_k \left\{ \langle H \rangle_{ik} - \tilde{\mathrm{E}} \delta_{ik} \right\} = 0, i = 1,2 \tag{2.16}$$

here i corresponds to two configurations or two levels. where

$$\left\langle \vec{H} \right\rangle_{11} = \varepsilon_{j_1} + \varepsilon_{j_2} + \mathrm{E}_J(j_1 j_2, j_1 j_2) \tag{2.17}$$

with

$$\mathrm{E}_J(j_1 j_2, j_1 j_2) \equiv \left\langle \psi_{JM}(j_1 j_2) \mid \vee_{12} \mid \psi_{JM}(j_1 j_2) \right\rangle \tag{2.18}$$

and

$$\left\langle \vec{H} \right\rangle_{22} = \varepsilon_{j_3} + \varepsilon_{j_4} + \mathrm{E}_J(j_3 j_4, j_3 j_4) \tag{2.19}$$

where

$$\mathrm{E}_J(j_3 j_4, j_3 j_4) \equiv \left\langle \psi_{JM}(j_3 j_4) \mid \vee_{12} \mid \psi_{JM}(j_3 j_4) \right\rangle \tag{2.20}$$

$$\left\langle \vec{H} \right\rangle_{12} = \left\langle \vec{H} \right\rangle_{21} = \mathrm{E}_J(j_1 j_2, j_3 j_4) \tag{2.21}$$

where

$$\mathrm{E}_J(j_1 j_2, j_3 j_4) \equiv \left\langle \psi_{JM}(j_1 j_2) \mid \vee_{12} \mid \psi_{JM}(j_3 j_4) \right\rangle \tag{2.22}$$

Here V_{12} is Hermitian. These equations are solved through perturbation theory. The resulting wave functions are

$$\psi_{JM}(jj) = \alpha_1 \psi(j_1 j_2 : m_1 m_2) + \alpha_2 \psi(j_3 j_4 : m_3 m_4) \quad (2.23)$$

2.5.2 For three or more particles out side the core

If there are n particles outside closed shell, the anti-symmetrised wave-function for nucleons outside the closed shell is given by Slater determinant:

$$\psi^n_{JM}(r) = (n!)^{-1/2} \begin{vmatrix} \phi_{j_1 m_1}(1) & \phi_{j_1 m_2}(1) & \cdots & \phi_{j_n m_n}(1) \\ \phi_{j_1 m_1}(2) & \phi_{j_2 m_2}(2) & \cdots & \phi_{j_n m_n}(2) \\ \vdots & \vdots & \vdots & \vdots \\ \phi_{j_1 m_1}(n) & \phi_{j_2 m_2}(n) & \cdots & \phi_{j_n m_n}(n) \end{vmatrix} \equiv \left| \phi_{j_1 m_1} \quad \phi_{j_2 m_2} \quad \cdots \quad \phi_{j_n m_n} \right|$$

(2.24)

This is antisymmetric (from the properties of the determinant), to the interchange of any two particles and vanishes when two particles occupy the same quantum state. Thus the only possible M state, for the configuration $J=j^{(2J+1)}$, when orbital is completely occupied, is

$$M = \sum_i m_i = 0 \quad where \quad m_i \equiv j_{m_1}$$

(2.25)

For the calculation of matrix elements of the residual interaction V_{ij} the slater determinant is expressed in such a way that the single particle wave function of one particle (say nth) is explicitly separated and the slater

integral is expanded in terms of the minor of the last row, excluding the wave function of the nth particle.

$$\psi_{JM}(1,2...n) = \sum_{J\beta} \left\langle j^{n-1} J\beta \middle| j^n I\alpha \right\rangle \left[\Phi_{J\beta}(1...n-1)\phi_j(n) \right]_{IM} \quad (2.26)$$

Where $\left\langle j^{n-1} J\beta \middle| j^n I\alpha \right\rangle$ are called the coefficients of fractional parentage (c.f.p) which are so chosen that wave function to be antisymmetric to the interchange of any two particles and are real quantities in the representation chosen above.

It may be seen, that the wave-function has been divided between the $\Phi_{J\beta}(1...n-1)$, which will be written in the form of Slater determinant of the terms of minors of the last row and $\phi_j(n)$ the single particle wave function of the nth particle. A further reduction leads to division between the wave function of (n-2) particles and a product of two single particle wave function of nth, (n-1)th particles respectively. This reduction continues till one obtain a coupled to particle wave function and product of coupled two nucleon function and (n-2) single particle wave function. The matrix element of two body operator V_{ij} can easily be calculated.

2.6 Techniques of calculations and Shell-Model code

The Nuclear Shell-Model (SM) is the most general microscopic nuclear model and is in principle able to describe all properties of nuclei. In the shell model calculations one calculates the total energy relative to a closed core instead of calculating the total energy of the entire system of A valence nucleons. Modern large-scale shell-model calculations give the most accurate and comprehensive description of nuclei far from β-stability. It is a most powerful tool for the study of nuclear structure and is one of the most important theoretical predictions to compare with the experimental data like low-lying energy levels, transition properties, g-factor, magnetic moments and quadrupole moments of very exotic nuclei. To derive the effective interaction used in the shell-model calculations from the nucleon nucleon interaction, less work has been done to understand the effective operators employed in the calculating different nuclear, usually electromagnetic, properties.

There is three part in the shell-model to calculate the nuclear properties, namely, model space, effective interaction and shell-model code to diagonalize the matrices. By choosing appropriate model space and construct suitable effective interaction one can obtain nuclear data close to experimental one. But two main problems appear in a shell-model description of the nuclear structure is, first, the possibility of obtaining a regularized effective interaction in a given valence space, from the bare nucleon-nucleon force. In its present state, effective interactions cannot be

used in SM calculations without some phenomenological corrections. And second one is, with the increase of the size of the valence space or (and) the increase of the number of particles (holes) the dimension of matrices explodes. This explains why SM calculations have been only extensively done for light nuclei, *p* shell and *s* - *d* shell and heavy nuclei with only few particles (holes) outside an inert core or for semi-magic nuclei. Nuclear shell model calculations in large and realistic single particle model spaces are very difficult to make due the extremely large Hilbert space dimension involved.

2.6.1 Model space

A model space is a set of quantum numbers describing all the states that are occupied by the 'active nucleon' or valence nucleons outside the inert core. It is assumed that all the properties of the nucleus are governed by these nucleons. Generally, the best and most complete results are obtained when the model space is as large as possible. However, the computation time increases with the size of model space and empirical Hamiltonians are better determined in smaller model spaces. Thus the choice of model space is a compromise between what one would like to describe and what is computationally practical. The continuous increase in computing power has made it possible to make progressively larger nuclear calculation in restricted model space. Currently existing nuclear shell model calculation methods/programs make it possible to calculate nuclear wave functions

exactly in the model space sd and fp and in $f_{5/2}pg_{9/2}$ model space with somewhat truncated calculations.

2.6.2 Effective interactions

Different theories based on realistic nuclear forces and the microscopic theories are used to develop a effective interaction. The effective interaction for the shell model is normally different from the bare realistic nuclear force. First, the free nuclear force exhibits a strong coupling between low-momentum and high-momentum degrees of freedom. This coupling is due to the short range properties of the interaction. Furthermore, the effective interaction for the shell model is defined in a restricted configuration space. An effective interaction for the shell model is started from realistic nuclear forces (bare nucleon-nucleon interaction) and perturbative many-body methods is used to derive it. Any effective interaction is valid only for the model space used in its derivation (and if necessary for the truncation scheme employed). Any change in model space and/or truncation requires a renormalization of the residual interaction.

2.6.3 Shell model code: Nushell

Nushell [8] is a shell model code developed by Alex Brown from MSU to tackle dimension up to 10^5 in the J-T scheme and about 2×10^6 in the M-

scheme. Nushell generates the basis states in m-scheme and then computes the matrix in the j scheme. Therefore, it bypass the complication of the angular momentum algebra in j-j coupled basis and also avoids the huge matrix dimension generated during m-scheme. Nushell consists of seven main programs and some supporting codes. SHELL makes a batch file .*bat that coordinates the program sequence and their inputs. NUBASIS makes a list of all possible M-scheme basis states for a given model space together with a given set of restrictions. NUPROJ makes linear combinations of the M-scheme basis states that have good J values in p/n formalism or good J and T in isospin formalism. NUMATRIX makes the matrix corresponding to the J (or JT) dimension of the problem. NULANCZOS find the lowest N eigen values for the matrix. MVEC reads the output of Proj and Lanczos to make the eigenvectors in the M-scheme basis. TRAMP calculates overlaps between two wavefunctions. DENS calculates the radial wavefunctions for a given nucleus with oscillator, Woods-Saxon or skyrme Hartree-Fock potentials and reads the .*obd from nushell to calculate B(EL), B(ML) and B(GT) values. It comes with a library of model spaces and interactions.

2.7 Electromagnetic Transition in Nuclei

In a quantum-mechanical treatment of a radiating system, the multipole moments of the charge, current and magnetization of the emitting system

are replaced by matrix elements of corresponding opertors between the initial and final states of the system. The electric multipoles are defined as

$$B(el,L)=\frac{1}{2J_i+1}|(J_f \parallel \frac{1}{e}\sum_i e_i r_i^L Y_L(\theta_i\phi_i) \parallel J_i)|^2 \quad (2.27)$$

where L is the sum of obital and intrinsic angular momenta, J_i and J_f are the initial and final state spins respectively, e is the effective charge. Thus B(E2) in unit of e^2fm^{2L} becomes

$$B(el,L)=\frac{1}{2J_i+1}|(J_f \parallel \frac{1}{e}\sum_i e_i r_i^2 Y_2(\theta_i\phi_i) \parallel J_i)|^2 \quad (2.28)$$

The transformation from B(E2,$2^+\rightarrow 0^+$) e^2fm^4 units to W.u. is given by

$$B(E2,2^+\rightarrow 0^+)_{W.u.}=\frac{16.8}{A^{4/3}}B(E2,2^+\rightarrow 0^+)e^2\,fm^4 \quad (2.29)$$

References:

[1] K.S. Krane, Introductory Nuclear Physics (Wiley, 1988)

[2] M. Bender et al., Rev. Modern Phys. 75 (2003), 121

[3] D. Vretenar et al., Phys. Rep. 101 (2005), 409

[4] M. G. Mayer, Phys. Rec. 75, 1969 (1949)

[5] M. G. Mayer and J. H. D. Jensen, *Elementary Theory of Nuclear Shell Structure* (John Wiley and Sons., New York, 1955)

[6] M. Goeppert-Mayer, Phys. Rev. **75**, 1969 (1949)

[7] O. Haxel, J. Jensen, and H. Suess, Phys. Rev. **75**, 1766 (1949)

[8] Nushell@MSU, B. A. Brown and W. D. M. Rae (unpublished).

Chapter 3

Nucleon Nucleon Interaction

Two body matrix element can be calculated either by Talmi Mossunky method or by Slater method in any general basis. The bare nucleon-nucleon interaction is a starting point to derive an effective interaction to be used in nuclear calculations. With the restriction to two-body interactions, the interaction energy in a many particle configuration can be reduced to a weighted sum over TBME only. The value of the matrix elements depends on the residual interaction, the single particle wave functions and on the total spin and isospin of the two particle system. The basic TBME of the residual interaction can be evaluated in three different way.

3.1 Realistic (Microscopic) effective interactions

In a microscopic approach, one starts from a bare NN potential and derives the Brueckner G-matrix which, in turn, is used to calculate certain classes of diagrams defining the effective interaction in an open shell, V_{eff}. The matrix elements of V_{eff} can then be used to calculate, for example, the

energy spectrum of an open-shell nucleus including both the ground state and the excited states.

The most fundamental way to get the two-nucleon interaction to be exploited in the many-body calculations is to derive it from a bare NN potential for free nucleons in a vacuum, by taking into account medium effects, the Pauli principle and truncated model space. This is why such an interaction is called an effective interaction. This approach treats two nucleons in nuclear medium in a way analogous to the scattering of two nucleons in vacuum . The resulting effective interaction is well-behaved at short distances. At the same time many-body effects are consistently treated when just applying the bare force. To eliminate hard core repulsion the G-matrix has been introduced which is obtained by solving the Bethe-Goldstone equation [1] and NN interaction V is used to calculate the G-matrix [2-4] .

$$G(\omega) = V + V\frac{Q_2 P}{\omega - H_0}G(\omega) \tag{3.1}$$

Here, ω is the `starting energy' at which G is computed. H_0 is the unperturbed Hamiltonian for the intermediate two-particle state. V is the bare interaction between two nucleons unmodified for the nuclear medium. Q_{2P} is a two-particle projection operator that guarantees that the scattered particle obey the Pauli exclusion principle: the two nucleons can only be scattered to unoccupied states, hence to states that lie above the

Fermi energy. The effective interaction derived from this *G*-matrix can be expressed as:

$$\nu_{eff} = G + G\frac{Q'}{E_{0_V} - H_0^V}\nu_{eff} \tag{3.2}$$

where H_{V0} is describing the single-particle Hamiltonian for the valence space, and E_{0V} is the corresponding single-particle energy. The prime on the projection operator Q` indicates that the expansion of v_{eff} does not sum over two-particle ladder diagrams already included in G, in order to avoid double-counting. This method introduces a mass (A) dependence in the extracted TBME, thus requiring a new calculation for every new core nucleus. The first such derived effective interaction is the one of Kuo and Brown in the sd-shell. Another example of often used effective interaction based on the G-matrix is by Hjorth-Jensen[4] developed for the $1p_{3\backslash2}$, $0f_{5\backslash2}$, $1p_{1\backslash2}$, $0g_{9\backslash2}$ space, Lisetskiy [5] developed Bonn-C NN potential (JJ4APN) based interaction for N=50 isotones in the vicinity of ^{78}Ni, Honma et al. developed GXPF1-interaction [6] for the mass range $47 \leq N \leq 66$.

Recently a method has been developed to eliminate the hard core repulsive (high momentum) contributions to V_{NN} directly [7]. The resulting smooth and non-singular V_{low-k} can then be used to calculate core polarization corrected TBME carrying no mass(A) dependence.

As a general rule it should be noticed that any effective interaction is valid only for the model space used in its derivation (and if necessary for the truncation scheme employed). Any change in model space and/or truncation requires (and justifies) a renormalization of the residual interaction.

3.2 Phenomenological (Empirical) effective interactions

Empirical interactions are extracted from experimental data, in the simplest approach, from the binding energies of *CS*,*CS* ± 1 and *CS* ± 2 nuclei. In the case of a single *j* shell:

$$\left\langle j^2 J \middle| V \middle| j^2 J \right\rangle = BE\left(CS \pm 2; j^2, I = J\right) - BE\left(CS; g.s.\right) - 2\varepsilon_j \tag{3.3}$$

Where $\varepsilon_j = BE(CS \pm 1; j^2, I = j) - BE(CS; g.s.)$ (3.4)

Thus the single-particle energies are taken from the spectrum of the nucleus with the some core plus one nucleon and two body matrix elements which are taken as free parameters in a fit for a particular mass region[8]. The energy levels calculated with these parameters are compared to the experimental energy levels and the parameter values are adjusted by means of a least-square fitting procedure. The energy eigen values obtained after diagonalization can be represented as linear

combinations of these parameters. The approach allows to get a good description of nuclei in a given model space. The drawback is that as the model space increases, the number of parameters increases drastically, 15 TBME's for (0p)-shell with two single particle energies, 63 TBME's in (1s0d)-shell with three single particle energies, 195 TBME's in (1p0 f) shell with four single particle energies and so on. To reach convergence, one uses the so-called linear combination method [9,10]. Its meaning is to choose the most important linear combinations of TBME's to be determined in a fit. The interaction found in this way describes very accurately the data. The examples of empirical interactions are the (0p) shell interaction of Cohen and Kurath [11], the so-called universal(1s0d) interaction (USD) [9, 12], the (1p0f)-shell GXPF1[13, 6], GXPF1A[14] interaction. However some of these interactions do not reproduce the results very close to the experimental data in some cases, that's why some semi empirical interaction are made by experimental data fitting in realistic interaction for a particular mass region to reproduce the better results close to the experimental data like JUN45[15] and Lisetskiy[16].

3.3 Schematic effective interactions

Departing from the basic properties of the nuclear force, we also use the properties of some of the simple forces such as multiple forces, zero-range or delta-forces and spin exchange component. Such type interaction is Schematic interactions. The earlier interactions are

parameterized functions of nucleon coordinates. They are used to calculate all TBME's in a given model space:

$$\langle ab;JT|V(1,2)|cd;JT\rangle \tag{3.5}$$

In schematic interactions, interaction between two nucleons can be imagined to be of zero-range (delta type):

$$V_\delta(1,2) = -V(r)\delta(\vec{r_1} - \vec{r_2}), \tag{3.6}$$

and the simplest approximation for the short range character of the nuclear force. Moreover, the δ-force can be extended by including a spin-exchange component:

$$V_\delta(1,2) = -V_0(1 - \alpha + \alpha\vec{\sigma_1}.\vec{\sigma_2})\delta(\vec{r_1} - \vec{r_2}) \tag{3.7}$$

with α the degree of spin-exchange, varying between 0 and 1, and V_0 the strength of the interaction and given in units MeV.fm^3. The delta interaction which is more popular in the sd-shell is SDM whose modified version is MSDI.

A few parameters, characterizing a schematic interaction, such as V_0 and α , are adjusted to reproduce low-energy spectra of a few neighboring nuclei of interest. These parameters are then supposed to change from one region of the nuclear chart to another. Another important interaction is the pairing interaction between alike nucleons. For a constant pairing force, it is defined as an extra attraction between coupled to J = 0,T = 1 pairs of nucleons, which results in only non-zero TBME's of the type

$$\langle a^2;01|V_{pairing}(1,2)|b^2;01\rangle = -(-1)^{l_a+l_b}\frac{1}{2}G\sqrt{(2j_a+1)(2j_b+1)}\,,$$

(3.8)

where G is the strength, and zero matrix elements otherwise.

The last schematic interaction we would like to mention here is the quadrupole-quadrupole interaction which is necessary, in particular, its proton-neutron part, to describe rotation of deformed nuclei. This is a λ = 2 component of the general (proton-neutron) multipole-multipole interaction (a separable interaction) of the type:

$$V(1,2) = \sum_{\lambda}\chi_{\lambda}(Q_{\lambda}\cdot Q_{\lambda}) = \sum_{\lambda}\chi_{\lambda}\, r_{\pi}^{\lambda} r_{\nu}^{\lambda} Y_{\lambda}(\Omega_{\pi})\cdot Y_{\lambda}(\Omega_{\nu}) \qquad (3.9)$$

Historically, interactions of the Yukawa [17], Gaussian [17], delta [17] and surface delta [18] types, as detailed in various textbooks [19,20,17], have played a significant role in the evolution of shell model calculations. The restrictions and symmetries are imposed on the TBME by a given analytic function and radial dependence introduce deficiencies in the energies (pairing, level density) and electromagnetic transition rates (configuration mixing) calculated in the shell model application. Another type of schematic interaction is widely used in mean field calculations employing the HF method , namely the Skyrme [21,22] and Gogny forces [23]. They have been successfully used to calculate such gross properties as masses, shapes, radii, level densities and single

particle energies, but have been scarcely applied to detailed shell model spectroscopy.

References:

[1] H. Bethe et al., Proc. Roy. Soc. (London) A 238 (1957), 551

[2] T.T.S. Kuo, G.E. Brown, Nucl. Phys. A **114**, 241 (1968)

[3] T.T.S. Kuo, E. Osnes, Springer Lecture Notes of Physics **364**, 1 (190)

[4] M. Hjorth-Jensen et al., Phys. Rep. **261**, 125 (1995)

[5] A. Lisetski et al., Phys. Rev. C 69 (2004), 044314

[6] M. Honma et al., Phys. Rev. C 69 (2004), 034335

[7] S. Bogner, T.T.S. Kuo, L. Coraggio, Nucl. Phys. A **684**, 432c (2001)

[8] P. Brussaard, Shell-Model Applications in Nuclear Spectroscopy, North- Holland, Amsterdam, 1977

[9] B. A. Brown and B. H. Wildenthal. Ann. Rev. Nucl. Part. Sci., 38:29, 1988

[10] T. Otsuka, M. Honma, T. Mizusaki, et al. Prog. Part. Nucl. Phys., 47:319, 2001

[11] S. Cohen and D. Kurath. Nucl. Phys., 73:1, 1965

[12] E. Caurier and F. Nowacki. Acta Physica Polonica, 30,705, 1999

[13] M. Honma, T. Otsuka, B. A. Brown, and T. Mizusaki. Phys. Rev. C, 65, 061301(R), 2002

[14]M. Honma, T. Otsuka, B.A. Brown and T. Mizusaki, Eur. Phys. J. A 25 Suppl. 1, 499 (2005).

[15] M. Honma et al., Phys. Rev. C 80, 064323 (2009)

[16] A.F.Lisetskiy et al., PRC70, 044314 (2004)

[17] K. Heyde, The Nuclear Shell Model, Springer, Berlin, 1994

[18] S. Arvieu, S.A. Moszkowski, Phys. Rev. **145**, 830 (1966)

[19] A. de Shalit, I. Talmi, Nuclear Shell Theory, Academic Press, New York, 1963

[20] P.J. Brussaard, P.W.M. Glaudemans, Shell model applications in nuclear spectroscopy, North-Holland, Amsterdam, 1977

[21] T.R.H. Skyrme, Nucl. Phys. **9**, 615 and 635 (1959)

[22] D. Vautherin and D.M. Brink, Phys. Rev. C **5**, 626 (1972)

[23] D. Gogny, Nucl. Phys. A **237**, 399 (1975)

Chapter 4

Shell Model Description of N=51 Isotones

4.1 Introduction

With the development of first generation radioactive ion beam facilities over the last decade it is now possible to access very neutron rich nuclei in few specific regions of the nuclear chart which do not even survive on the earth. Further, the study of these nuclei is considered as an ideal testing ground for a number of important issues: e.g. the evolution of shell structure concentrating on the neutron rich regions around Z = 20 and 28, relation between single particle and collective behavior etc. The study of nuclei with two magic numbers Z = 28 and N = 50 and in its vicinity has already been undertaken for a long time towards and beyond ^{78}Ni and is still the objective of active experimental and theoretical research. Previously neutron rich nuclei in the vicinity of ^{78}Ni have been produced and studied using deuteron beam available at the Tandem Accelerator in Orsay[1]. Since ^{78}Ni is the most neutron rich example of doubly magic nucleus in whole nuclide chart with an extreme N/Z ratio of 1.79 and further away from the stability on the neutron rich side, this region of nuclide chart remains extremely hard to reach experimentally. So far, only a dozen of ^{78}Ni could be successfully synthesized and identified with most advanced techniques of production of rare isotopes using high energy beam fragmentation. The most practical method of exploring the ^{78}Ni region is to study the decay of fission product to the levels of the N = 50 isotones above ^{78}Ni [2] and the study of nuclei with few valence particle or holes provides best testing ground for the basic ingredients of the shell model calculations. So N = 51 nuclide form an

interesting example of nuclei where the variation of the neutron single-particle energies can be investigated and nuclei in this mass region are particularly important to understand astrophysical processes. Also neutron rich nuclei between N = 50 and N = 82 shells cover waiting point in r-processes. Properties of low lying states in these nuclei near closed shell are useful for the description of nuclear structure, quenching of shell gaps and a more uniform spacing of single-particle energy levels [3,4,5] and influence how heavier nuclei are produced in astrophysical rapid neutron capture (r−) process [6,7]. A large number of nuclei can be populated by means of binary reactions such as multinucleon transfer and deep inelastic collisions with a stable beam. Such reactions combined with modern -detection array have increased substantially the available data on nuclei far from stability. Recently an experiment has been performed at LNL to study the nature of the low lying yrast or quasi yrast $7/2^+$ states in $32 < Z < 40$, N = 51 nuclei in order to assess their collective or ν1g7/2 single-particle origin and better constrain the relative position of the latter with respect to other neutron single-particle states above a ^{78}Ni core [8].

In the present work we have chosen N = 51 isotone nuclide viz. ^{83}Ge, ^{85}Se, ^{87}Kr, ^{89}Sr and ^{91}Zr which form an interesting region to study the validity of nuclear shell model in modeling of the available nuclear data [9,10]. Recently single neutron transfer reaction have been measured on two N= 50 isotones at HRIBF. The single particle like states of ^{83}Ge and

^{85}Se have been populated using radioactive ion beams of ^{82}Ge and ^{84}Se and the (d, p) reaction in inverse kinematics. This experiment has provided data on level structure of ^{83}Ge and ^{85}Se [9] including data on ^{87}Kr, ^{89}Sr and ^{91}Zr with references therein.

The nuclear shell model is the most powerful tool for giving a quantitative interpretation to the experimental data. Recent shell model calculations for neutron-rich F isotopes [11], odd and even isotopes of Fe [12,13], odd-odd Mn isotopes [14] odd-mass ^{61,63,65}Co isotopes [15], even-even Ni and Zn and odd-A Cu isotopes [16,17], odd-mass Ga isotopes [18] and neutron deficient $^{102-108}$Sn isotopes [19] have been carried out in an extended configuration space with suitably renormalized effective interaction, give a satisfactory account of the experimental data of unstable nuclei. Following this in the present work we have performed large scale shell model calculation for neutron rich ^{83}Ge, ^{85}Se, ^{87}Kr, ^{89}Sr and ^{91}Zr nuclei which form the N = 51 isotonic chain. The effective interaction used in the present work is renormalized G matrix obtained from CD Bonn N-N interaction and adopted to the model space based on a ^{78}Ni core (referred to as jj45pna interaction in the literature). Earlier jj45pna interaction has been used in the study of ^{128}Cd [20] and its monopole corrected version in the study of Zr isotopes in this region [21]. G-matrix derived from CD-Bonn potential have also been widely used in the theoretical calculations performed by the Oslo group and their coworkers in ^{132}Sn region [22,23,24,25,26].

The aim of this work is to test the suitability of the model space and the effective interaction in interpreting the experimental data of these highly unstable nuclei on the neutron rich side.

4.2 Details of Calculation

4.2.1 Configuration Space

Large scale shell model calculations have been performed for even Z neutron-rich N = 51 isotones in mass region A=83 - 91 treating ^{78}Ni as a core. The configuration space comprises of ν($0g_{7/2}$, $1d_{5/2}$, $1d_{3/2}$, $2s_{1/2}$, $0h_{11/2}$) orbitals for neutrons and π($0f_{5/2}$, $1p_{3/2}$, $1p_{1/2}$, $0g_{9/2}$) orbitals for protons with all Pauli allowed combinations of valence particles. The calculated single particle energies for model space π($0f_{5/2}$, $1p_{3/2}$, $1p_{1/2}$, $0g_{9/2}$) and ν($0g_{7/2}$, $1d_{5/2}$, $1d_{3/2}$, $2s_{1/2}$, $0h_{11/2}$) are

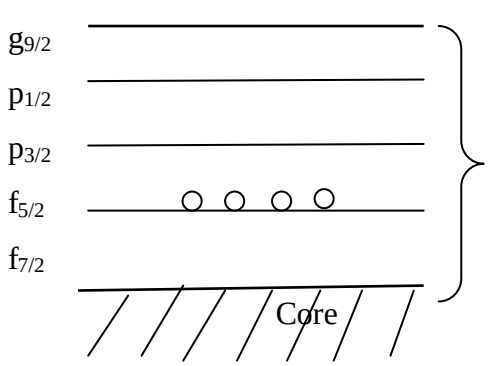

Figure 4.1: Model Space For the Proton

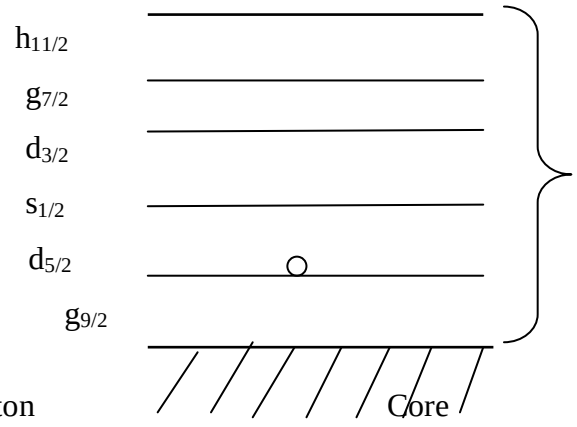

Figure 4.2: Model Space For the Neutron

respectively -0.7166, 1.1184, 1.1262 and 0.1785 MeV for proton orbitals and 5.7402, 2.4422, 2.5148, 2.1738 and 2.6795 MeV for neutron orbitals.

4.2.2 Effective Interaction

The calculations have been performed with a state of art effective interaction (jj45pna) derived from high precision, charge dependent version of Bonn N-N potential, known as CD-Bonn potential [27]. This potential is a charge-dependent one-boson-exchange nucleon-nucleon (*NN*) potential the parameters of which fit the proton- proton and neutron-proton data available till 2000 with χ^2 per datum close to 1. This reproduction of the *NN* data is more accurate than by any phase-shift analysis and any other *NN* potential. The high precision is obtained by the introduction of two effective σ mesons with partial wave dependent parameters. This potential model is an extension of the one-boson-exchange models of the Bonn group [28], where mesons like π,ρ,η,δ,ω and the fictitious σ meson are included. In the charge-dependent version, the first five mesons have the same set of parameters for all partial waves, whereas the parameters of the σ meson are allowed to vary. Earlier one-boson-exchange (OBE) model was designed which includes only single-meson exchanges (which can be represented in an energy-independent way). Usually, this model includes all mesons with masses below the nucleon mass, i.e., π, η , ρ and ω . In addition, the OBE model typically

introduces a scalar, isoscalar boson commonly denoted by σ (or ε). Based upon multimeson exchange contributions, this σ must approximate more than just the 2π exchange. In particular, it has to simulate 2π+πρ exchanges which are clearly not of purely scalar, isoscalar nature. Consequently, the σ approximation is poor (as demonstrated in Fig. 11 of Ref. [29]). This deficiency is overcome by readjusting the parameters of the σ boson in each partial wave. Moreover, the 2π+πρ exchanges create, in terms of ranges, a very broad contribution that cannot be reproduced well by a single boson mass but with two masses it can be reproduced. The *NN* potential with introducing two σ meson thus is energy independent and defined in the framework of the usual (nonrelativistic) Lippmann-Schwinger equation. The charge dependence of the CD-Bonn potential which is based upon the Bonn full model [30] have charge symmetry and charge independence breaking in all partial wave with $J \leq 4$.

The strong short range repulsion is overcome by Brueckner (reaction) G-matrix renormalization which accounts for the effects of two nucleon correlations [31]. The jj45pna effective interaction has been obtained by adopting G-matrix to the chosen model space above the ^{78}Ni core by using many body perturbation technique.

4.3 Results and Discussion

4.3.1 Excitation Energies

The results of our calculations for different isotones are shown in fig. 4.3-4.7 along with the experimental data for comparison . The excited states up to 2.5 MeV have been calculated. Experimentally it is well established that the $\nu 1d_{5/2}$ subshell is the ground state for all the isotones considered here i.e. $1d_{5/2}$ is first valence orbit above the N=50 shell gap which is well reproduced in our results for all isotones. Our calculations predict $1/2^+$ as the first excited state in agreement with the experimental data for all the isotones considered, except for ^{91}Zr in which $7/2^+$ state is predicted as the first excited state and $1/2^+$ state lies slightly higher. The predicted $E(1/2^+)$ state lies lower than the corresponding experimental values in all the cases. The special feature of the experimental energy spectra of N = 51 isotones is increase in the $E(1/2^+)$~$E(5/2^+)$ splitting in going from Z= 32 to Z=40. This trend is also reproduced in the theoretical spectra.

The variation of the excitation energy of first $1/2^+$ state with proton number is shown in fig 4.8. If energies relative to the $2s_{1/2}$ are considered, the monopole residual interaction between spin-flip $\Delta\ell$=1 pair of $0f_{5/2}$ proton orbital and $1d_{5/2}$ neutron orbital could be lowering $1d_{5/2}$ excitation with respect to $2s_{1/2}$ orbital as the stable ^{89}Sr and ^{91}Zr are approached. Since $1/2^+$ level is attributed to the excitation of neutron to $2s_{1/2}$ level, this variation of $E(1/2^+)$ with filling of proton orbitals is a signature of monopole effect [9,10]. Alternatively the raising of the $2s_{1/2}$ orbital in neutron rich N=51 isotones could be evidence for a reduced diffuseness

of the nuclear surface, which preferentially raises $2s_{1/2}$ orbitals relative to the increased binding of lower j-states [32].

In all the isotones with the exception of ^{91}Zr, the $7/2^+$ level is predicted to lie higher than the $3/2^+$ level contrary to the experimental results. $7/2^+$ state for ^{85}Se and ^{87}Kr have small deviations from corresponding experimental values. For ^{83}Ge its value is too high and for ^{89}Sr and ^{91}Zr its value is too low in comparison to the experimental data. So this interaction gives poor results for $7/2^+$ state. It finally becomes first excited state for ^{91}Zr. This indicates that the considered model space is not enough for ^{91}Zr. Rising trend of calculated E($3/2^+$) values with increasing Z is supported by the experimental data although their values are comparatively low. $7/2^+$ state is single particle energy in nature with weaker amount of mixing of neutron single particle $0g_{7/2}$ with coupled configuration. On the other hand $3/2^+$ state is single particle energy in nature with partial mixing of neutron single particle $1d_{3/2}$ with coupled configuration [33]. Single particle energies used in our calculations are 5.7402 for $0g_{7/2}$ and 2.5148 for $1d_{3/2}$. The calculated levels are sensitive to the single particle energies of the neutron orbitals which in turn get renormalized due to the monopole correction. Thus use of effective single particle energies can change the results.

The agreement of the E($9/2^+$) with experimental data for ^{89}Sr and ^{91}Zr is reasonably good. For ^{87}Kr and ^{85}Se theoretical E($9/2^+$) levels lie higher as compared to the corresponding experimental values but rising trend of

$E(9/2^+)$ state with increasing Z shows the nearly correct systematic for all nuclei. The experimental data for $E(9/2^+)$ state for ^{83}Ge is not available and theoretically predicted value is 1.856 MeV. The $9/2^+$ state is likely to have a rather pure coupled configuration $\nu 1d_{5/2} \otimes 2^+$, as $0g_{9/2}$ orbit is too deeply bound (by about 3.5 MeV) to give a fraction of single particle state at low energy . Such a configuration for the $9/2^+$ state is confirmed by the fact that its energy follows closely that of the 2^+ state [34].

The discrepancy between the calculated values and the experimental data can also be attributed to the core excitation effect and neglect of contributions arising due to 3N forces [35] . The coupling of the $\nu 1d_{5/2}$ orbit to the first 2^+ excitation of the core provides a multiplet of states with spin between $1/2^+$ and $9/2^+$. Therefore the $1/2^+$, $3/2^+$ and $7/2^+$ states originating from the $2s_{1/2}$,$1d_{3/2}$ and $0g_{7/2}$ orbits can be mixed to those obtained with the coupling to the core excitation. But experimentally $1/2^+$ and $7/2^+$ significantly depart from that of 2^+ core indicating that their composition is likely to be mostly of single particle origin with a weaker amount of mixing with the coupled configuration. So they are originating mainly from $2s_{1/2}$ and $0g_{7/2}$ subshell [34] and observed as first and second excited state experimentally. While $3/2^+$ state close to one of 2^+ state of core [10] is originating with a partial mixing of neutron single particle state $1d_{3/2}$ with coupled configuration [33]. Recent studies [36-38] have shown that 3N forces play an important role in the evolution of shell structure in neutron rich nuclei. Explicit calculations carried out for

neutron rich light mass oxygen [36] and medium mass calcium isotopes [37] have shown that 3N forces add a repulsive term to the monopole component of the two nucleon interaction and are key to explain the doubly magic nature of ^{24}O and ^{48}Ca nuclei. Inclusion of 3N forces substantially increases the energy gap between $0d_{5/2}$ and $1s_{1/2}$ levels in oxygen and between $0f_{7/2}$ and $1p_{3/2}$ levels in calcium leading to shell closure at N=16 and N=28. Three body forces also play an important role in the nuclear saturation properties in nuclear matter [38] ,which can be demonstrated typically in the Bruckener (G-Matrix) theory. Thus 3N forces are likely to play an important role in the ^{78}Ni region as well. The poor agreement of the $1/2^+$ single particle states with the experimental levels is an indication of the importance of 3N component in the interaction. Such forces, if included ,will shift the levels upwards due to increased repulsion and are likely to improve the agreement with the experimental data.

4.3.2 Wave Function

Most dominant configuration of wave function for ground state and first three excited states for all the isotones are shown in table 4.1. It is observed that in all the isotones except in ^{91}Zr, the structure of the proton part of the wave function for the ground state and first excited state $1/2^+$ remains the same confirming that the excited state is due to the excitation of neutron from ($d_{5/2}$) to ($s_{1/2}$). In ^{91}Zr the structure of the proton wave

function changes indicating the more complex nature of $7/2^+$ and $1/2^+$ excitations. In ^{83}Ge and ^{87}Kr the proton wave functions for $7/2^+$ state remains unchanged whereas in ^{85}Se, ^{89}Sr and ^{91}Zr their structure changes. The proton wave function for $3/2^+$ state also remains same in all the isotones except for ^{91}Zr. The difference can be attributed to the variation in proton single particle energies with changing Z.

4.3.3 Electromagnetic Properties

Theoretically calculated B(E2) values for the transition $1/2^+ \rightarrow 5/2^+$ and $7/2^+ \rightarrow 5/2^+$ are shown in table 4.2 for each of the N=51 isotonic nuclei. The effective charges used for proton and neutron are e_π^{eff} = 1.50 and e_ν^{eff} = 0.5 respectively. The calculations show that B(E2; $1/2^+ \rightarrow 5/2^+$) values first increase up to ^{87}Kr and then decreases for ^{89}Sr. No experimental data is available for comparison. The decrease in B(E2;$7/2^+ \rightarrow 5/2^+$) values in going from midshell to ^{89}Sr supports the onset of shell closure at Z=40.

Table 4.1 Main configurations in the wave functions of the ground state and first exited state for N = 51 isotones.

Nuclei	J^{π}	Wave function		Probability
		Proton	Neutron	
^{83}Ge	$5/2^{+}_{gs}$	$(f_{5/2})^2,(p_{3/2})^0,(p_{1/2})^0,(g_{9/2})^2$	$(d_{5/2})^1$	34.3
	$1/2^{+}_{1}$	$(f_{5/2})^2,(p_{3/2})^0,(p_{1/2})^0,(g_{9/2})^2$	$(s_{1/2})^1$	27.0
	$7/2^{+}_{2}$	$(f_{5/2})^2,(p_{3/2})^0,(p_{1/2})^0,(g_{9/2})^2$	$(g_{7/2})^1$	16.2
	$3/2^{+}_{3}$	$(f_{5/2})^2,(p_{3/2})^0,(p_{1/2})^0,(g_{9/2})^2$	$(d_{3/2})^1$	32.9
^{85}Se	$5/2^{+}_{gs}$	$(f_{5/2})^4,(p_{3/2})^0,(p_{1/2})^0,(g_{9/2})^2$	$(d_{5/2})^1$	20.0
	$1/2^{+}_{1}$	$(f_{5/2})^4,(p_{3/2})^0,(p_{1/2})^0,(g_{9/2})^2$	$(s_{1/2})^1$	15.6
	$7/2^{+}_{2}$	$(f_{5/2})^2,(p_{3/2})^0,(p_{1/2})^0,(g_{9/2})^4$	$(g_{7/2})^1$	17.0
	$3/2^{+}_{3}$	$(f_{5/2})^4,(p_{3/2})^0,(p_{1/2})^0,(g_{9/2})^2$	$(d_{3/2})^1$	19.9
^{87}Kr	$5/2^{+}_{gs}$	$(f_{5/2})^4,(p_{3/2})^0,(p_{1/2})^0,(g_{9/2})^4$	$(d_{5/2})^1$	19.0
	$1/2^{+}_{1}$	$(f_{5/2})^4,(p_{3/2})^0,(p_{1/2})^0,(g_{9/2})^4$	$(s_{1/2})^1$	14.4
	$7/2^{+}_{2}$	$(f_{5/2})^4,(p_{3/2})^0,(p_{1/2})^0,(g_{9/2})^4$	$(g_{7/2})^1$	22.4
	$3/2^{+}_{3}$	$(f_{5/2})^4,(p_{3/2})^0,(p_{1/2})^0,(g_{9/2})^4$	$(d_{3/2})^1$	19.5
^{89}Sr	$5/2^{+}_{gs}$	$(f_{5/2})^4,(p_{3/2})^2,(p_{1/2})^0,(g_{9/2})^4$	$(d_{5/2})^1$	14.7
	$1/2^{+}_{1}$	$(f_{5/2})^4,(p_{3/2})^2,(p_{1/2})^0,(g_{9/2})^4$	$(s_{1/2})^1$	11.8
	$7/2^{+}_{2}$	$(f_{5/2})^4,(p_{3/2})^0,(p_{1/2})^0,(g_{9/2})^6$	$(g_{7/2})^1$	16.5
	$3/2^{+}_{3}$	$(f_{5/2})^4,(p_{3/2})^2,(p_{1/2})^0,(g_{9/2})^4$	$(d_{3/2})^1$	14.1
^{91}Zr	$5/2^{+}_{gs}$	$(f_{5/2})^6,(p_{3/2})^2,(p_{1/2})^0,(g_{9/2})^4$	$(d_{5/2})^1$	12.4
	$1/2^{+}_{1}$	$(f_{5/2})^4,(p_{3/2})^2,(p_{1/2})^0,(g_{9/2})^6$	$(s_{1/2})^1$	9.1
	$7/2^{+}_{2}$	$(f_{5/2})^6,(p_{3/2})^0,(p_{1/2})^0,(g_{9/2})^6$	$(g_{7/2})^1$	14.3
	$3/2^{+}_{3}$	$(f_{5/2})^4,(p_{3/2})^2,(p_{1/2})^0,(g_{9/2})^6$	$(d_{3/2})^1$	11.3

Table 4.2 The B(E2) values for N = 51 isotones calculated with e_{π}^{eff} = 1.50e and e_{ν}^{eff} = 0.50e.

-	^{83}Ge	^{85}Se	^{87}Kr	^{89}Sr
B(E2; $1/2^+ \rightarrow 5/2^+$)(W.u.)	17.9	24.5	26.7	12.7
B(E2; $7/2^+ \rightarrow 5/2^+$)(W.u.)	32.0	17.2	11.2	0.9

4.4 Conclusions

In the present work large scale shell model calculations have been performed for N = 51 isotones nuclide ^{83}Ge, ^{85}Se, ^{87}Kr, ^{89}Sr and ^{91}Zr in valence space ν($0g_{7/2}$, $1d_{5/2}$, $1d_{3/2}$, $2s_{1/2}$, $0h_{11/2}$) orbitals for neutrons and π($0f_{5/2}$, $1p_{3/2}$, $1p_{1/2}$, $0g_{9/2}$) orbitals for protons with ^{78}Ni core. The effective interaction is based on the renormalization of CD-Bonn nucleon-nucleon potential developed by G - matrix theory for nuclei above ^{78}Ni core. Thus simple and pure neutron configurations of $(1d_{5/2})^{1\nu}$ and $(2s_{1/2})^{1\nu}$ above the N=50 shell closure can be assumed to describe the ground state and first excited state of all isotones. Ground state spin $5/2^+$ for all the isotones is associated with the last odd neutron in $d_{5/2}$ state. Similarly $1/2^+$ spin of first excited state can be attributed to the excitation of the last neutron from $1d_{5/2}$ to $2s_{1/2}$ level. The increase in $E(1/2^+)$~$E(5/2^+)$ splitting in going from Z=32 to 40 is direct reflection of the monopole effect wherein the energy of $1/2^+$ state is gradually increasing with the filling of proton orbitals.

The calculated $1/2^+$ levels are consistently lower than the corresponding

experimental values. The fitting of higher $3/2^+$,$7/2^+$ and $9/2^+$ states with the corresponding experimental data is not good. Thus, the present interaction in the chosen model space does not give good agreement with the experimental data. The reason for this could be manifold. Firstly, all these states have admixtures of coupling of single particle states with core excitation. Secondly, it is well known that the neutron single particle orbital changes with filling of proton number due to the attracting monopole pairing interaction between proton and neutron in spin-orbit partners [39]. So minor adjustment in the monopole part of the neutron proton interaction and renormalization of the single particle energies of the neutron orbitals can lead to better agreement with the experimental data. Thirdly, recent studies have shown that 3N forces have important effect on the evolution of shell structure in neutron rich nuclei. The three body component of these interactions gives rise to a repulsive contribution to the monopole interaction. These forces when included can give a shift to $1/2^+$ states in the right direction . Lastly, the wave functions of the $7/2^+$ states in ^{85}Se, ^{87}Kr, and ^{91}Zr and $1/2^+$ and $3/2^+$ states of ^{91}Zr have main components in which proton configuration is different than the ground state configuration showing that these states are not pure neutron excitation states.

References:

[1] F. Ibrahim *et al.*, Nucl. Phys. A **787**, 110c (2007).

[2] J. A. Winger, *et al.*, Phys. Rev. C **38**, 285 (1988).

[3] D. Verney *et al.*, Phys. Rev. C **76**, 054312 (2007).

[4] M. Lebois *et al.*, Phys. Rev. C **80**, 044308 (2009).

[5] K. Sieja and F. Nowacki, Phys. Rev. C **81**, 061303(R) (2010).

[6] J.A. Cizewski *et al.*, Nucl. Instum. Methods Phys. Res., Sect. B **241**, 200 (2005).

[7] J.S. Thomas *et al.*, Phys. Rev. C **71**, 021302 (2005).

[8] Andrea Gottardo, Ph.D. thesis, INFN-Legnaro (2007)

[9] J.S. Thomas *et al.*, Eur. Phys. J. A **25**, s01, 371 (2005).

[10] O. Perru *et al.*, Eur. Phys. J. A **28**, 307 (2006).

[11] P. C. Srivastava and I. Mehrotra, Int. J. Mod. Phys. E **20**, 637 (2011).

[12] P. C. Srivastava and I. Mehrotra, J. Phys. G : Nucl. Part. Phys. **36**, 105106 (2009).

[13] P. C. Srivastava and I. Mehrotra, Phys. At. Nucl. **73**, 1656 (2010).

[14] P. C. Srivastava and I. Mehrotra, Eur. Phys. J. A **45**, 185 (2010).

[15] P. C. Srivastava and V.K.B. Kota, Phys. At. Nucl. **74**, 971 (2011).

[16] P. C. Srivastava and I. Mehrotra, Int. J. Mod. Phys. E **21**, 1250007 (2012).

[17] P. C. Srivastava, Mod. Phys. Lett. A **27**, 1250061 (2012).

[18] P. C. Srivastava, J. Phys. G : Nucl. Part. Phys. **39**, 015102 (2012).

[19] T. Trivedi, P. C. Srivastava, D. Negi and I. Mehrotra, Int. J. Mod. Phys. E **21**, 1250049 (2012).

[20] L. C´aceres *et al.*, Phys. Rev. C **79**, 011301(R) (2009).

[21] K. Sieja *et al.*, Phys. Rev. C **79**, 064310 (2009)

[22] J. Shergur *et al.*, Phys. Rev. C **71**, 064321 (2005).

[23] J. Shergur *et al.*, Phys. Rev. C **72**, 024305 (2005).

[24] M. P. Kartamyshev, T. Engeland, M. Hjorth-Jensen, and E. Osnes, Phys. Rev. C **76**, 024313(2007).

[25] J. Shergur *et al.*, Phys. Rev. C **65**, 034313 (2002).

[26] B. A. Brown, N. J. Stone, J. R. Stone, I. S. Towner, and M. Hjorth-Jensen, Phys. Rev. C **71**, 044317 (2005).

[27]R. Machleidt, Adv. Nucl. Phys. 19, 189 (1989).

[28] R. Machleidt, K. Holinde, and Ch. Elster, Phys. Rep. **149**, 1(1987).

[29] R. Machleidt, Phys. Rev. C **63**, 024001 (2001).

[30] R. Machleidt, K. Holinde, and Ch. Elster, Phys. Rep. **149**, 1 (1987).

[31] L. Coraggio, A. Covello, A. Gargano, N. Itaco, and T.T.S. Kuo, Prog. in Part and Nucl. Phys. **62**, 135 (2009).

[32] J. Dobaczewski, W. Nazarewicz, T. R. Werner, J. F. Berger, C. R. Chinn, and J. Decharg´e, Phys. Rev. C **53**, 2809 (1996).

[33] E. A. Henry, W. L. Talbert, Jr., and J. R. McConnell, Phys. Rev. C **7**, 222 (1973).

[34] J. Fujita and M. Miyazawa, Prog. Theor. Phys. **17**, 360 (1957).

[35] O. Sorlin and M.-G. Porquet, Prog. in Part and Nucl. Phys. **61**, 602 (2008).

[36] T. Otsuka, T. Suzuki, J. D. Holt, A. Schwenk, and Y. Akaishi, Phys. Rev. Lett. **105**, 032501 (2010).

[37] J. D. Holt, T. Otsuka, A. Schwenk and T. Suzuki J. Phys. G : Nucl. Part. Phys. **39**, 085111 (2012).

[38] G. Hagen, T. Papenbrock, D. J. Dean, A. Schwenk, A. Nogga,M.Włoch, and P. Piecuch Phys. Rev. C **76**, 034302 (2007).

[39] P. Federman and S. Pittel Phys. Lett. B **69**, 385 (1977).

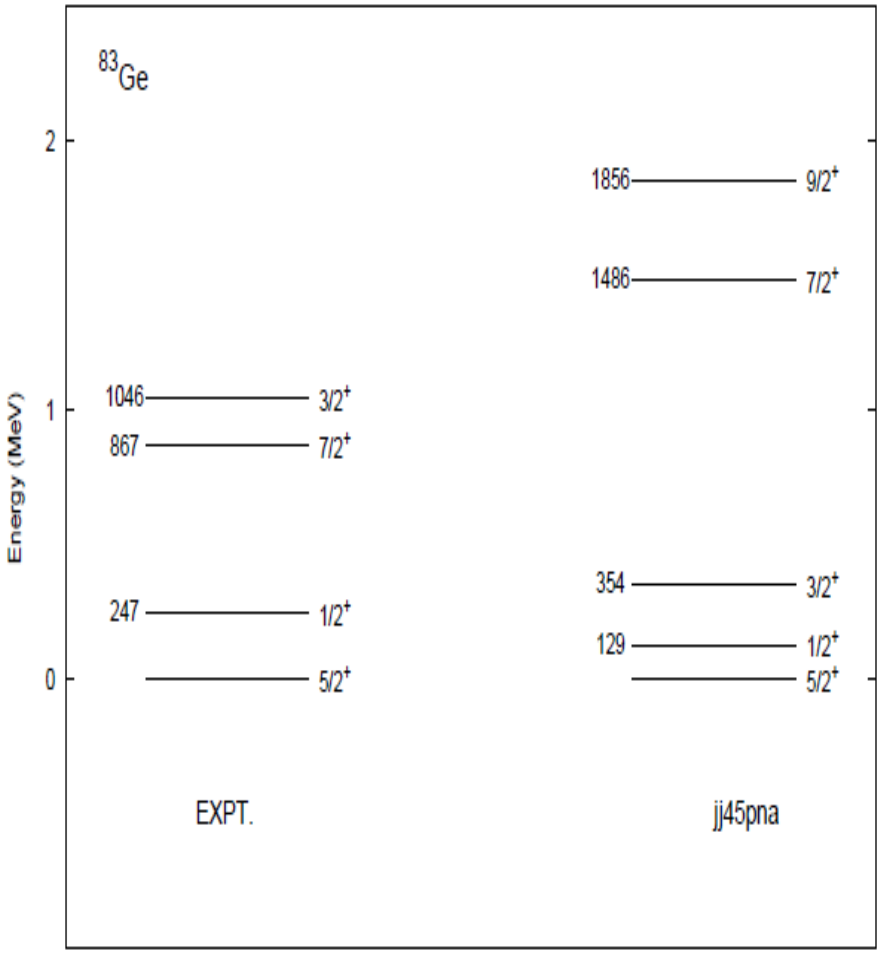

Figure 4.3: Calculated and experimental spectra for ^{83}Ge.

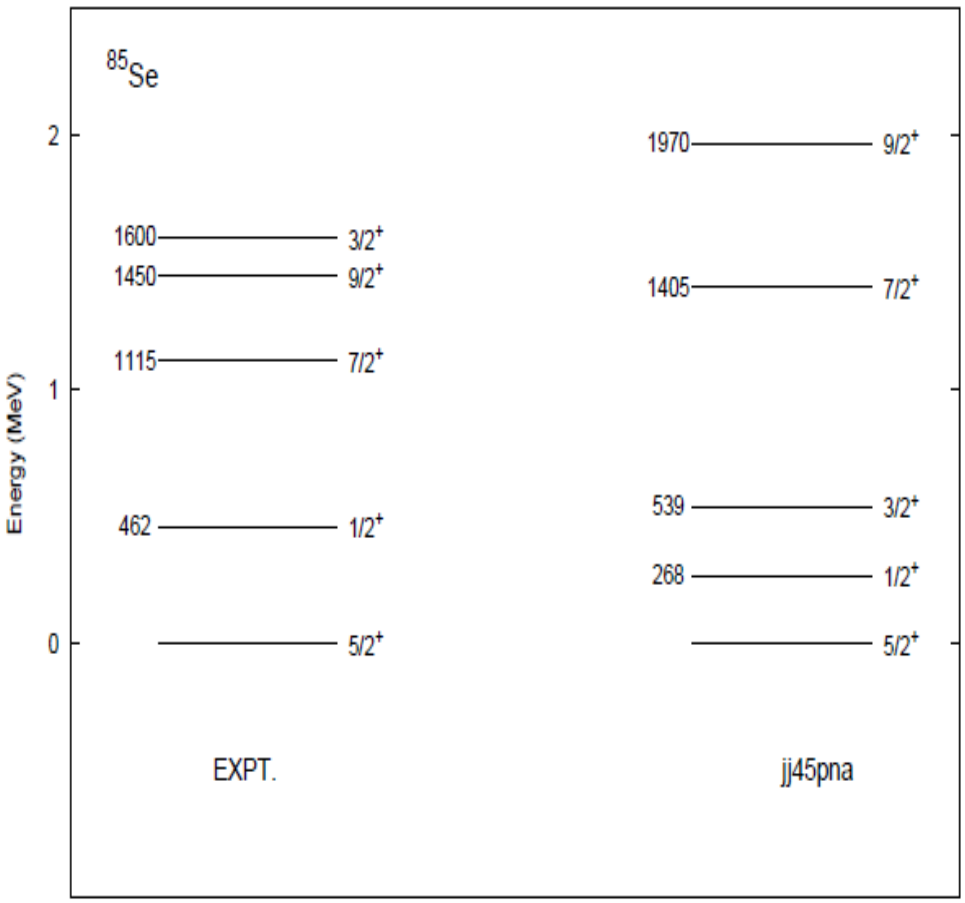

Figure 4.4: Calculated and experimental spectra for ^{85}Se.

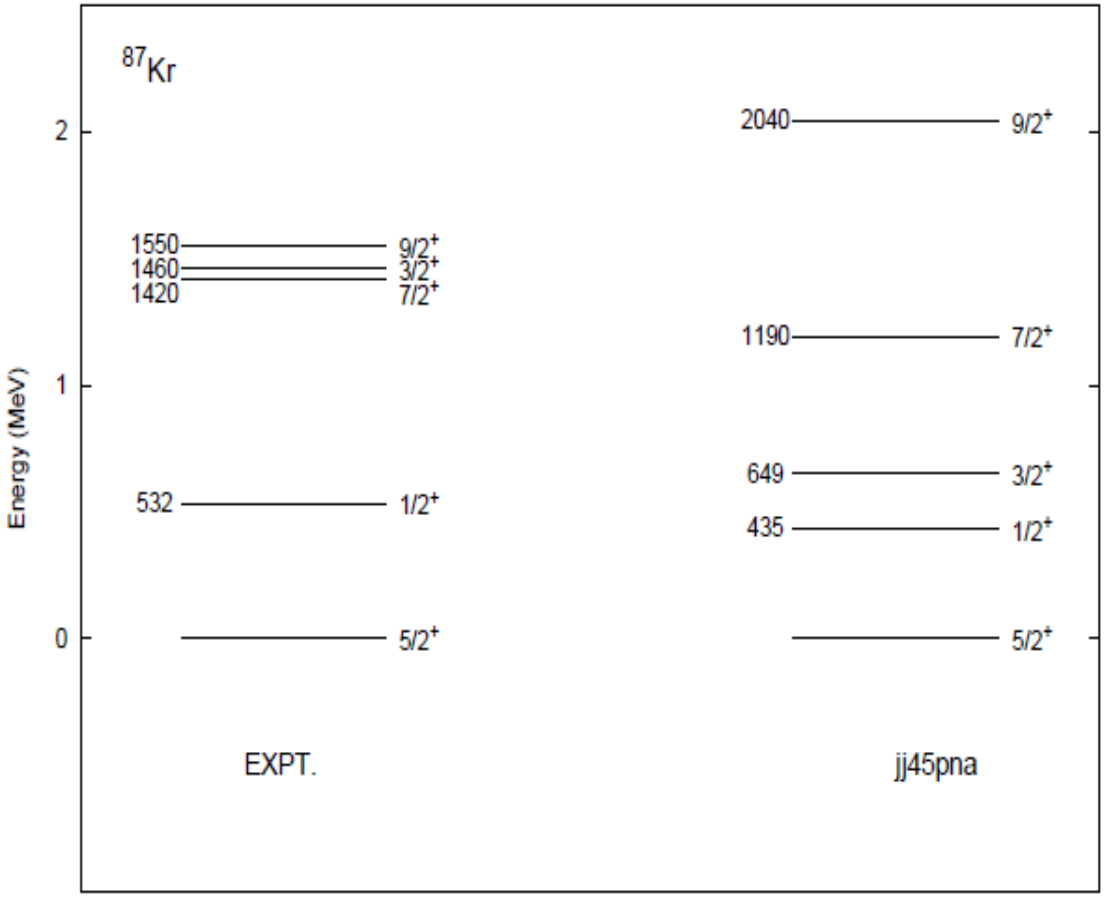

Figure 4.5: Calculated and experimental spectra for ^{87}Kr.

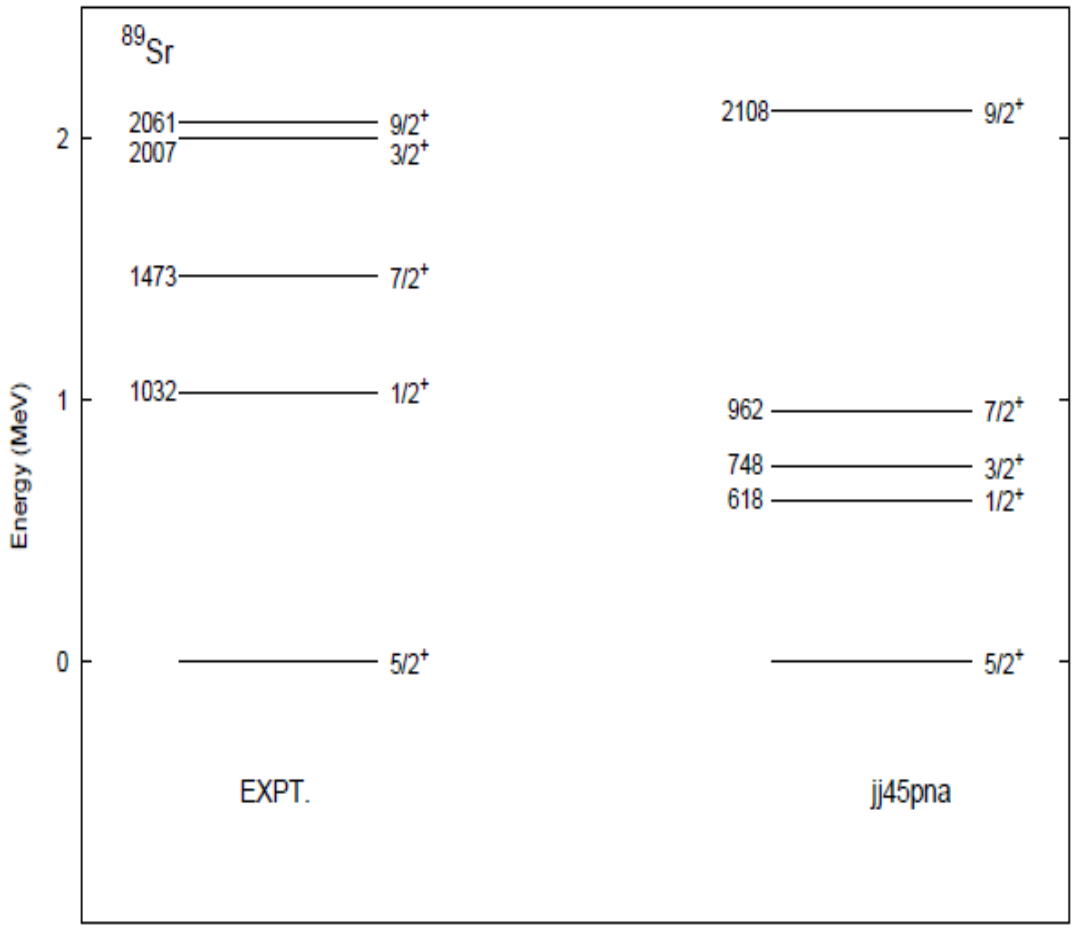

Figure 4.6: Calculated and experimental spectra for ^{89}Sr.

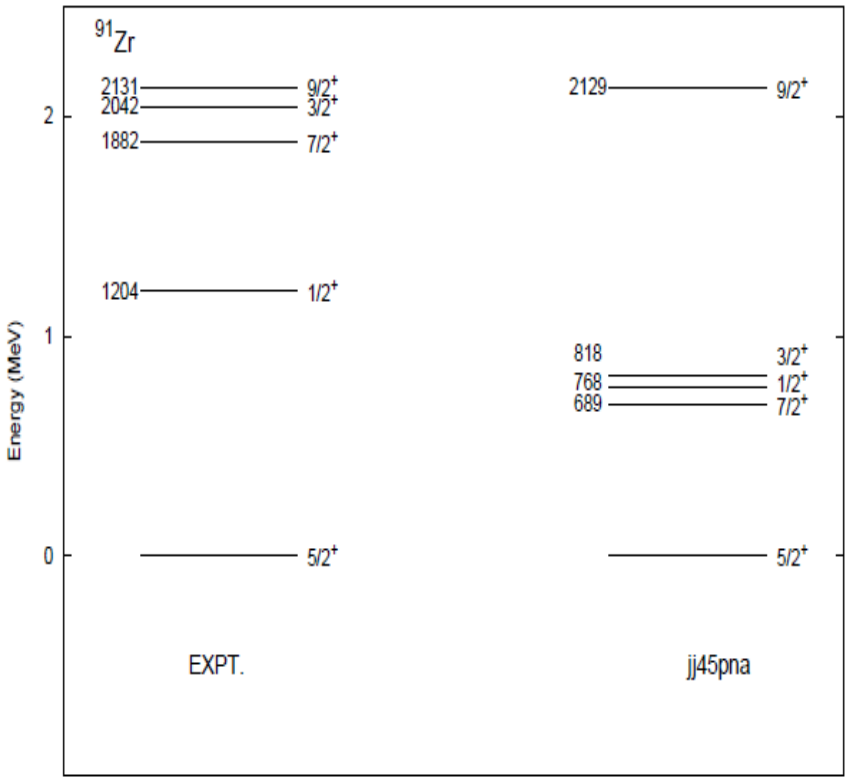

Figure 4.7: Calculated and experimental spectra for ^{91}Zr.

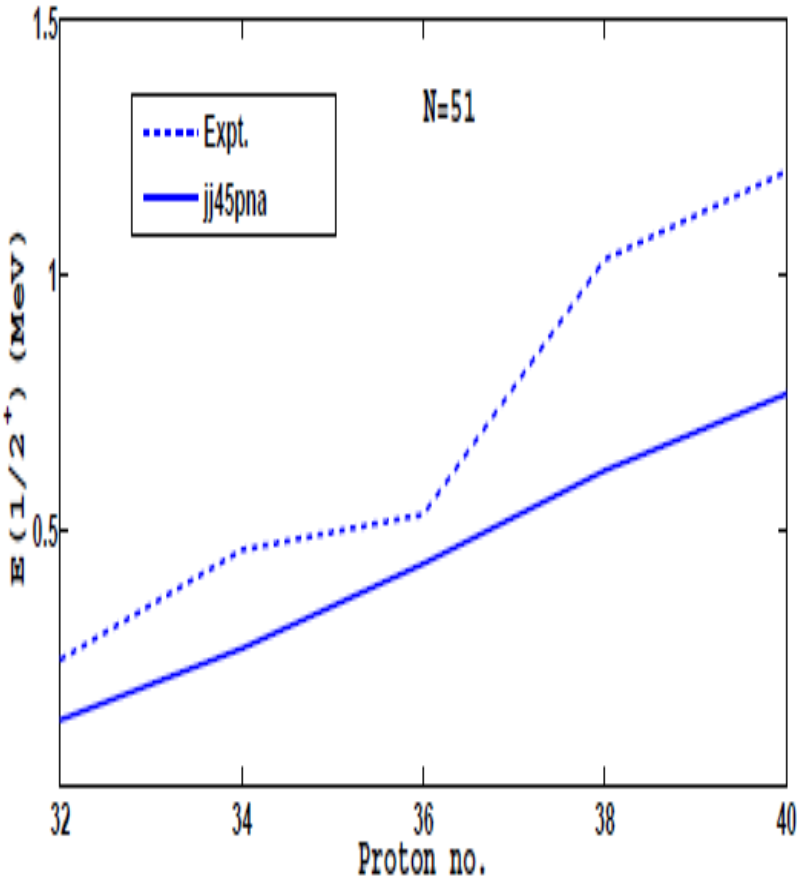

Figure 4.8 : Variation of E($1/2^{+}$) with proton no.

Chapter 5

Shell Model Study of Ca Isotopes

5.1 Introduction

One of the most important and challenging frontiers of nuclear structure physics is the study of nuclei at the limit of stability, especially neutron-rich nuclei with weakly bound neutrons. A topic of particular interest is the evolution of the shell structure in those nuclei. That is, the magic number may change dramatically depending on the N/Z ratio when we move towards the particle drip lines [1]. Such study is important not only due to the expected variation in properties of nuclei and the formation of island of inversion but also for the understanding of nuclear astrophysics as well as the nucleon-nucleon interaction. The exotic regions of the chart of nuclides have been expanded during the last few years with discovery of a large number of exotic nuclei of which one is Ca isotopic chain. The Ca isotopic chain spans over about 22 hitherto discovered isotopes, with the well known N=20 and N=28 the major shell closure [1]. As the size of Z=20 gap remains large and almost constant along the whole Ca isotopic chain, core excitation of the Ca isotopes should remain relatively weak at low excitation energy. This isotopic chain is therefore an ideal test bench for exploring the possibility of subshell closures at neutron numbers other than 20, as their existence would be decoupled from the proton core excitations. This assertion of a weak core excitation is corroborated by the behavior of the 2^+ state and the $B(E2;2^+\rightarrow 0^+)$ values in Ca isotopic chain. As ^{40}Ca core is hardly polarized by adding neutron, the neutron single particle energies in

the Ca and neighboring isotopes serve as references to the constraint effective nuclear interaction used for the shell model or mean field calculation.

Heavy-mass calcium isotopes (N > 28) have recently been the subject of a renewed experimental and theoretical attention, since they lie far from the stability valley, thus allowing to explore the evolution of the shell structure when approaching the neutron drip line. This has resulted in a large number of experiments in this region [2-11] aiming to study the evolution of the single particle (SP) orbitals. An 879.9 keV γ -ray transition has been identified following the β decay of 58V and assigned as the $2^+ \rightarrow 0^+$ transition in $^{58}Cr_{34}$ by Prisciandaro et al. [12]. In this experiment a peak in the energies of the first excited 2^+ states for the even–even chromium isotopes has been observed at $^{56}Cr_{32}$, providing empirical evidence for a significant subshell gap at $N = 32$. Experimental evidence for the subshell closure at N=32 also has been observed in the ^{52}Ca nucleus through the observation of the first 2^+ state at 2.52 MeV. This state was populated through the β-decay of ^{52}K at the CERN/ISOLDE facility [13]. On the theoretical side calculations performed by Honma et. al. for fp shell nuclei (Ca, Ti, Cr, Fe, and Ni isotopic chains) using GXPF1 interaction have predicted subshell closure at both N=32 and N=34 [14] in all the above isotopes. But a modified version of the GXPF1 interaction, dubbed as GXPF1A, shell closure is predicted only at N= 34 [15]. Theoretical calculation with the FPD6 interaction [16] and also the spherical Hartree-

Fock calculations with the semi-realistic NN interactions [17] give the shell closer at N = 32 with Ca and Sc isotopes.

In the work of Crawford [18] the low-energy level structures of the neutron-rich ^{53,54,56}Sc isotopes were investigated and compared with advanced shell-model calculations using the GXPF1[14], GXPF1A[15] and KB3G[19] effective interactions and the results confirm the *N*=32 subshell closure, but suggest a compression of the ν2 $p_{1/2}$-ν1$f_{5/2}$ spacing ,which may preclude formation of a *N*=34 subshell closure in the Ca isotopes.

We have performed shell model calculation for even mass Ca isotopes up to N=38 neutrons in the frame work of Shell Model for yrast states. The calculations have been carried out with three different interactions GXFP1A[15], KB3G[19], and FPD6N[20] in full fp shell ($f_{7/2}$ $P_{3/2}$ $P_{1/2}$ $f_{5/2}$) for neutrons above the ^{40}Ca core using Nushell code [21]. The first two interactions are modified versions of the Kuo and Brown reaction matrix elements[22] whereas the GXPF1A is based on Bonn C interaction [23]. All these interactions are based on the experimental energy data mainly on stable nuclei. Some of these interactions can predict the properties of light pf shell nuclei but have limited applicability towards the end of pf shell. Thus it is a challenging task to apply these interactions to describe the structure of unstable nuclei. The aim of the present work is to study the evolution of shell closure along the neutron rich Ca isotopic chain .

The paper is organized as follows: section 2 gives detail of calculations. Results and discussion are given in section 3 and finally in section 4 conclusions are given.

5.2 Detail of Calculations

5.2.1 Choice of Model Space

Shell model calculations have been performed with different interactions for even mass neutron-rich Ca isotopes in mass region A= 42 - 58 treating ^{40}Ca as a core. The configuration space is taken as full fp shell which is made up of all Pauli allowed combinations of valence particles in the $0f_{7/2}$, $1p_{3/2}$, $0f_{5/2}$ and $1p_{1/2}$ orbitals for neutrons. The corresponding single particle energies for different interaction for the model space $0f_{7/2}$, $1p_{3/2}$, $0f_{5/2}$ and $1p_{1/2}$ are shown in fig.1. The single particle energy for FPD6N is adopted to suit the heavier pf shell nuclei and exhibits different with large difference between $f_{5/2}$ and $p_{1/2}$.

5.2.2 Effective Interaction

The effective interaction can in principle be derived from the free NN interaction. Several such microscopic interactions have been proposed for the pf shell. Most successful of these are the KB3 series based on Kuo-Brown reaction matrix element [22] and GXPF series based on Bonn-C

interaction [23]. In the present work we have performed calculations with three different interactions GXFP1A[15], KB3G[19], and FPD6N[20].

GXPF1A is modified version of GXPF1 which is based on Bonn-C potential. Starting from microscopic effective interaction, it has been derived by Hjorth-Jensen based on renormalized G matrix theory[24]. It is obtained by modifying 70 well-determined linear combinations of 4 single-particle energies and 195 two-body matrix elements by iterative fitting calculations to about 700 experimental energy data out of 87 nuclei from A=47 to A=66. Five matrix elements have been changed in GXFP1A to overcome some shortcoming of the GXPF1 interaction for the region of the neutron rich Sc, Ti, and Ca isotopes [15]. GXPF1 interactions are successful in predicting the experimental data of wide region of pf shell nuclei but have limited applicability near the end of pf shell.

The KB3G is the latest version of the family of KB3 interactions [25]. KB3 is the monopole modification of the Kuo-Brown reaction matrix elements. These interactions, obtained from Hamada-Johnston realistic potential[26], consist of two part: the bare reaction matrix elements and the renormalization due to core polarization effect. KB3G is obtained from KB3 by introducing mass dependence and refining its monopole changes to adjust the shell gap at N=Z=20 and its surroundings [27]. Both these interactions (KB3G & KB3) are quite successful in the lower pf shell($A \leq 52$) [28,29]. The core polarizations are evaluated for two cases; for ^{40}Ca core and then for a ^{48}Ca core.

FPD6N interaction has been obtained by adjusting the single particle energy for ^{56}Ni. This interaction has been derived for nuclei in the low lying states of the 0f1p shell by fitting semi-empirical potential form and two-body matrix elements to 61 binding energy and excitation energy data in the mass range 41 to 49. The intruder states have been excluded from the selected data set. Starting from a slightly modified Kuo-Brown G-Matrix, and proceeding from the successive interactions involving recalculation of the transition densities and determination of new parameter sets by fitting to a selection of 61 experimental binding and excitation energies, good convergence of the interaction has been obtained. It successfully describes heavier pf shell nuclei , such as ^{56}Ni and ^{64}Ge . There are however some defects, for instance in the single particle aspect of ^{57}Ni.

5.3 Results and Discussion

We have performed shell model calculations for even-even Ca isotopes from neutron number N=22 to N=38 with three different interactions. The results obtained for $^{42-52}$Ca are shown in figures 1-6 along with experimental data whatever available. The results for $^{54-58}$Ca are shown in figures 7-9. It is seen that KB3G and GXPF1A give almost similar results for first three low lying states in lighter Ca isotopes upto ^{50}Ca. Departures are observed in first 6^+ and 8^+ states which have dominant configurations. For more neutron rich Ca isotopes the two interactions gives significantly different results when cross shell excitation excitations across N=28 shell come into play.

This is mainly due to large difference in their single particle energy structure.

The first 2^+ energy level in nuclei is a good systematic measure of the structure.The most two important signature of shell\subshell closure in even-even nuclei are (i) high excitation energy of the fisrt 2^+ state and (ii) small value of the B(E2;$2^+ \rightarrow 0^+$) transition rate indicating the single particle structure of the state. In fig. 11 variation of E(2^+) is shown with neutron number for all the interactions along with the experimental data. In fig. 11 B(E2;$2^+ \rightarrow 0^+$) transition rate and the experimental data, which is known upto N=30, are shown in table 5.1.

Table 5.1: Value of B(E2) for $^{50\text{-}56}$Ca

Interaction / Nucleus	KB3G	GXFP1A	FPD6N
^{50}Ca	6.008	0.411	0.608
^{52}Ca	4.998	0.339	0.485
^{54}Ca	5.399	0.249	0.316
^{56}Ca	5.850	0.334	0.390

The calculated 2^+ states are in good agreement with corresponding experimental levels in all the cases for $^{42\text{-}46}$Ca and $^{50\text{-}52}$Ca isotopes while for ^{50}Ca 2^+ state is compressed with FPD6N interaction as shown in figure 8. The calculated 4^+ and 6^+ levels are also somewhat compressed compared to their experimental counterparts for KB3G and GXFP1A while for FPD6N

these states are shifted upward for $^{42-46}$Ca. In the case of ^{48}Ca results are just opposite. 4^+ state is reproduced very well for ^{50}Ca with all interactions. For ^{52}Ca only 2^+ level is known experimentally . A large gap with KB3G interaction between 0^+ and 2^+ state shows a subshell closure at N=32 which is further supported by corresponding low value of B(E2;$2^+ \rightarrow 0^+$) value at this neutron number. There is no indication of any shell closure at N=32 with other interactions. Subshell closure at N=34 is predicted for GXFP1A and FPD6N with large gap between 0^+ and 2^+ state and corresponding low values of B(E2;$2^+ \rightarrow 0^+$) as shown in figure11-12. B(E2;$2^+ \rightarrow 0^+$) values for neighboring isotopes are also shown in table 1. High energy of 4^+ state in ^{52}Ca also underlines the validity of the N=32 subshell closure with KB3G and at N=34 in ^{54}Ca with other interactions [30]. There is no indication of shell closure at any other neutron numbers with all interactions. 28 is a well established magic number and ^{48}Ca is known to be a magic nucleus. The theoretical results predict the next magic nucleus as ^{52}Ca in the Ca isotonic chain with KB3G while ^{54}Ca with other interactions. The most direct evidence for large energy separation between the $f_{5/2}$ and $p_{3/2}$ neutron orbitals, which results in the N=32 closure, comes from the excitation energies of corresponding states observed in the one neutron ^{49}Ca isotope [31]. The most dominant configurations in the wave functions of the ground state and first excited state for Ca isotopes are given in table 5.2.

5.4 Conclusion

In this work we have performed the shell model calculation using Nushell code for neutron rich even mass Ca isotopes covering N = 22 to N=38. In our calculation ^{40}Ca is chosen as core and valence space comprises of full fp shell $0f_{7/2}$, $1p_{3/2}$, $0f_{5/2}$ and $1p_{1/2}$ for neutrons. Calculations have been carried out with three different interactions, viz. GXFP1A, KB3G and FPD6N which are specially developed for fp shell and suitably modified for monopole correction. We have studied the shell structure along the Ca isotopic chain and have observed the subshell closure existence at N=32 with KB3G while GXFP1A and FPD6N interactions predict the subshell closure at N=34. Shell closure at any other neutron number has not been observed. KB3G interaction best suited for lighter pf shell nuclei. FPD6N is based on Kuo-Brown matrix element interaction but the single particle energy are matched with ^{56}Ni. GXPF1A interaction is modified to reproduce the properties of pf shell nuclei heavier region. From this point of view the results obtained with GXPF1A interaction and to some extent with FPD6N interaction for heavier Ca isotopes should be more reliable. But there is experimental evidence [13,14] for subshell closure at N=32 whereas still now no such evidence has been observed for N=34 subshell closure. Further $B(E2;2^+ \rightarrow 0^+)$ transition rate for GXPF1A and FPD6N interactions are much smaller than corresponding experimental values. But shell model calculations suggest that N = 34 may be a magic number in Ca isotopes, depending on the effective interactions used [32]. This is again clearly a

region where more experimental data are needed. The availability of experimental data in nuclei with large N/Z ratios may provide a ground to constrain the properties of different components of the interaction, such as the isovector channel of the spin-orbit interaction, which are not well defined but may be responsible for the shell evolution.

References:

[1] O. Sorlin, M.-G. Porquet, Prog. Part. Nucl. Phys. 61, 602(2008).

[2] Liddick S N et al 2004 Phys. Rev. Lett. 92 072502

[3] Liddick S N et al 2004 Phys. Rev. C 70 064303

[4] Dinca D -C et al 2005 Phys. Rev. C 71 041302(R)

[5] Gade A et al 2006 Phys. Rev. C 74 021302(R)

[6] Perrot F et al 2006 Phys. Rev. C 74 014313

[7] Rejmund M et. al.,(2007)Phys. Rev. C 76 021304(R)

[8] Mantica P F et al 2008 Phys. Rev. C 77 014313

[9] Fornal B et al 2008 Phys. Rev. C 77 014304

10] Maierbeck P et al 2009 Phys. Lett. B 675 22

[11] Bhattacharyya S et al 2009 Phys. Rev. Lett. 101 032501

[12] J.I. Prisciandaro et. al., Phys. Lett. B 528 58 (2002); J.I. Prisciandaro et al.,

Phys. Lett. B 510, 17 (2001).

[13] A. Huck et. al., Phys. Rev. C 31 (1985) 2226

[14] M. Honma et. al., Phys. Rev. C 65 (2002) 061301.

[15] Honma M, Otsuka T, Brown B A and Mizusaki T 2005 Eur. Phys. J. A 25, s01 499

[16] Richter W A, der Merwe M G V, Julies R E and Brown B A 1991 Nucl. Phys. A 523, 325

[17] H. Nakada, arXiv:1003.572v2 [nucl-ph],2010.

[18]Crawford, Heather Lynn, Ph.D., MSU, 2010, 164 pages; 3435145

[19] A. Poves et. al. Nucl. Phys. A 694 (2001) 157-198.

[20] Richter et al., Nucl. Phys. A523, 325 (1991)

[21] Nushell@MSU, B. A. Brown and W. D. M. Rae (unpublished).

[22] Kuo and Brown, Nucl. Phys. A 114 (1968) 241

[23] M. F. Jiang et. al., Phys. Rev. C Vol 46, No. 3, (1992)

[24] M. Hjorth-Jensen, T. T. S. Kuo and E. Osnes, Phys. Rep. 261, 125 (1995).

[25] A. Poves and A. P. Zuker, Phys. Rep. 70 (1981) 235

[26] T. Hamada and I. D. Johnston, Nucl. Phys. 34 (1962) 382.

[27] A. Poves et al., Nucl. Phys. A 403 (2001), 213.

[28] D. Rudolph, Phys. Rev. Lett. 82 (1999) 3763.

[29] P. von Neumann-Cosel, A. Poves, J. Retamosa, A. Richter, Phys. Lett. B 443 (1998) 1

[30] Nucl. Data Sheets 76, 2 (1995).

[31] E. Caurier et. al., Phys. Rev. C 50 (1994) 225.

[32] J.D. Holt, T. Otsuka, A. Schwenk, and T. Suzuki, J. Phys. G 39, 085111 (2012)..

Table 5.2: Main configurations in the wave functions of the ground state and first excited state for Ca isotopes.

Interaction	Nuclei	J^{π}	Neutron Wave Function				Probability
KB3G	^{32}Ca	0^+	$(f_{7/2})^8$	$(p_{3/2})^4$	$(f_{5/2})^0$	$(p_{1/2})^0$	80.833
		2^+	$(f_{7/2})^8$	$(p_{3/2})^3$	$(f_{5/2})^0$	$(p_{1/2})^1$	86.670
	^{34}Ca	0^+	$(f_{7/2})^8$	$(p_{3/2})^4$	$(f_{5/2})^0$	$(p_{1/2})^2$	77.160
		2^+	$(f_{7/2})^8$	$(p_{3/2})^4$	$(f_{5/2})^1$	$(p_{1/2})^1$	87.376
GXPFIA	^{32}Ca	0^+	$(f_{7/2})^8$	$(p_{3/2})^4$	$(f_{5/2})^0$	$(p_{1/2})^0$	83.113
		2^+	$(f_{7/2})^8$	$(p_{3/2})^3$	$(f_{5/2})^0$	$(p_{1/2})^1$	89.512
	^{34}Ca	0^+	$(f_{7/2})^8$	$(p_{3/2})^4$	$(f_{5/2})^0$	$(p_{1/2})^2$	95.093
		2^+	$(f_{7/2})^8$	$(p_{3/2})^4$	$(f_{5/2})^1$	$(p_{1/2})^1$	94.542
FPD6N	^{32}Ca	0^+	$(f_{7/2})^8$	$(p_{3/2})^4$	$(f_{5/2})^0$	$(p_{1/2})^0$	66.311
		2^+	$(f_{7/2})^8$	$(p_{3/2})^3$	$(f_{5/2})^0$	$(p_{1/2})^1$	77.319
	^{34}Ca	0^+	$(f_{7/2})^8$	$(p_{3/2})^4$	$(f_{5/2})^0$	$(p_{1/2})^2$	85.714
		2^+	$(f_{7/2})^8$	$(p_{3/2})^4$	$(f_{5/2})^1$	$(p_{1/2})^1$	85.365

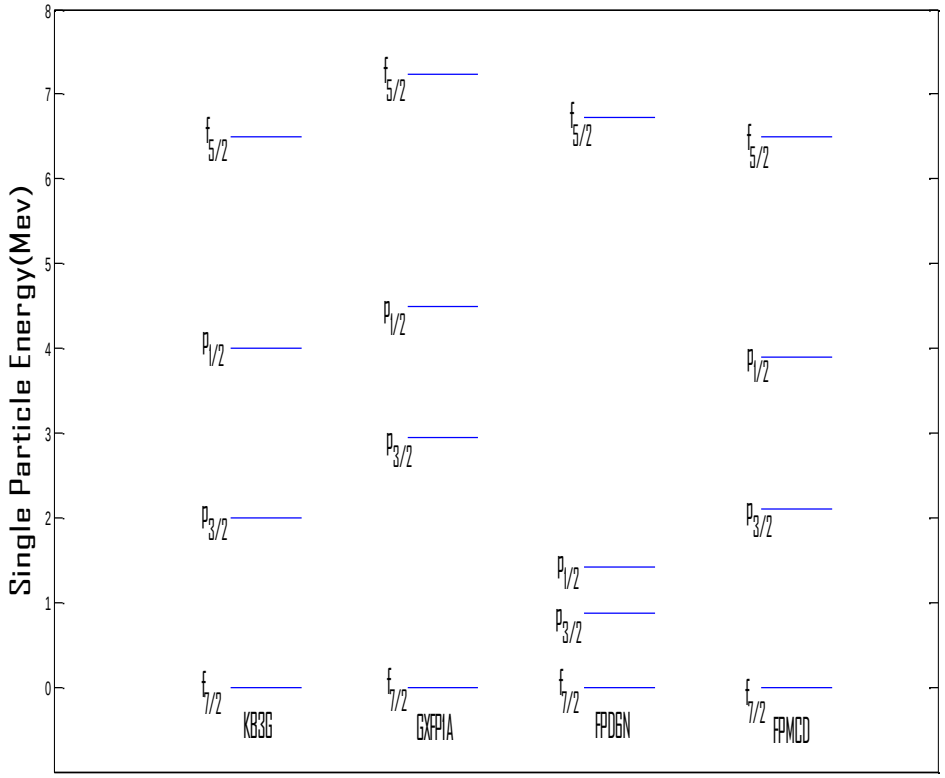

Figure 5.1: Single particle energies of neutron for different interactions

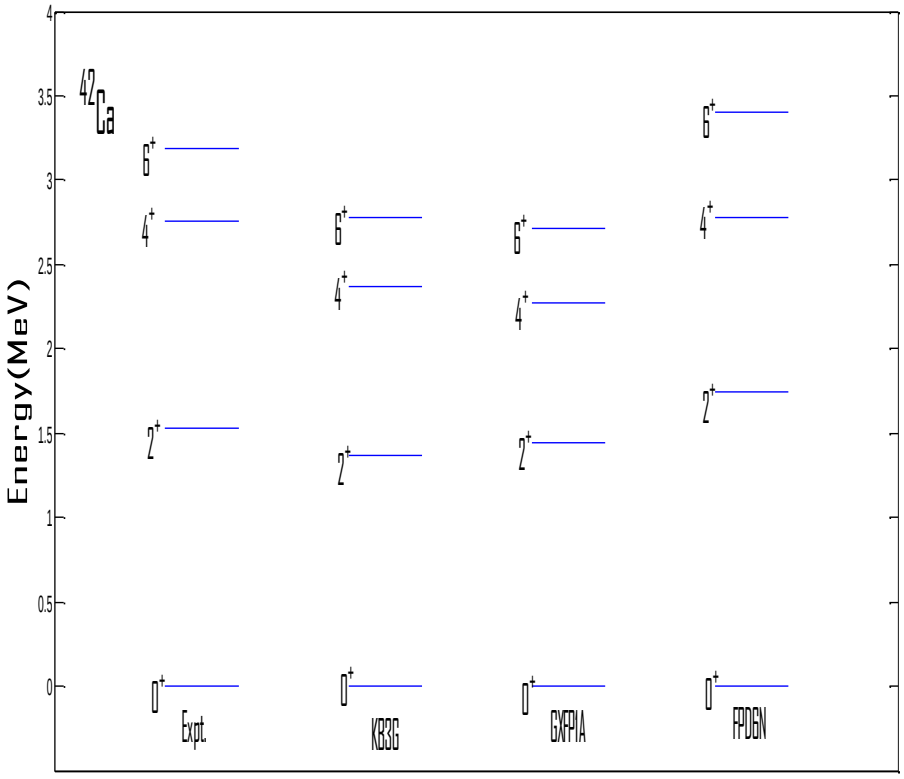

Figure 5.2: Experimental and theoretical values of ^{42}Ca

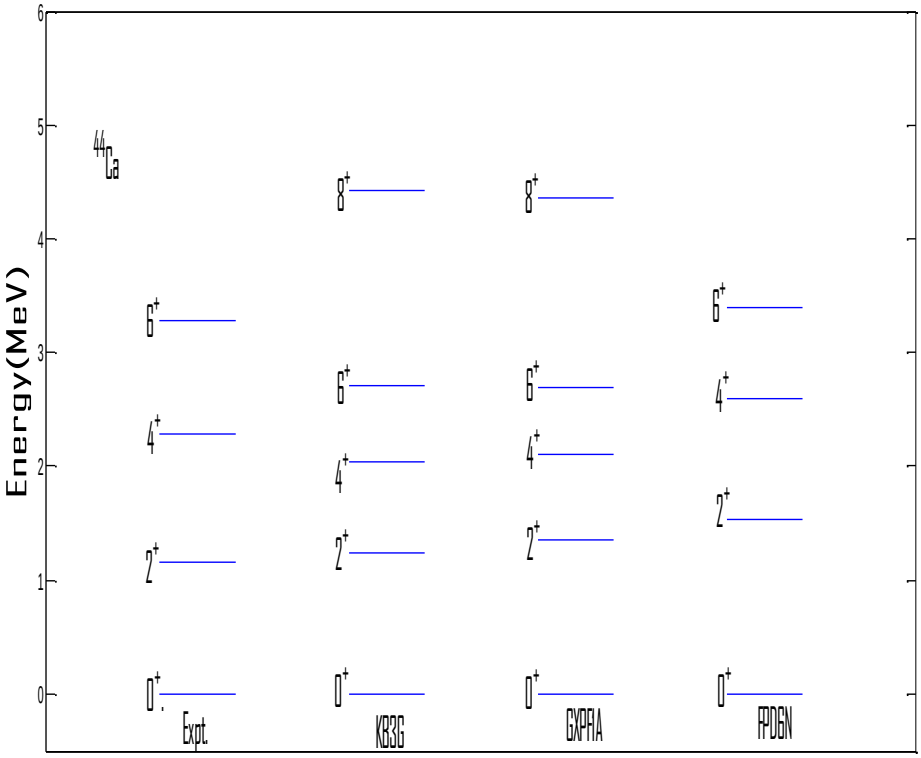

Figure 5.3: Experimental and theoretical values of ^{44}Ca

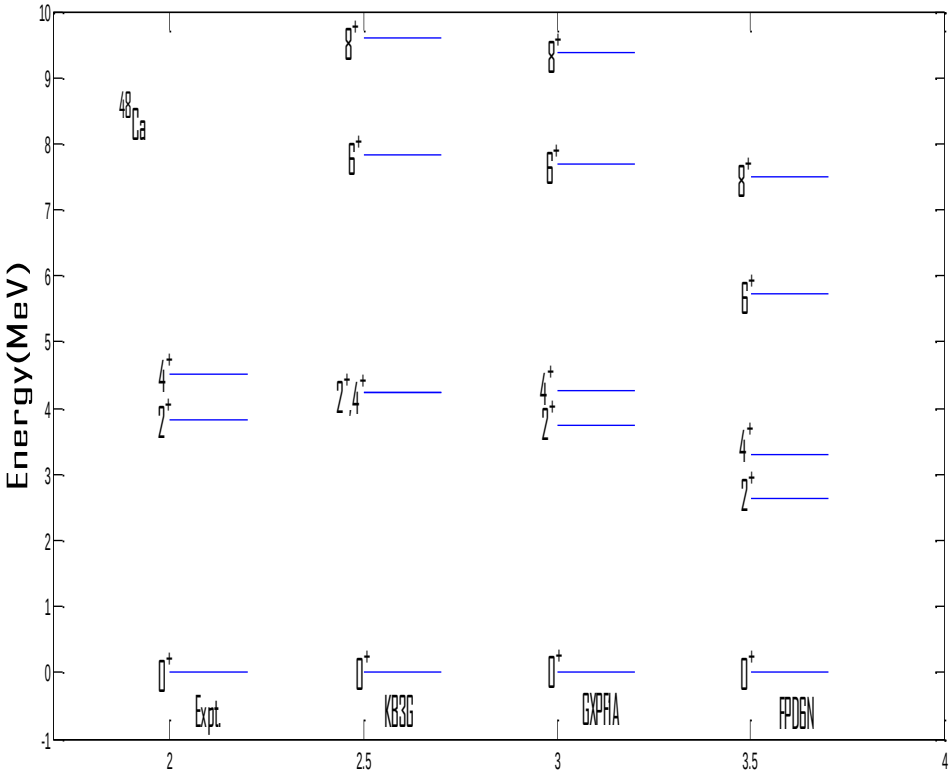

Figure 5.4: Experimental and theoretical values for ^{46}Ca

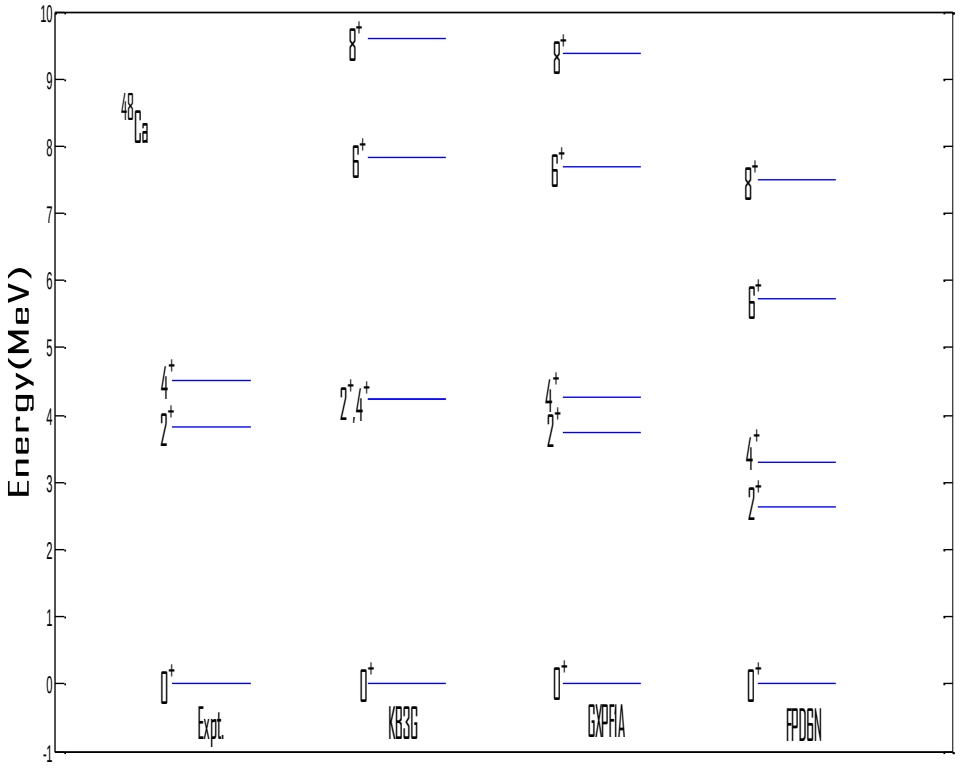

Figure 5.5: Experimental and theoretical values of ^{48}Ca

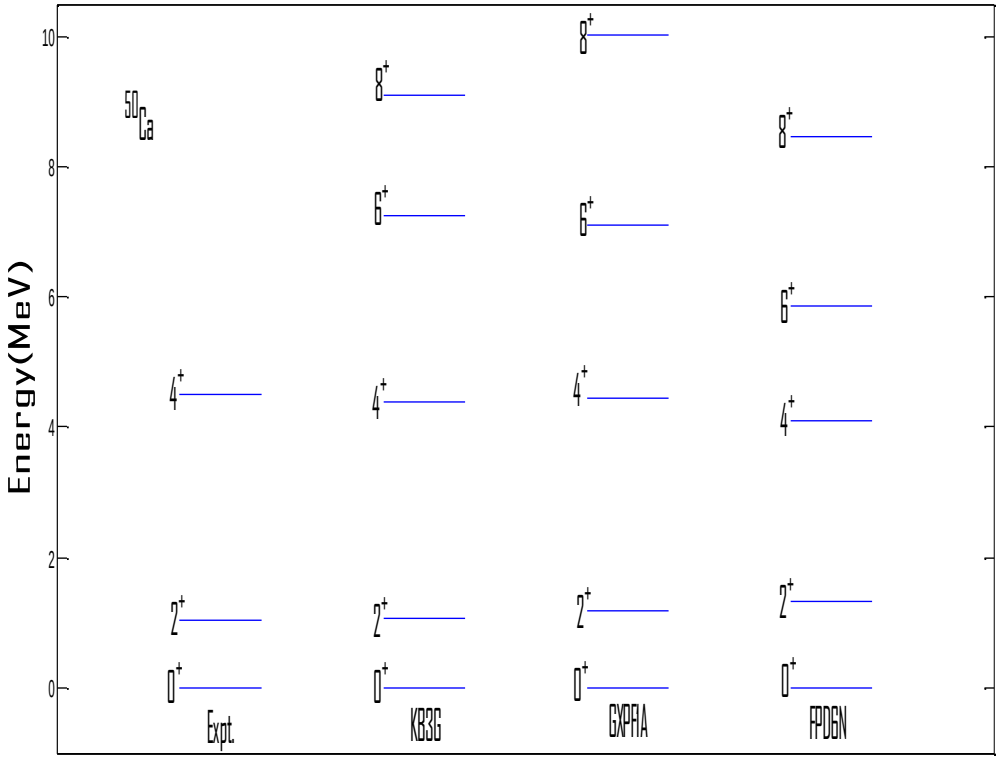

Figure 5.6: Experimental and theoretical values of ^{50}Ca

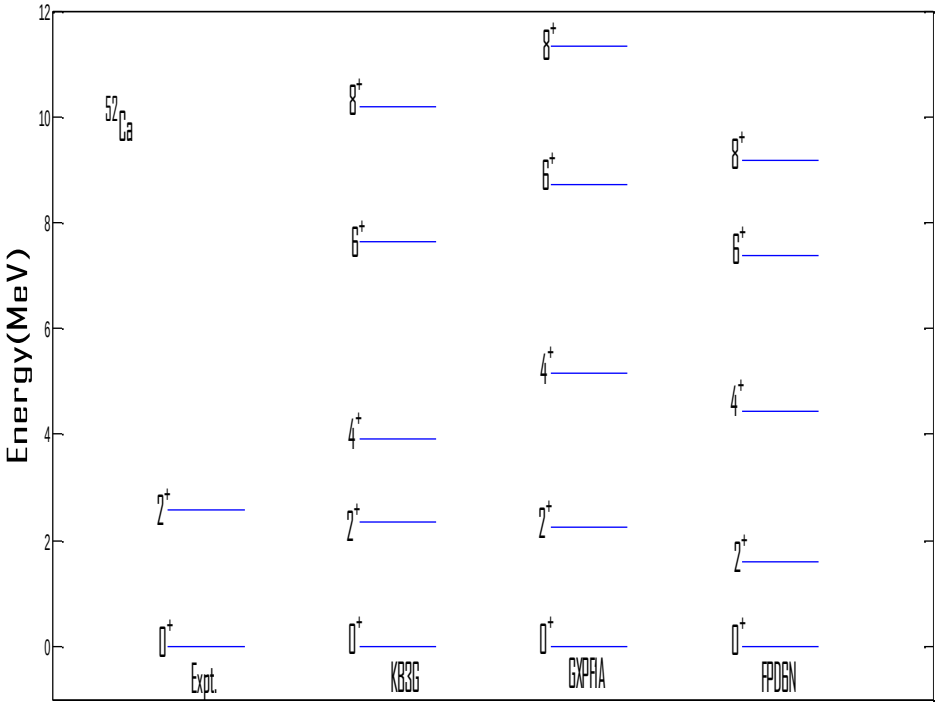

Figure 5.7: Experimental and theoretical values of ^{52}Ca

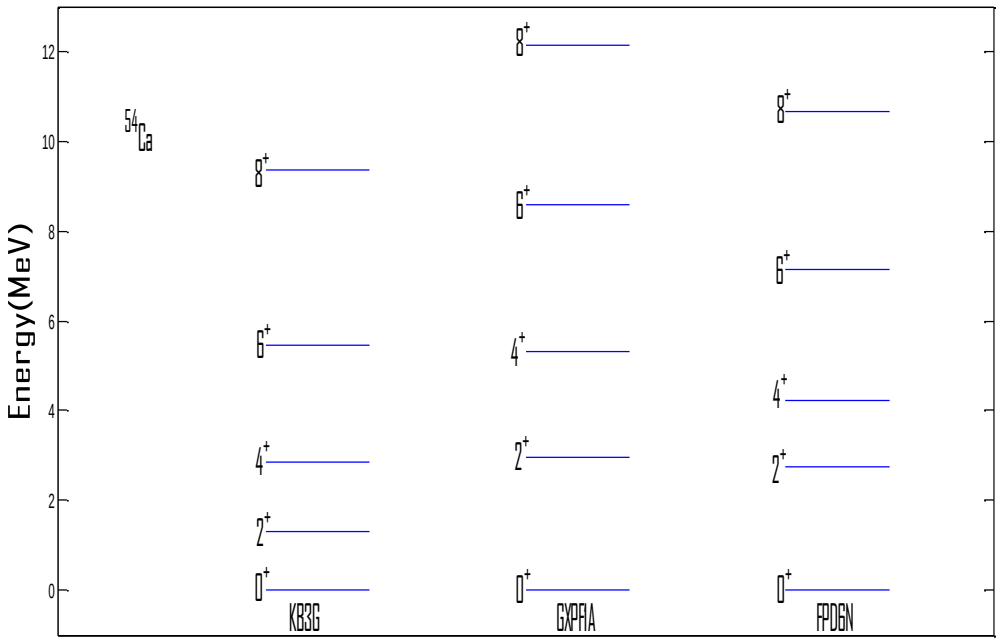

Figure 5.8: Theoretical values of ^{54}Ca

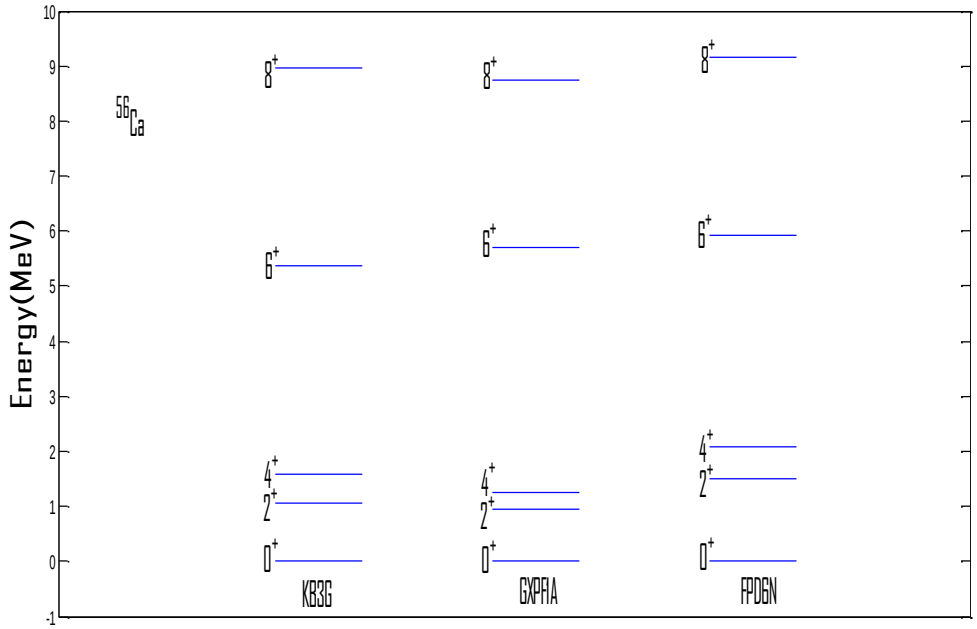

Figure 5.9: Theoretical values of ^{56}Ca

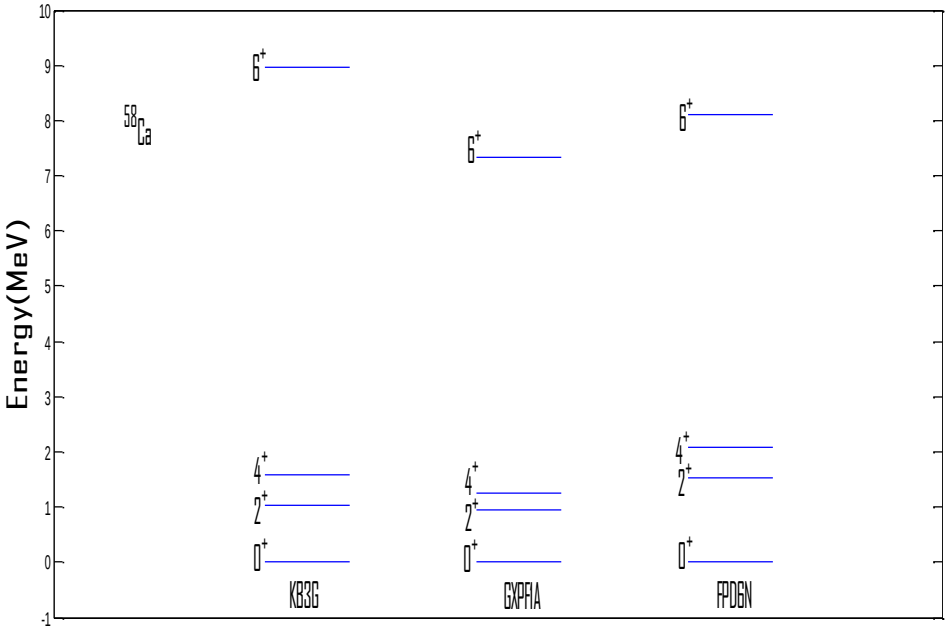

Figure 5.10: Theoretical values of ^{58}Ca

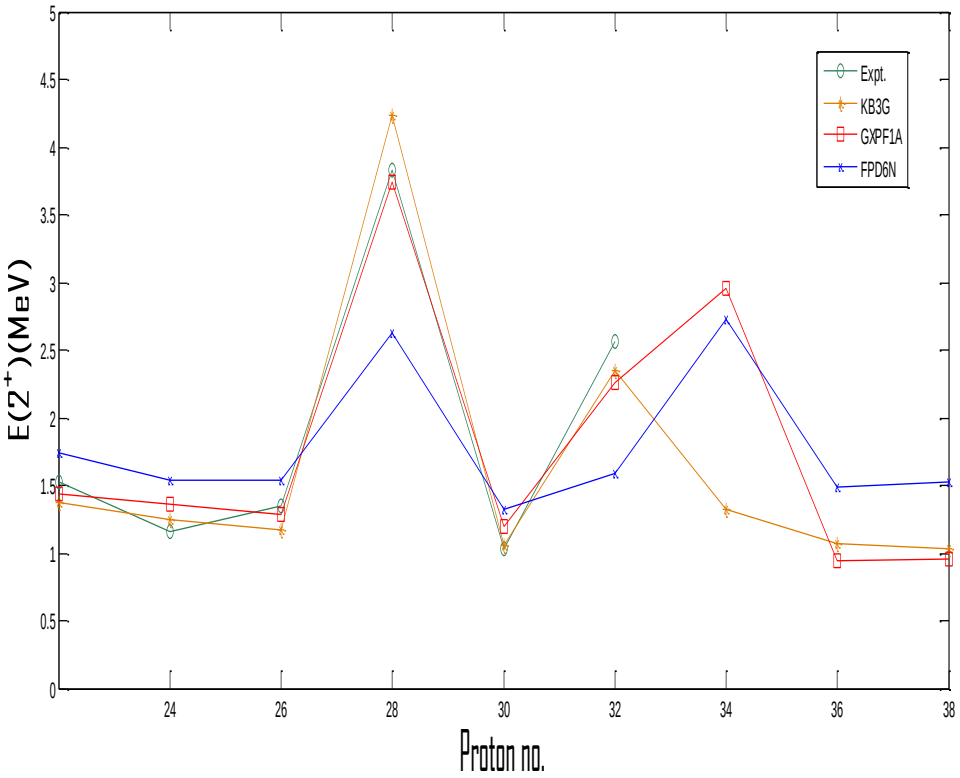

Figure 5.11: Energy of first 2^+ state of Ca isotopes

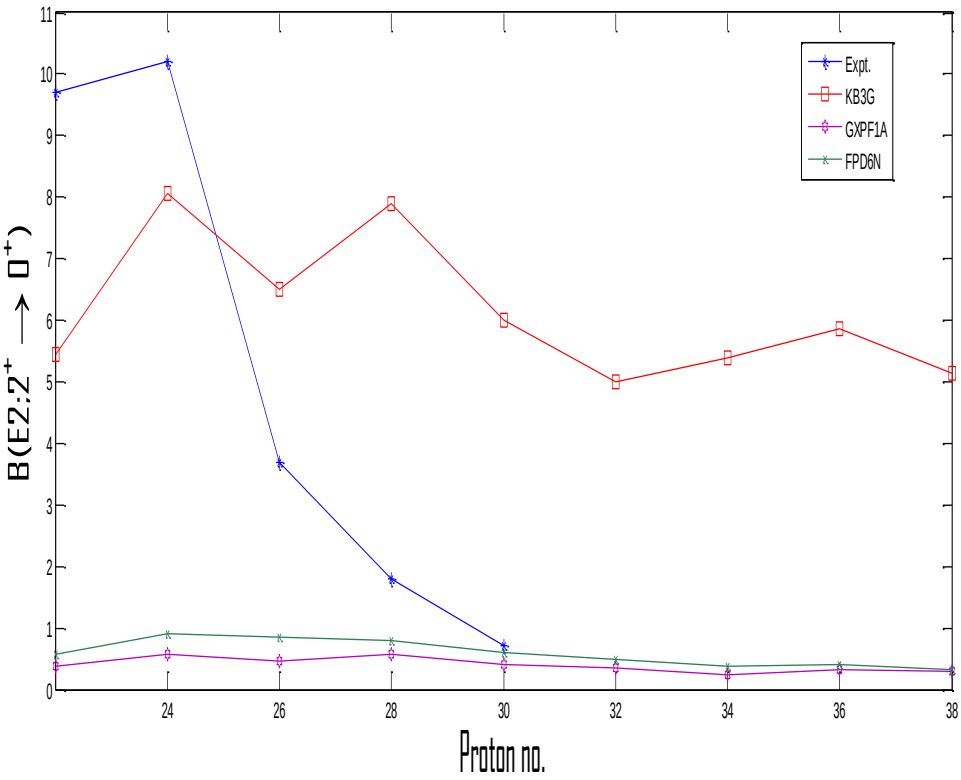

Figure 5.12: B(E2) values of first 2^+ state of Ca isotopes

Chapter 6

A Shell Model Study of N=50 Isotones with $30 \leq Z \leq 46$

6.1 Introduction

Nuclei are mesoscopic systems composed of fermions characterized, as other finite quantum mechanical many body systems, by a shell structure with the presence of gaps in the single particle spectra. The filling of the nucleon orbital up to the shell gaps give rise to the well known magic numbers in nuclei near stability. Nuclei having both nucleons as magic number with few valence nucleons are crucial for the understanding of nuclear structure and ideal for studying the effective nucleon nucleon interaction through comparison with shell model calculations[1]. Consequently the N=50 isotones above the ^{78}Ni have attracted physicists since the first developments of the nuclear shell model. ^{78}Ni also have astrophysicsl importance [2]. In ^{78}Ni the N=50 is situated deep into exotic region and Z=28 is a well established proton gap. So the doubly closed ^{78}Ni with an unusual proton to neutron ratio , lies between two regions: of the light nuclei, where experimental evidence for changing magic numbers going far from stability is well established, and of heavy ones, where no quenching of the known spin-orbit shell closures has been observed. Furthermore, because Z=50 is a jj-coupling closed shell and Z=40 is an LS-coupling closed shell, the active parts of the wave functions of the nuclei with Z from 40 to 50 should be dominated by excitations, within the $1p_{1/2}$ and $0g_{9/2}$ proton orbits which are being filled from Z=40 to 50. ^{78}Ni is therefore an interesting region to study the validity of nuclear shell model in modeling the available experimental nuclear data. The possible way to study experimentally these regions by observing the decay of

short lived neutron-rich nuclei produced in fission to levels of the N=50 isotones above the ^{78}Ni. *N*=50 nuclei have been the subject of a number of theoretical investigations which assumed closed-shell neutrons and active protons in either the $p_{1/2}$ and $g_{9/2}$ or $p_{1/2}$, $g_{9/2}$, $p_{3/2}$, and $f_{5/2}$ shells.

Neutron rich ^{78}Ni and proton rich ^{100}Sn are two doubly magic nucleus leads two different region of the nuclear chart. Since ^{78}Ni is further away from stability on the neutron-rich side and ^{100}Sn is near to the stability on the proton rich side, nuclei between these nuclei have unusual structural changes. The N =50 isotones from ^{82}Ge to ^{96}Pd span two rather distinct regions of shell-model configurations, above ^{90}Zr, the low-lying wave functions tend to be dominated by configurations constructed purely of $0g_{9/2}$ protons, or of $0g_{9/2}$ protons and $1p_{1/2}$ proton holes, while below ^{88}Sr the wave functions presumably are dominated by configurations constructed of mixtures of $0f_{5/2}$, $lp_{3/2}$, and $1p_{1/2}$ protons. Also the shell model orbitals for neutrons in nuclei with Z=28 and N=28-50 are the same as those for protons in nuclei with N=50 and Z=28-50 and the effective NN interaction is most easily studied in the N=50 isotones between these two doubly magic nuclei.

Since N=50 is a well-established shell closure, the low-lying states of the N=50 isotones should involve only proton excitations. They provide the best testing ground for the basic ingredients of shell-model calculations, especially regarding the matrix elements of the two-body effective interaction.

In most of the shell model calculations performed during the last two decades [3-10] study is focused on the isotones up to mass 95 [5] or 96 [4-7, 9, 10]. An extensive theoretical work on N=50 isotones from Z=34-96 have been performed by Sinatkas et. al.[7] with ^{100}Sn core and the effective two-body interaction and

the effective one body transition operators for this model space are derived by introducing second-order corrections to the Sussex matrix elements, while the one-hole energies are deduced by a least-squares fit to the observed levels. Ji and Wildenthal [4,5,6] also have studied the $N = 50$ isotones but only for nuclei ^{82}Ge up to ^{87}Rb. These results are obtained with a new effective Hamiltonian operator, obtained empirically from an iterative fit to experimental energies taken from all experimentally studied (A =82—96) N =50 nuclei. The model space for the calculations consists of active $0f_{5/2}$, $lp_{3/2}$ $lp_{1/2}$, and $0g_{9/2}$ proton orbits relative to a nominal ^{78}Ni core. This space is truncated internally by restricting the number of particles excited from the negative-parity orbits into the $0g_{9/2}$ orbit to be no greater than four. Ghugre *et al.* [8] have investigated both the low-lying and high-spin states in some N=50 isotones in an even larger model space $\pi(f_{5/2}, p_{3/2}, p_{1/2}, g_{9/2})$ and $\nu(g_{9/2}, p_{1/2}, d_{5/2}, d_{3/2}, s_{1/2})$ above the ^{66}Ni core. J. Blomqvist et. al. [3] have shown that it is possible to fit a large number of low lying energy levels in the N=50 isotones from ^{89}Y to ^{96}Pd within a model consisting of proton filling the shell $1g_{9/2}$ and $2p_{1/2}$, and treating the single particle energies and two particle interaction matrix element as free parameter.

Up to the present work the experimental information has been made available on the energy levels of N=50 isotones in the mass region A=80-87, are given in ref.[11].The experimental data for nuclei Mo, Ru and Pd are taken from ref [12] in which M. Gorska et. al. have compared their data to these N=50 nuclei, while for other nuclei data are taken from the site of NNDC[13].

In the present work even and odd mass N=50 isotones between ^{78}Ni and ^{100}Sn namely ^{80}Zn, ^{82}Ge, ^{84}Se, ^{86}Kr, ^{88}Sr, ^{90}Zr, ^{92}Mo, ^{94}Ru, ^{96}Pd and ^{81}Ga, ^{83}As, ^{85}Br, ^{87}Rb, ^{89}Y, ^{91}Nb, ^{93}Tc, ^{95}Rh have been studied. We have performed large scale shell model calculations using Nushell code [14] and ^{78}Ni core. The valence space comprises of $\pi(0f_{5/2}, {}_1p_{3/2}, {}_1p_{1/2}, {}_0g_{9/2})$ for protons. The calculations have been performed with jj44b Hamiltonian[15] which was obtained from a fit to experimental data of about 600 binding energies and excitation energies of nuclei with Z=28-30 and N=48-50. The main motivation for carrying out this work is (i) to test the suitability of the model space and the effective interaction in explaining the observed experimental data(ii) to test if the same effective interaction and model space are good choice for both the neutron rich nuclei near the drip line and proton rich line near the line of stability (iii) to study the evolution of shell structure if any in the case of even-even nuclei.

The paper is organized as follows: section 2 gives detail of calculations. Results and discussion are given in section 3 and finally in section 4 conclusions are given.

6.2 Detail of Calculations

Shell model calculations have been performed for the N=50 isotones for Z=30-46 treating ^{78}Ni as a core. The valence space comprises of ($0f_{5/2}$, $1p_{3/2}$, $1p_{1/2}$, $0g_{9/2}$)orbitals for protons which is made up of all Pauli allowed combinations of valence particles. Thus these isotones have 2 to 18 protons outside the core with

proton to neutron ratio changing from 0.60 to 0.92. The calculated single particle energies for the model space $0f_{5/2}$, $1p_{3/2}$, $1p_{1/2}$ and $0g_{9/2}$ are respectively -9.2859, -9.6566, -8.2695 and -5.8944 MeV.

The effective interaction of Lisetskiy et. al.[15] derived from a fit to existing data for the Ni isotopes from A=57 to A=76 and N=50 isotones from ^{79}Cu to ^{100}Sn. Thus it uses experimental data of about 600 binding energies and excitation energies for the fitting procedure. Most of the binding energies that were used in the interaction were of nuclei with Z=28-30 and N=48-50.The starting point is a realistic G-matrix interaction based on Bonn-C potential [16] together with core polarization corrections based on a ^{56}Ni core. Bonn-C potential is the stronger tensor force version of original Bonn potential [17,18]. This potential is derived from relativistic meson exchange theory and defined in the framework of the Blanckenbecler-Sugar reduction of the Bethe-Salpeter equation using one-boson-exchange (OBE) terms. Due to relativistic nonlocal terms, the tensor force of the Bonn potential is weaker than in local parametrizations of the nuclear force.

The calculations have been performed with the code NuShell [14]. It comes with a library of model spaces and interactions. This shell model code has been developed by Alex Brown from MSU to tackle the dimensions up to 10^6 in the J − T scheme and about $2x10^7$ in m-scheme. NuShell generates the basis states in m-scheme and then computes the matrix in j-scheme. Therefore, it bypasses the complication of angular momentum algebra in j − j coupled basis and also avoids the huge matrix dimension generated during m-scheme. NuShell consists of seven main programs and some supporting codes.

6.3 Results and Discussion

The results of our calculations for different even Z, N=50 isotones are shown in fig.6.1-6.9 along with the experimental data whatever available. The excited states up to 10.5 MeV have been calculated. On observing the results it is seen that for all nuclei systematic of levels are well reproduced. Experimentally it is well established that the 0^+ is the ground state for all the N=50 isotones considered here which is well reproduced in our results for all isotones. Towards the proton rich side levels are reproduced well for ^{90}Zr, ^{92}Mo and to some extent ^{94}Ru. For ^{96}Pd spectrum is compressed. For other nuclei towards the neutron rich side below the ^{90}Zr the spectra are start to become expand except for ^{86}Kr and ^{88}Sr in which only 4^+ state is compressed. From ^{90}Zn to ^{96}Pd 2^+ state reproduced very well as the first excited state in agreement with the experimental data . E(4^+) is reproduced as second excited state in our results but their energy are slightly greater than the experimental levels for nuclei ^{82}Ge, ^{84}Se, ^{90}Zr and lower for nuclei ^{86}Kr, ^{88}Sr, ^{94}Ru and ^{96}Pd. For ^{92}Mo 4^+ state have reproduced very well but for ^{88}Sr and ^{96}Pd its value is much lower than experimental value. The predicted E(6^+) state lies higher than the corresponding experimental values for all nuclei except ^{94}Ru and ^{96}Pd and have well reproduced for ^{92}Mo. Its value is maximum for ^{86}Kr in our work while maximum for ^{88}Sr in experimental results. E(8^+) is decreased continuously from Z=30 to 46 and reproduced well for ^{86}Kr, ^{88}Sr, ^{90}Zr and ^{94}Ru and very well for ^{92}Mo while for ^{82}Ge its value is much higher and for ^{96}Pd its value is much lower than experimental value. The over all result is that the low lying states are reproduced very well and higher levels are reproduced nearly to experiment except some levels. A large separation between 0^+ and 2^+ state in ^{90}Zr is an indication of shell closure at Z=40 which is further

supported by corresponding low value of B(E2) which is shown in fig 6.10-6.11. Most dominant configuration of wave function for ground state and first excited states for all the isotones are shown in table 6.1. On observing the structure of wave functions of these N=50 nuclei it is found that the ground state and first excited states configuration remains same except ^{80}Zn, ^{86}Kr, ^{88}Sr and ^{90}Zr nuclei. The difference can be attributed to the variation in proton single particle energies with changing Z.

The calculated energy levels of odd Z, N=50 isotones for $31 \leq Z \leq 45$ are shown in fig. 6.12-6.19 along with the experimental data. It is observed that the present calculation predict the ground state spins of ^{85}Br, ^{89}Y, ^{91}Nb, ^{93}Tc and ^{95}Rh correctly. Experimentally the ground state of ^{83}As is predicted as a ($3/2^-$,$5/2^-$) doublet. In our calculation also ($3/2^-$,$5/2^-$) difference is 0.09 MeV which is too small. However for ^{81}Ga and ^{87}Rb ground state is not reproduced correctly. The decreasing value of $9/2^+$ state are reproduced nearly well for all nuclei from ^{83}As to ^{89}Y and it finally becomes ground state for ^{91}Nb. $3/2^-$ state in ^{91}Nb have a very good agreement with experimental value but for ^{89}Y and ^{93}Tc it have some deviation. $5/2^-$ state has been reproduced nearly well for ^{93}Tc and ^{91}Nb but for other nuclei it is much deviated from the corresponding experimental value. $1/2^-$ state have a poor result for all nuclei. $7/2^-$ state shows a nearly good agreement for all nuclei with whatever experimental data is available. $9/2^-$ state is reproduced nearly well for ^{83}As, ^{85}Br and ^{91}Nb but for ^{81}Ga and ^{87}Rb corresponding energy of this state is much higher than the experimental values. This interaction gives poor results for ^{81}Ga and ^{87}Rb while some of the predicted levels are close to corresponding experimental values in all other nuclei.

Variation of $5/2^-$ and $3/2^-$ state which are varying nucleus to nucleus are shown in fig.6.20-6.21.

The calculation by Sinatkas et. al. are found to be in very satisfactory agreement with experiment for all nuclei with $38 < Z \leq 46$ but for $Z < 38$ his agreement begins to deteriorate rapidly while our results are in satisfactory agreement with experiment and with the results by Ji & Wildenthal (up to the Z=36) for all even mass nuclei. For odd mass nuclei our results showing disagreement for most of the states of nuclei with experiment and also with the results of Sinatkas et. al. and Ji & Wildenthal.

Theoretically predicted levels which have not been observed experimentally as yet are to be confirmed.

6.4 Conclusions

The large scale shell model calculations for even and odd mass N=50 isotones namely ^{80}Zn, ^{82}Ge, ^{84}Se, ^{86}Kr, ^{88}Sr, ^{90}Zr, ^{92}Mo, ^{94}Ru, ^{96}Pd and ^{81}Ga, ^{83}As, ^{85}Br, ^{87}Rb, ^{89}Y, ^{91}Nb, ^{93}Tc, ^{95}Rh have been performed. The calculations have been performed using Nushell code and ^{78}Ni core in the valence space $\pi(0f_{5/2,\ 1}p_{3/2,\ 1}p_{1/2,\ 0}g_{9/2})$ for protons. jj44b Hamiltonian have been used to find the results which has obtained from a fit to experimental data of about 600 binding energies and excitation energies of nuclei with Z=28-30 and N=48-50. The results of our analysis shows that in the chosen configuration space jj44b interaction gives nearly good agreement with the experimental data for 0^+,2^+ and 4^+ state of even mass N=50 nuclei except somelevels of N=50 isotones and all energy levels of

^{92}Mo are reproduced very well. A large separation between 0^+ and 2^+ state in ^{90}Zr is an indication of shell closure at Z=40 which is further supported by corresponding low value of B(E2). For odd mass nuclei results for most of the states are not satisfactory.

The results of our analysis shows that nearly good agreement with experimental levels for both even mass neutron rich nuclei near the drip line and proton rich nuclei near line of stability is obtained indicating suitability of model space and the interaction for these even mass nuclei. However for odd Z, N=50 isotones the poor agreement with experimental results for most of states suggest the need for minor monopole correction in the interaction and more experimental data fitting in this region.

References:

[1] B. A. Brown, Prog. Part. Nucl. Phys. 47, 517 (2001)

[2] H Grawe et. al., Rep. Prog. Phys. 70 (2007) 1525–1582

[3] Blomqvist J and Rydstr¨om L 1985 *Phys. Scr.* **31** 31

[4] Ji X and Wildenthal B H 1988 *Phys. Rev.* C **37** 1256

[5] Ji X and Wildenthal B H 1988 *Phys. Rev.* C **38** 2849

[6] X. Ji and B. H. Wildenthal, Phys. Rev. C **40,** 2415, No. 1 (July 1989)

[7] Sinatkas J, Skouras L D, Strottman D and Vergados J D 1992 *J. Phys. G: Nucl. Part. Phys.* **18** 1377

[8] Ghugre S S and Datta S K 1995 *Phys. Rev.* C **52** 1881

[9] Johnstone I P and Skouras L D 1997 *Phys. Rev.* C **55** 1227

[10] Zhang C-H, Wang S-J and Gu J-N 1999 *Phys. Rev.* C **60** 054316

[11] D. Verney *et. al*. **Phys. Rev. C 76**, 054312(2007)

[12] M. Gorska *et al*. **Phys. Rev. Lett. 79**, No. 13(1997)

[13] ***www.nndc.bnl.gov***

[14] NuShell @ MSU B. A. Brown and W. D. M. Rae (unpublished)

[15] Lisetskiy and Brown (unpublished)

[16] M. F. Jiang et. al., Phys. Rew. C Vol 46, No. 3(1992)

[17] R. Machleidt, Adv. Nucl. Phys. 19, 189 (1989).

[18] R. Machleidt, K. Holinde, and C. Elster, Phys. Rep. 149, 1 (1987).

Table 6.1 Main configurations in the wave functions of the ground state and first exited state for N = 50 isotones.

Nuclei	State	Proton Wave Function				Probability
^{30}Zn	0^+	$(f_{5/2})^0$	$(p_{3/2})^2$	$(p_{1/2})^0$	$(g_{9/2})^0$	45.3
	2^+	$(f_{5/2})^2$	$(p_{3/2})^0$	$(p_{1/2})^0$	$(g_{9/2})^0$	39.0
^{32}Ge	0^+	$(f_{5/2})^2$	$(p_{3/2})^2$	$(p_{1/2})^0$	$(g_{9/2})^0$	42.5
	2^+	$(f_{5/2})^2$	$(p_{3/2})^2$	$(p_{1/2})^0$	$(g_{9/2})^0$	34.4
^{34}Se	0^+	$(f_{5/2})^4$	$(p_{3/2})^2$	$(p_{1/2})^0$	$(g_{9/2})^0$	27.0
	2^+	$(f_{5/2})^4$	$(p_{3/2})^2$	$(p_{1/2})^0$	$(g_{9/2})^0$	15.6
^{36}Kr	0^+	$(f_{5/2})^4$	$(p_{3/2})^4$	$(p_{1/2})^0$	$(g_{9/2})^0$	28.2
	2^+	$(f_{5/2})^3$	$(p_{3/2})^4$	$(p_{1/2})^1$	$(g_{9/2})^0$	22.2
^{38}Sr	0^+	$(f_{5/2})^6$	$(p_{3/2})^4$	$(p_{1/2})^0$	$(g_{9/2})^0$	21.8
	2^+	$(f_{5/2})^5$	$(p_{3/2})^4$	$(p_{1/2})^1$	$(g_{9/2})^0$	32.6
^{40}Zr	0^+	$(f_{5/2})^6$	$(p_{3/2})^4$	$(p_{1/2})^2$	$(g_{9/2})^0$	31.9
	2^+	$(f_{5/2})^4$	$(p_{3/2})^4$	$(p_{1/2})^2$	$(g_{9/2})^2$	27.2
^{42}Mo	0^+	$(f_{5/2})^6$	$(p_{3/2})^4$	$(p_{1/2})^2$	$(g_{9/2})^2$	39.0
	2^+	$(f_{5/2})^6$	$(p_{3/2})^4$	$(p_{1/2})^2$	$(g_{9/2})^2$	46.0
^{44}Ru	0^+	$(f_{5/2})^6$	$(p_{3/2})^4$	$(p_{1/2})^2$	$(g_{9/2})^4$	62.0
	2^+	$(f_{5/2})^6$	$(p_{3/2})^4$	$(p_{1/2})^2$	$(g_{9/2})^4$	65.7
^{46}Pd	0^+	$(f_{5/2})^6$	$(p_{3/2})^4$	$(p_{1/2})^2$	$(g_{9/2})^6$	100.0
	2^+	$(f_{5/2})^6$	$(p_{3/2})^4$	$(p_{1/2})^2$	$(g_{9/2})^6$	100.0

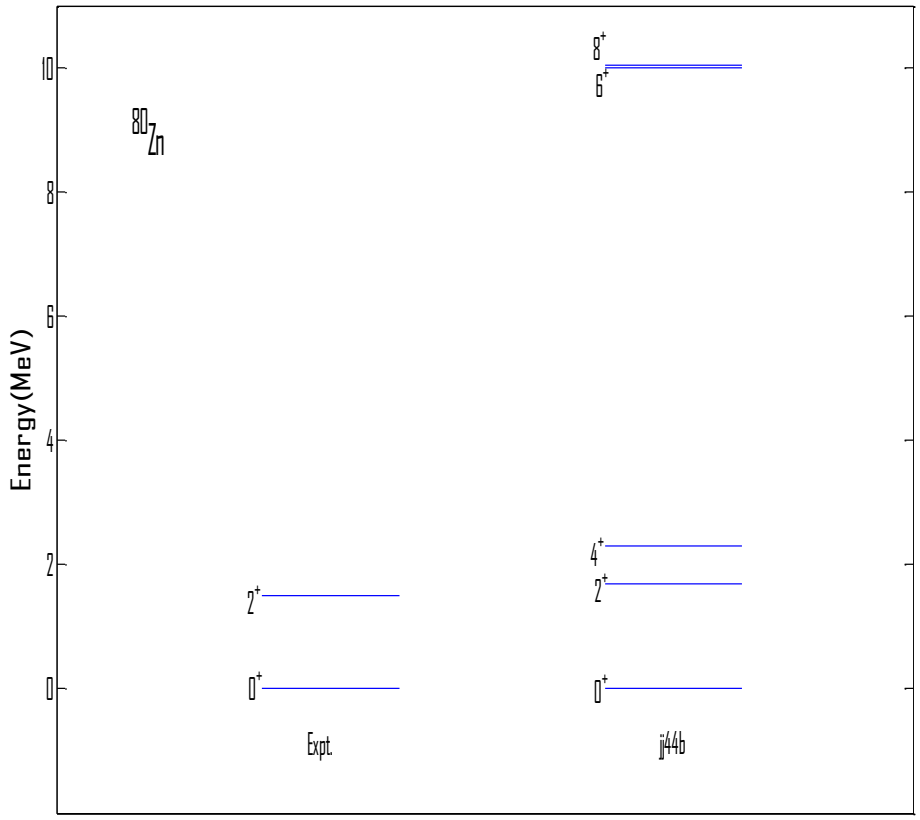

Figure 6.1: Calculated and experimental spectra for ^{80}Zn.

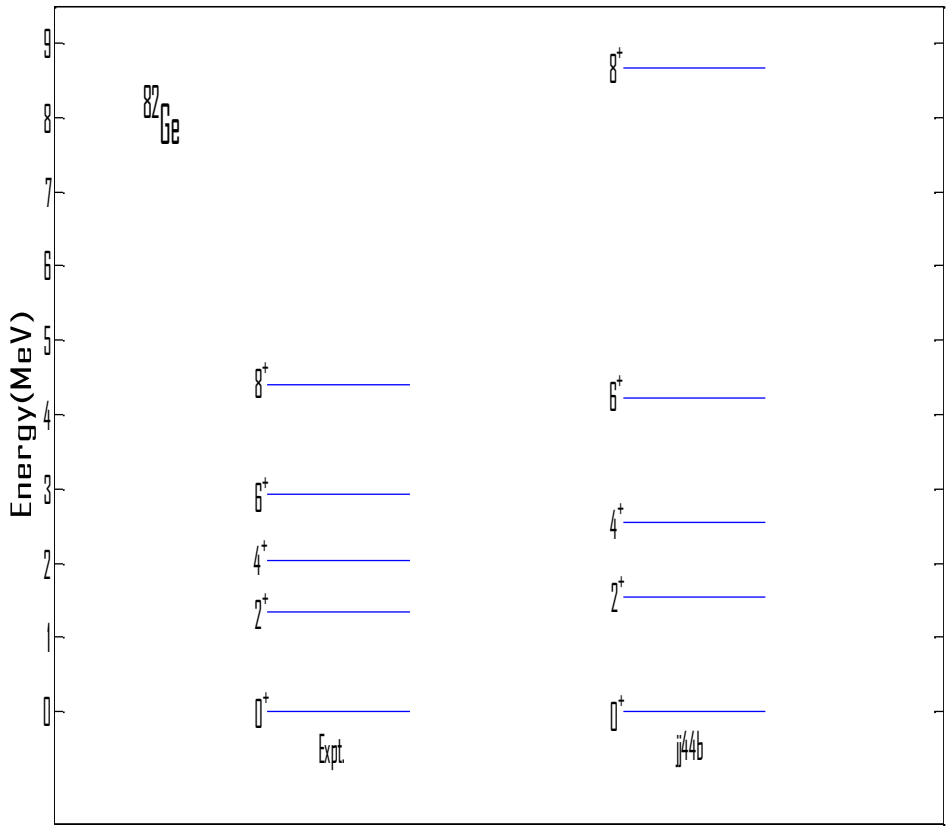

Figure 6.2: Calculated and experimental spectra for ^{82}Ge.

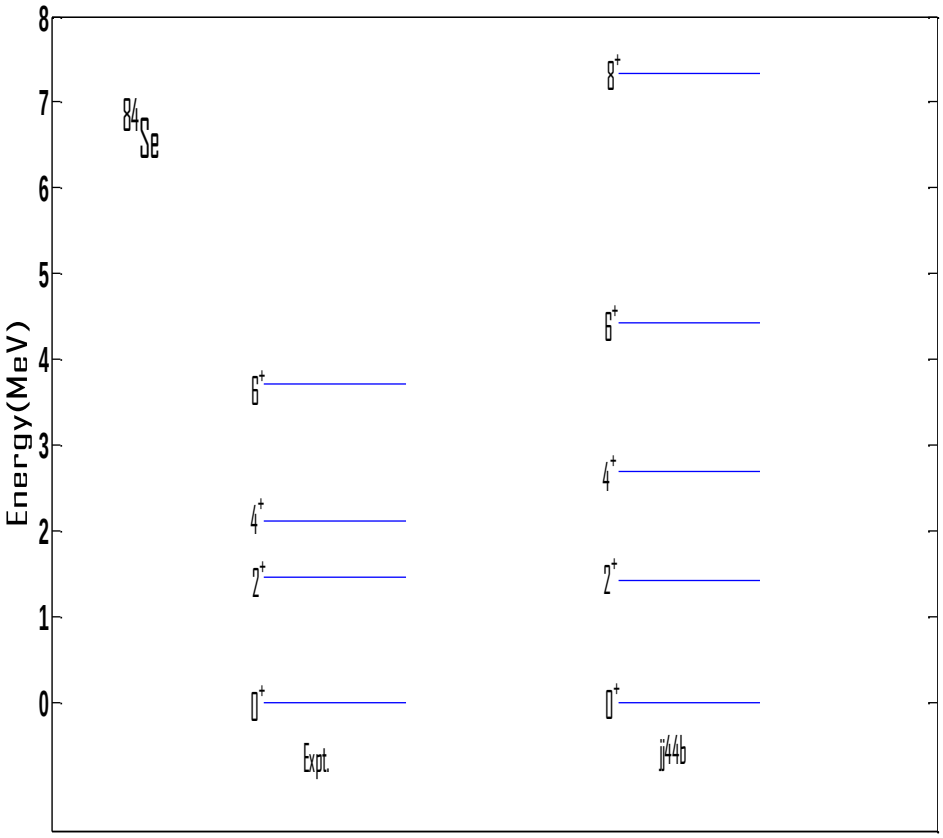

Figure 6.3: Calculated and experimental spectra for ^{84}Se.

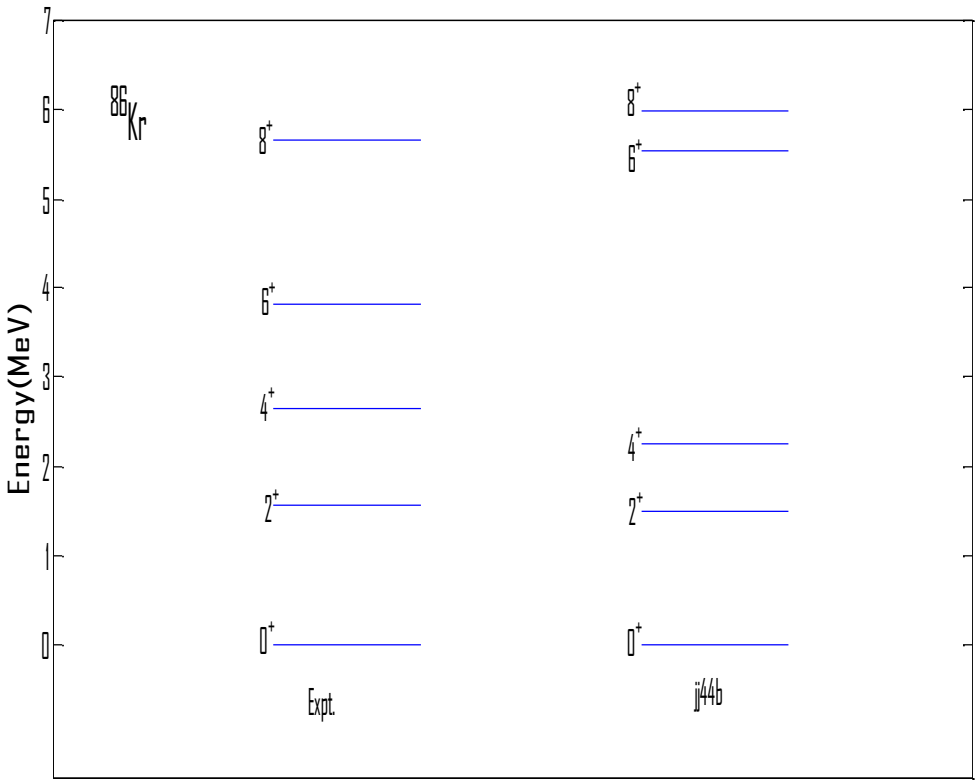

Figure 6.4: Calculated and experimental spectra for ^{86}Kr.

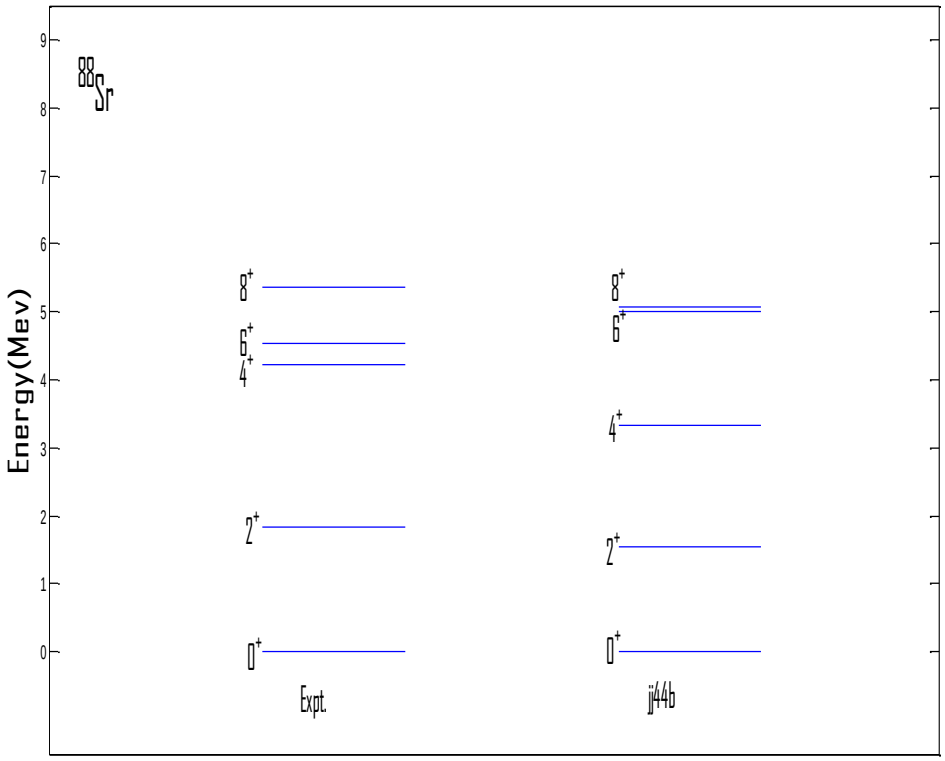

Figure 6.5: Calculated and experimental spectra for ^{88}Sr

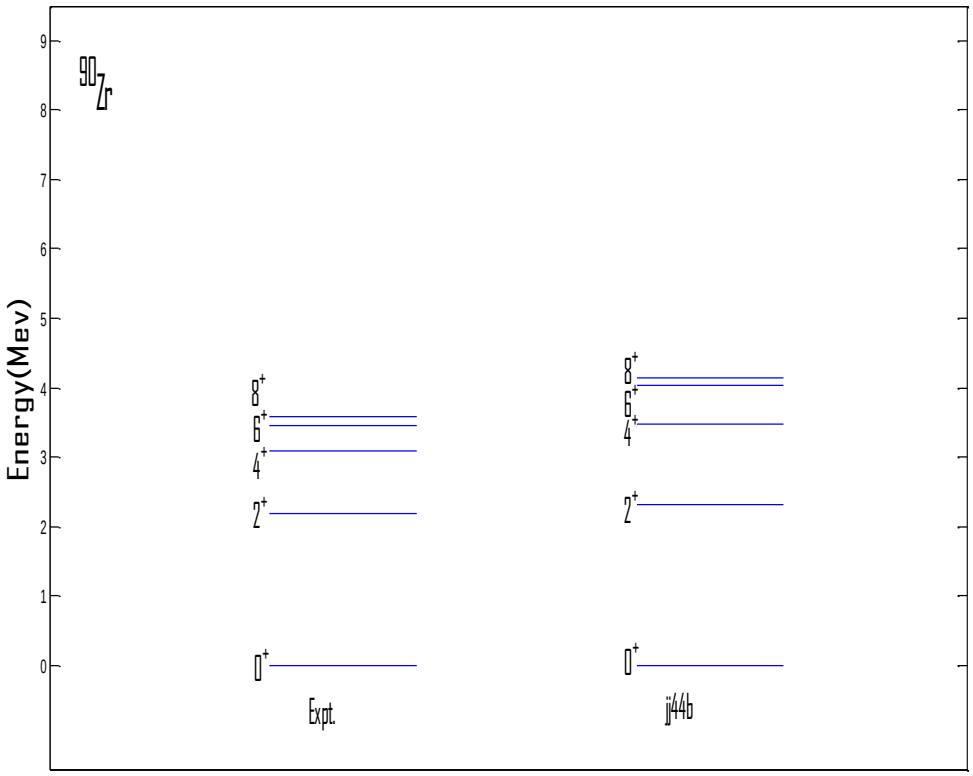

Figure 6.6: Calculated and experimental spectra for ^{90}Zr.

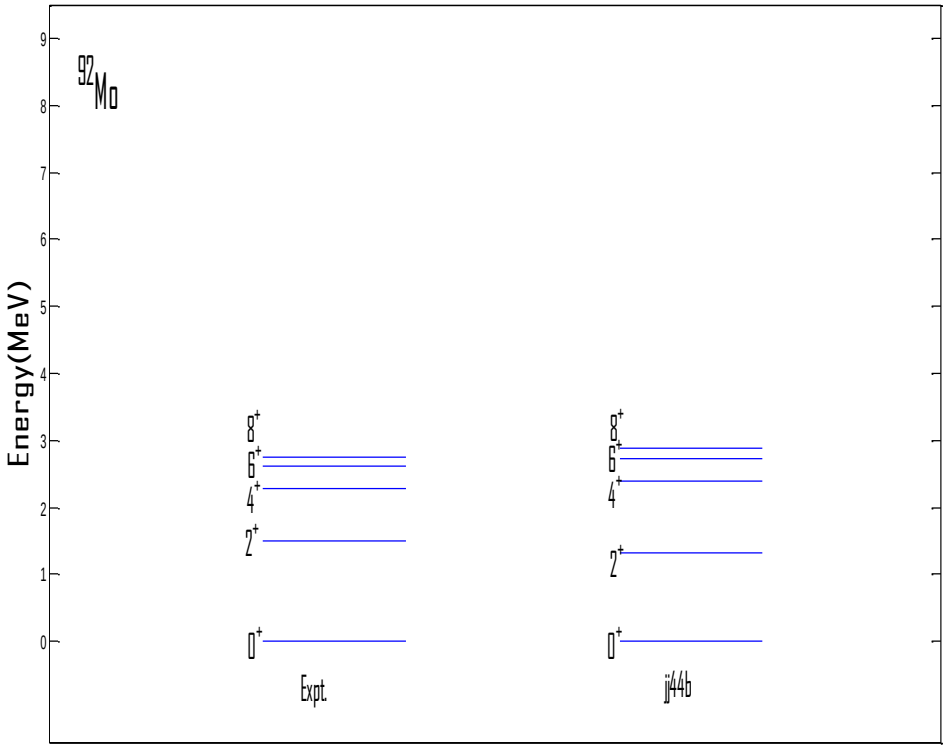

Figure 6.7: Calculated and experimental spectra for ^{92}Mo.

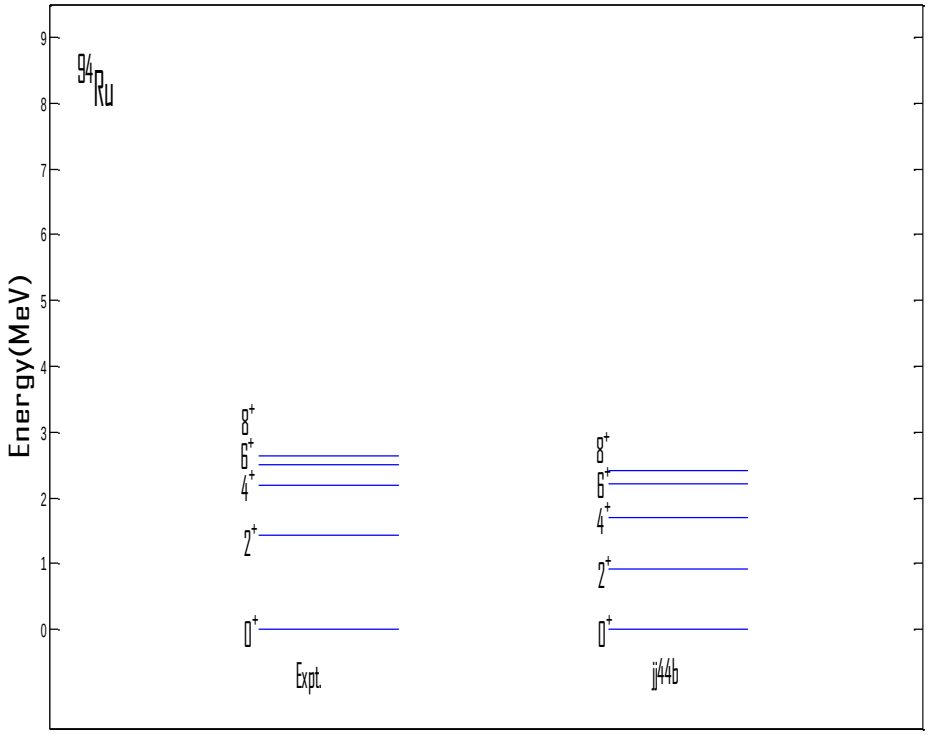

Figure 6.8: Calculated and experimental spectra for ^{94}Ru.

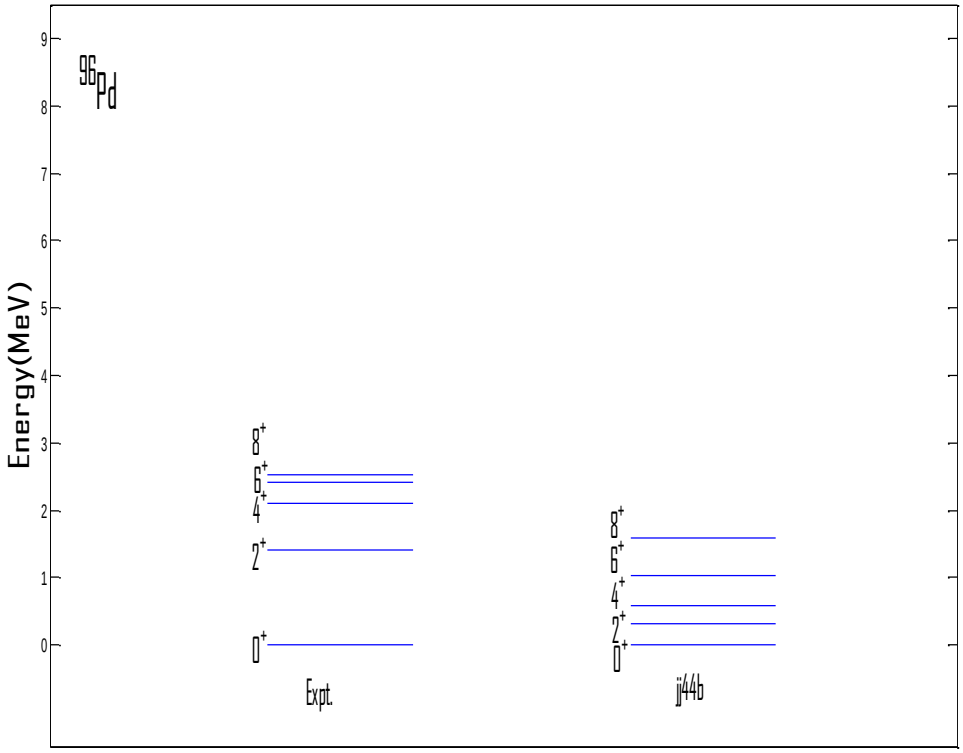

Figure 6.9: Calculated and experimental spectra for ^{96}Pd.

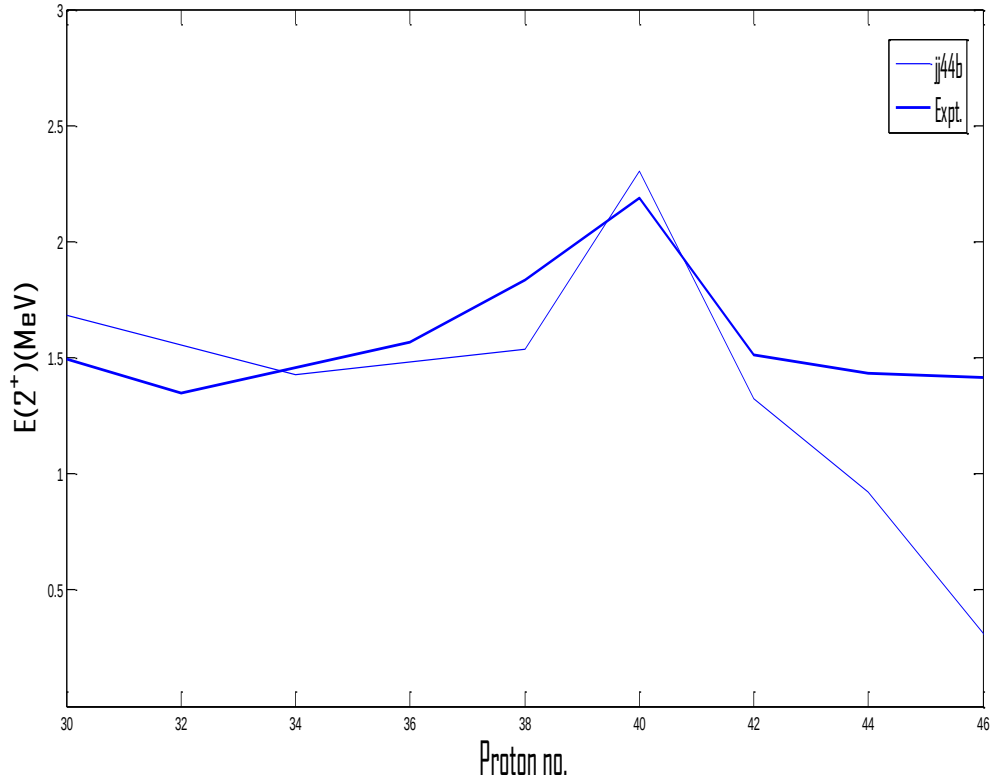

Figure 6.10 : Variation of $E(2^+)$ with proton no.

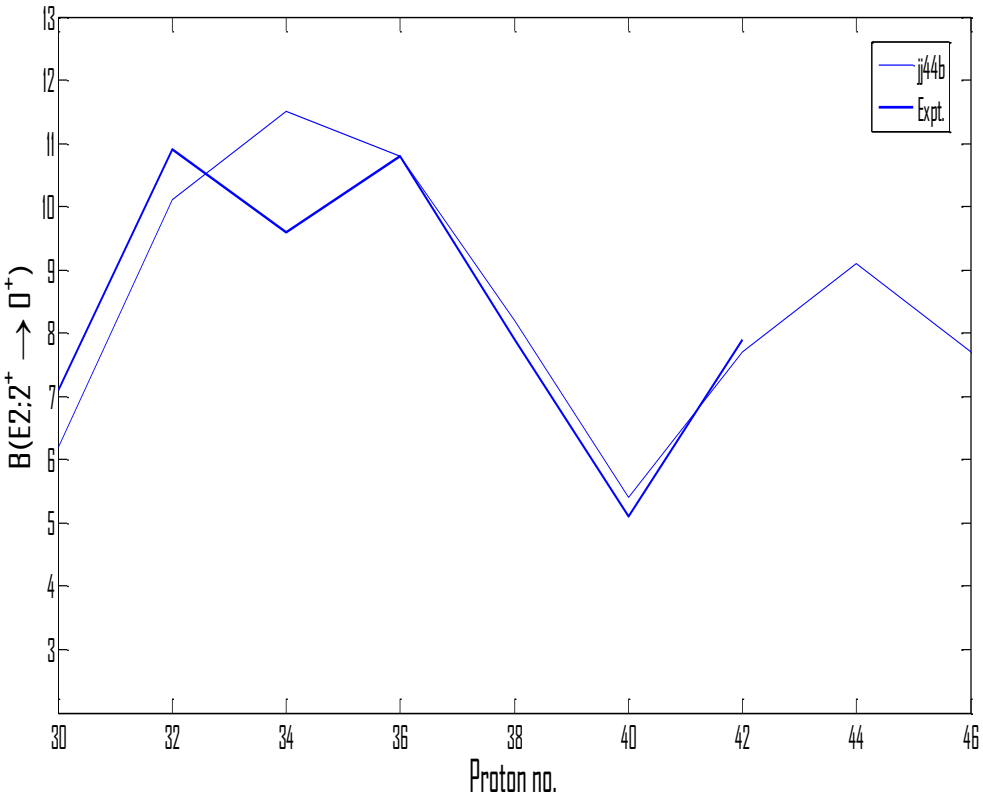

Figure 6.11 : Variation of B(E2;$2^+ \rightarrow 0^+$) with proton no.

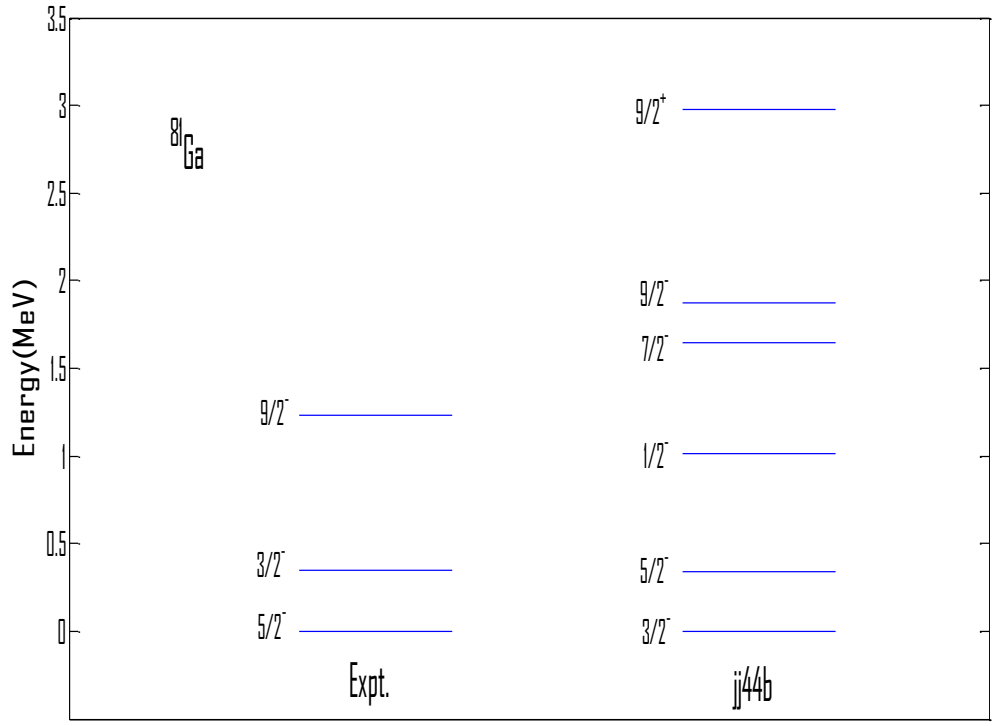

Figure 6.12: Calculated and experimental spectra for ^{81}Ga.

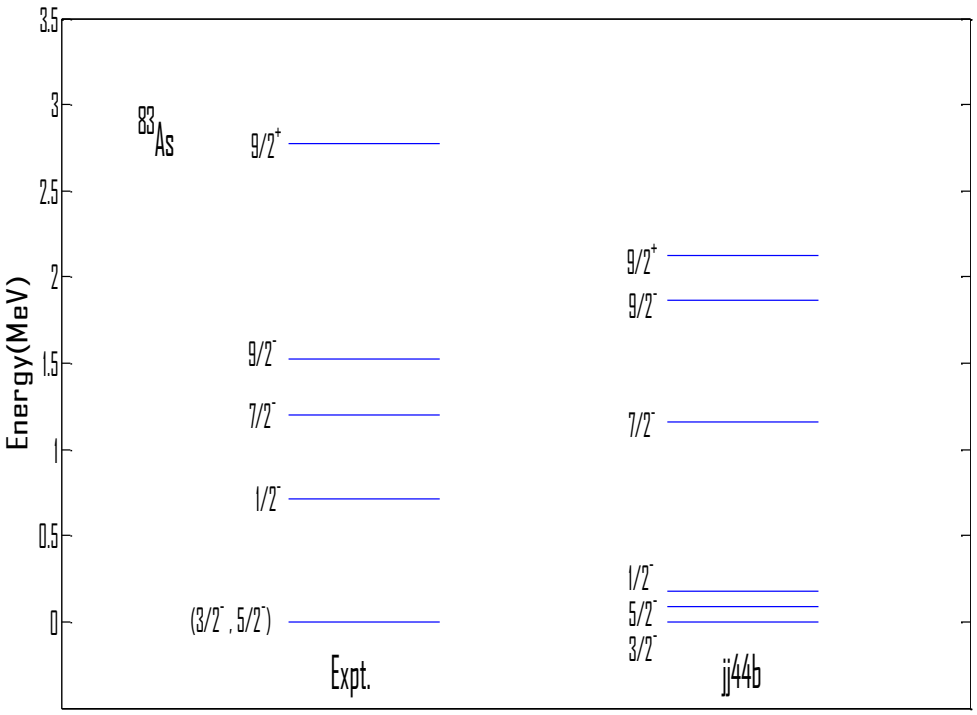

Figure 6.13: Calculated and experimental spectra for ^{83}As.

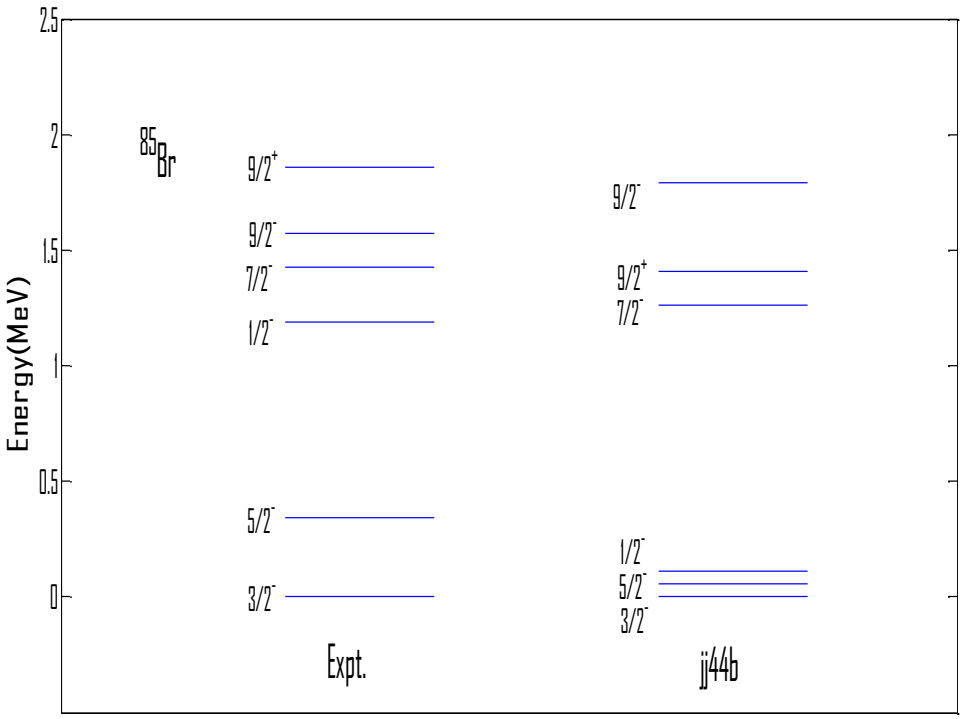

Figure 6.14: Calculated and experimental spectra for ^{85}Br.

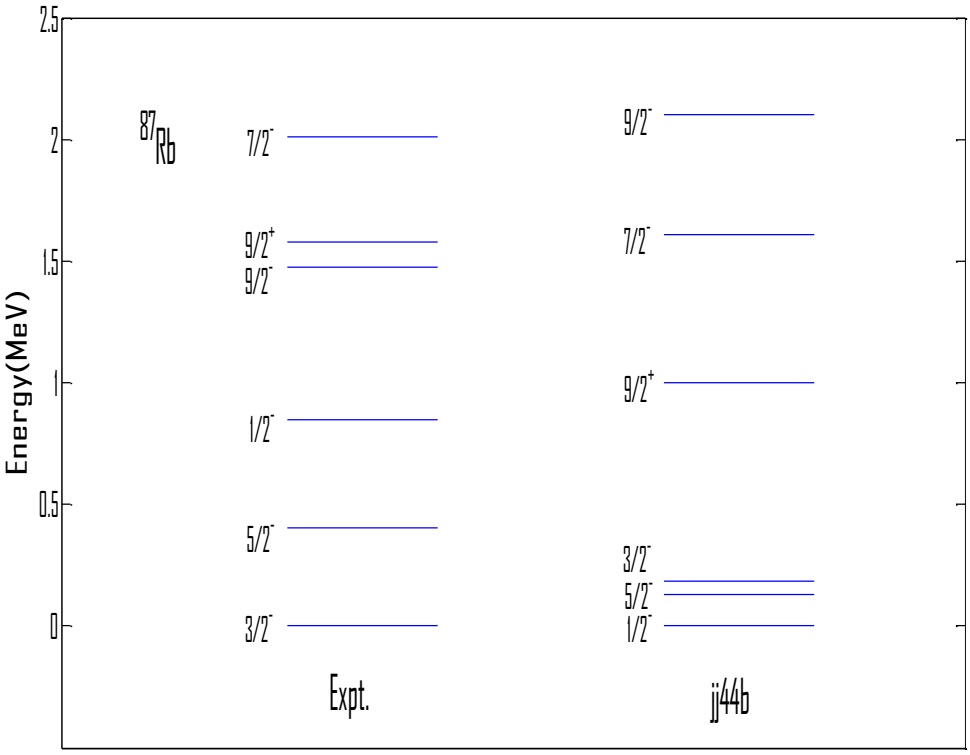

Figure 6.15: Calculated and experimental spectra for ^{87}Rb.

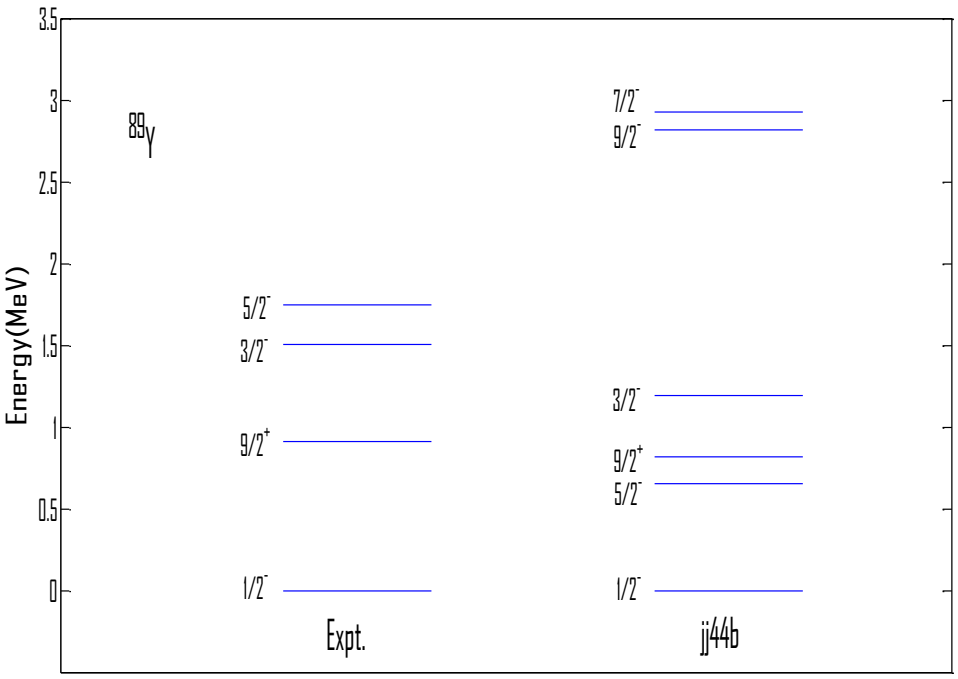

Figure 6.16: Calculated and experimental spectra for ^{89}Y.

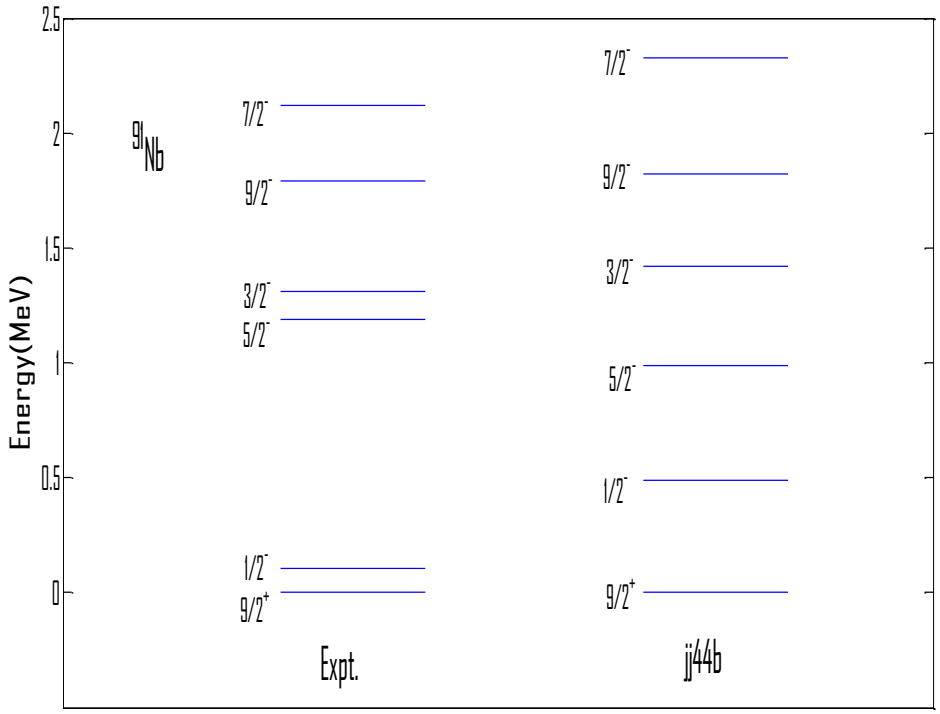

Figure 6.17: Calculated and experimental spectra for ^{91}Nb.

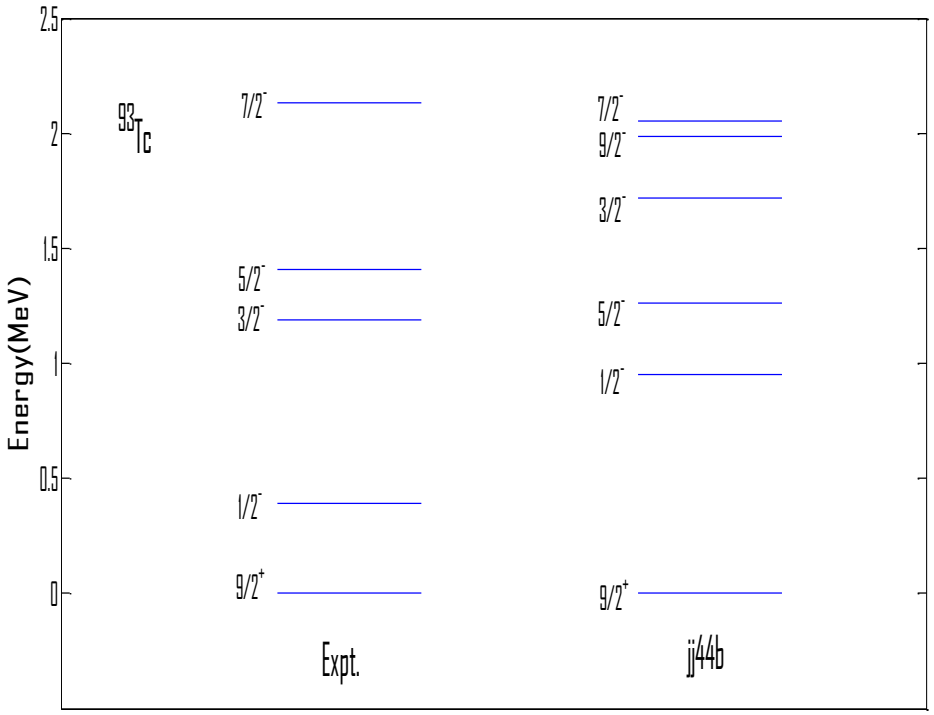

Figure 6.18: Calculated and experimental spectra for ^{93}Tc.

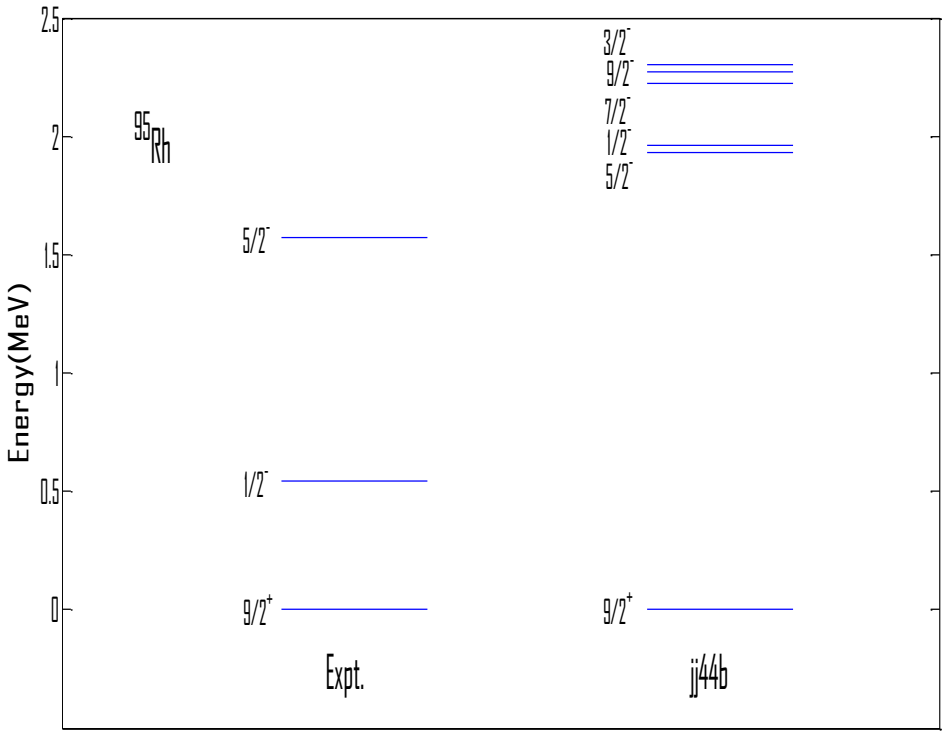

Figure 6.19: Calculated and experimental spectra for ^{95}Rh.

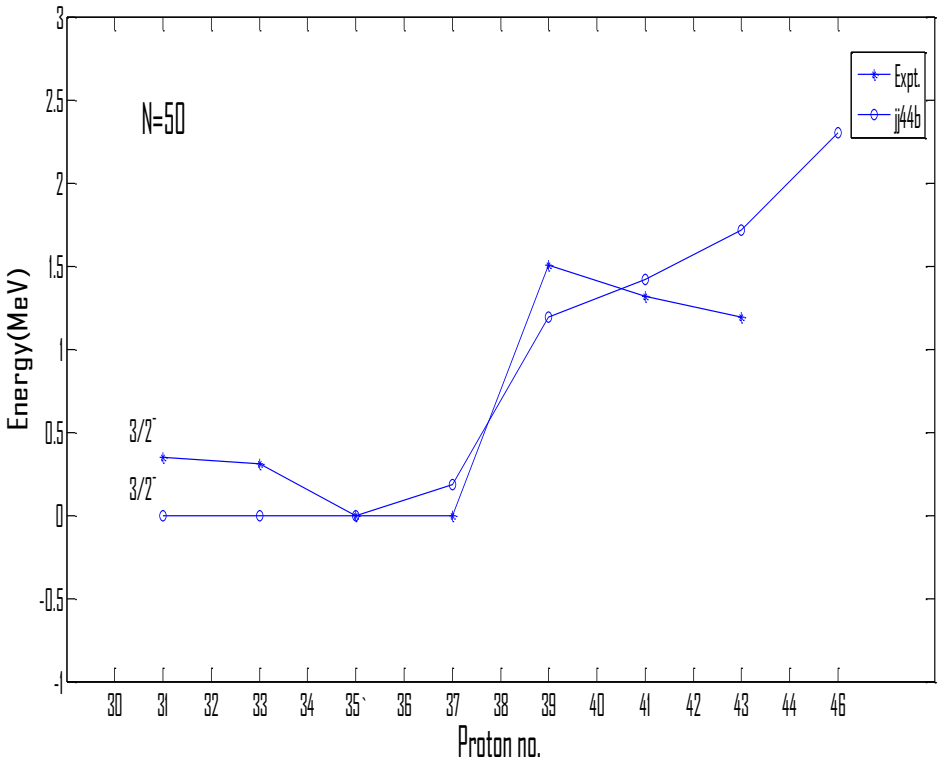

Figure 6.20: Variation of $3/2^-$ state of N=50 nuclei

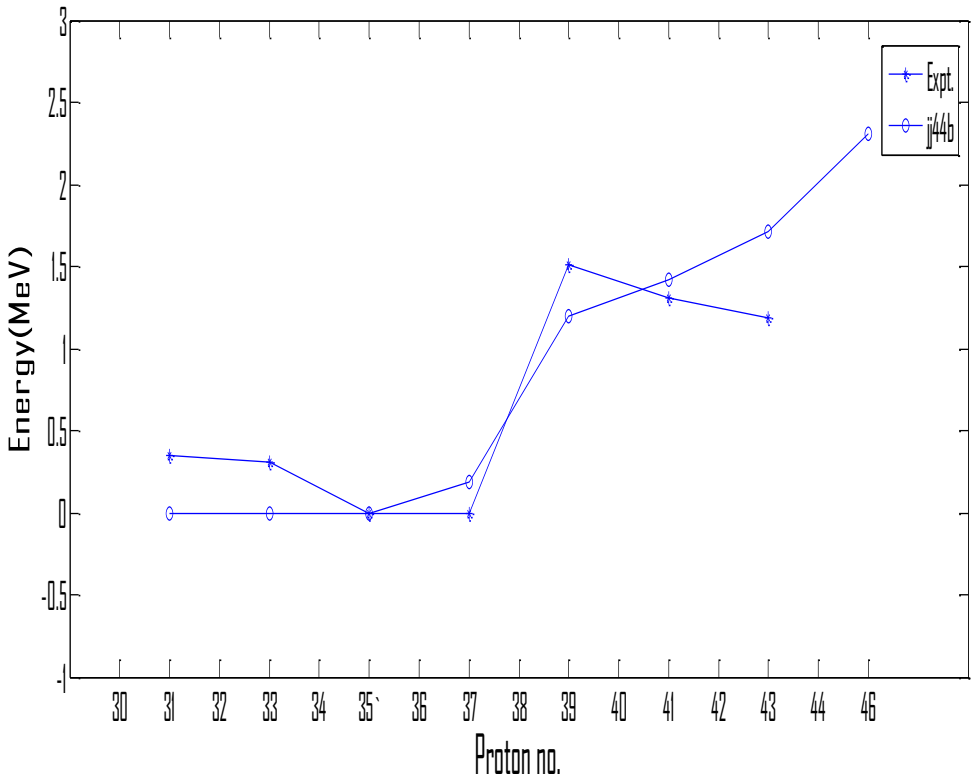

Figure 6.21: Variation of $3/2^-$ state of N=50 nuclei

Chapter 7

Importance and Future prospects

Nuclear structure physics and the visible Universe are intimately related since nuclear physics drives many astrophysical processes. These include Big Bang nucleosynthesis and the evolution and final fate of stars. A reliable description of the underlying astrophysical scenarios depends crucially on the knowledge of nuclear properties in the relevant regions of the Segr´e chart involving both nuclei close to stability, in the heavy-ion fusion below the nickel–iron region, which is important for the slow neutron capture (s-process) beyond, as well as exotic nuclei far-off stability in the rapid neutron capture (r-process) on the neutron-rich side and the rapid proton capture (rp-process) close to the proton dripline.

The binding energy per nucleon peaks around iron, energy is only released in fusion processes occurring below this point. Since the creation of heavier nuclei by fusion costs energy, nature resorts to the process of neutron capture. Neutrons(due to their lack of charge) are readily absorbed by a nucleus. Thus heavy elements are created by either a *slow* neutron capture process (the so-called *s* process) or by the *rapid*, or *r* process. The *s* process occurs in thermally pulsing stars (called AGB, or asymptotic giant branch stars) and takes hundreds to thousands of years to reach the heaviest elements of lead and bismuth. The *r* process is thought to occur in supernova explosions because the conditions of high temperature, high neutron flux and ejected matter are present. These stellar conditions make

the successive neutron captures very fast, involving very neutron-rich species which then beta-decay to heavier elements, especially at the so-called waiting points that correspond to more stable nuclides with closed neutron shells (magic numbers).

N = 51 nuclide are particularly important to understand astrophysical processes since neutron rich nuclei between N = 50 and N = 82 shells cover waiting point in r-processes. Properties of low lying states in these nuclei near closed shell are useful for the description of nuclear structure, quenching of shell gaps and a more uniform spacing of single-particle energy levels [1-3] and influence how heavier nuclei are produced in astrophysical rapid neutron capture (r−) process [4,5]. The astrophysical importance of ^{78}Ni is related to the understanding of the nuclear mechanism of the rapid capture of neutrons by seed nuclei through the r-process. The path of this reaction network is expected in neutron-rich nuclei for which there is little experimental data, and the precise trajectory is dictated by the details of the shell structure far from stability. Synthesis of heavier elements proceeds by r-process from the seed nucleus Fe following the path among neutron rich nuclei and closing at ^{78}Ni. Since nuclear structure of mostly r process nuclei is not known, the study of these neutron rich nuclei near the ^{78}Ni region will throw light on r-process in nucleosynthesis

Today research on nuclear physics focuses on exploring nucleonic matter under extreme conditions such as those that can be created in modern accelerator laboratories. The opportunities offered by beams of exotic nuclei for research in the areas of nuclear structure physics and nuclear astrophysics are exciting and world-wide activity in the construction of different types of radioactive beam facilities bears witness to the strong scientific interest in the physics that can be probed with such beams.

Nuclei far from stability allow us to amplify and isolate particular aspects of the nuclear interaction and dynamics. Future work will involve, for example, mapping the neutron drip line further up, investigating neutron halo systems, learning about the astrophysical rp- and r-process paths, exploring the evolution of shell structure and neutron skins, creating further super heavy nuclei, studying super-allowed beta-decay in very light proton rich nuclei, developing a deeper understanding of proton-neutron pairing and studying the exotic phenomenon of proton radioactivity.

The actual mechanism which causes the changes in nuclear structure as neutron/proton number increases in a nuclear system is still an open question. The present work can be extended to the study of following aspects:

Publications

In Journals

1. Shape evolution of the highly deformed Kr nucleus examined with DSAM

   K. Muarya in T. Trivedi et. al., Physical Review C 80, 047302 (2009)

2. Lifetime measurement of high spin states in ^{75}Kr

   K. Muarya in T. Trivedi et. al., Nuclear Physics A 834 (2010) 72c-74c

3. Large scale shell model calculations for N=51 isotonic chain

   Accepted to publish in IOSR Journal of Applied Physics

4. Large scale shell model calculations for Ca isotopic chain from N=22 to N=38

   Pramana-Journal of Physics (under review)

5. A Shell Model Study of Nuclei Between ^{78}Ni and ^{100}Sn

   To be communicated

In Conferences

1. Shape transition in ^{75}Kr and ^{75}Br nuclei

   Proceeding of DAE-BRNS Symposium on Nuclear Physics 54, 60 (2009)

2. Lifetime measurement of high spin states in ^{75}Kr

   NN2009, Beijing, China, August 16-21, 2009

3. Large scale shell model calculations for N=51 isotonic chain

   Proceeding of DAE-BRNS Symposium on Nuclear Physics 54, 140 (2009)

4. Large scale shell model calculations for Ca isotopic chain from N=22 to N=38

   Proceeding of DAE-BRNS Symposium on Nuclear Physics 55, 142 (2010)

5. A Shell Model Study of Even Nuclei Between ^{78}Ni and ^{100}Sn

   Proceeding of DAE-BRNS Symposium on Nuclear Physics 56, 384 (2011)

6. Nuclear Spectroscopy of N=50 Isotones With $29 \leq Z \leq 36$

   FIG-12, IUAC, New Delhi, 5^{th}-7^{th} March, 2012

7. A Shell Model Description of Odd Z N=50 Isotones Above the ^{78}Ni

   Proceeding of DAE-BRNS Symposium on Nuclear Physics (2012)

Appendix A

Nushell code: Sequence of programs for energies

SHELL: It creates batch file *.bat that coordinates the program sequence and their inputs. Alternatively, the input is from a .ans file that has been made by a previous run of shell.

NUBASIS: It makes a list of all possible M-scheme basis states for a given model space together with a given set of restrictions.

NUPROJ: It makes linear combinations of the M-scheme basis states that have good J values in p/n formalism or good J and T in isospin formalism.

NUMATRIX: It makes the matrix corresponding to the J (or JT) dimension of the problem. Only the non-zero matrix elements are stored.

NULANCZOS: It find the lowest N eigenvalues for the matrix. The default value of N is 10.

Sequence of programs for overlaps and transitions

MVEC: It reads the output of Proj and Lanczos to make the eigenvectors in the M-scheme basis and it is used as input to Tramp.

TRAMP: It calculates overlaps between two wave functions. It can be used with the den option within shell to obtain:
t - one-body transition density.

TBTDOP: It makes an intermediate file needed for two-body transition densities.*

Other programs

DENS - calculates the radial wave functions for a given nucleus with oscillator, Woods-Saxon or Skyrme Hartree-Fock potentials and reads the *.obd from nutshell to calculate B(EL), B(ML) and B(GT) values.

LEVEL - provides a level scheme for a given set of J values.

PN - converts a given set of *.sp and *.int files in isospin formalism into their equivalent in proton-neutron (pn) formalism.

Appendix B

Conversion of isospin to proton-neutron two-body matrix elements

The conversion of normalized isospin wavefunctions to normalzied proton-neutron (pn) wave functions is (a≠b):

$$
\begin{aligned}
| aa, J >_{pp} &= | aa, J = even, T = 1 > \\
| ab, J >_{pp} &= | ab, J, T = 1 > \\
| aa, J = even >_{pn} &= | aa, J = even, T = 1 > \\
| aa, J = odd >_{pn} &= | aa, J = odd, T = 0 > \\
| ab, J >_{pn} &= \sqrt{\frac{1}{2}} [| ab, J, T = 1 > + | ab, J, T = 0 >]
\end{aligned}
$$

Thus the normalized proton-proton (and neutron-neutron) matrix elements are just the T = 1 matrix elements, and the normalized proton-neutron matrix elements are (a≠b and c≠d):

$$< aa, J \mid V \mid cc, J >_{pn} = < aa, J, T = 1 \mid V \mid cc, J, T = 1 > + < aa, J, T = 0 \mid V \mid cc, J, T = 0 >$$

$$< ab, J \mid V \mid cc, J >_{pn} = \sqrt{\frac{1}{2}} [< ab, J, T = 1 \mid V \mid cc, J, T = 1 > + < ab, J, T = 0 \mid V \mid cc, J, T = 0 >]$$

$$< aa, J \mid V \mid cd, J >_{pn} = \sqrt{\frac{1}{2}} [< aa, J, T = 1 \mid V \mid cd, J, T = 1 > + < aa, J, T = 0 \mid V \mid cd, J, T = 0 >]$$

$$< ab, J \mid V \mid cd, J >_{pn} = \frac{1}{2} [< ab, J, T = 1 \mid V \mid cd, J, T = 1 > + < ab, J, T = 0 \mid V \mid cd, J, T = 0 >]$$

In the first three of these equations one of the matrix elements on the right-hand side is zero. Nushell uses unnormalized proton-neutron matrix elements (upn) of the form

$$< aa, J \mid V \mid cc, J >_{upn} = [< aa, J, T = 1 \mid V \mid cc, J, T = 1 > + < aa, J, T = 0 \mid V \mid cc, J, T = 0 >]$$

$$< ab, J \mid V \mid cc, J >_{upn} = [< ab, J, T = 1 \mid V \mid cc, J, T = 1 > + < ab, J, T = 0 \mid V \mid cc, J, T = 0 >]$$

$$< aa, J \mid V \mid cd, J >_{upn} = [< aa, J, T = 1 \mid V \mid cd, J, T = 1 > + < aa, J, T = 0 \mid V \mid cd, J, T = 0 >]$$

$$< ab, J \mid V \mid cd, J >_{upn} = [< ab, J, T = 1 \mid V \mid cd, J, T = 1 > + < ab, J, T = 0 \mid V \mid cd, J, T = 0 >]$$

The program PN converts an isospin interaction file into an unnormalized proton-neutron interaction file. In the proton-neutron file there is a label T′. For the pp and nn matrix elements you must have T′ = 1. For the proton-neutron matrix elements the T′ label must be 0 or 1 but its value does not affect the calculation. T′ can be used (as in the program PN) to keep track of where the proton-neutron matrix element came from in terms of the isospin matrix elements.

If you are given a set of normalized proton-neutron matrix elements they must be converted into unnormalized matrix elements to use in nushell (set T′ = 0):

$$< aa, J \mid V \mid cc, J >_{upn} = < aa, J \mid V \mid cc, J >_{pn}$$

$$< ab, J \mid V \mid cc, J >_{upn} = \sqrt{2} < ab, J \mid V \mid cc, J >_{pn}$$

$$< aa, J \mid V \mid cd, J >_{upn} = \sqrt{2} < aa, J \mid V \mid cd, J >_{pn}$$

$$< ab, J \mid V \mid cd, J >_{upn} = 2 < ab, J \mid V \mid cd, J >_{pn}$$

The Changing Mean Field in Exotic Nuclei: A Shell Model Study of Neutron Rich Nuclei

A Summary of the Thesis Submitted
to the

University of Allahabad
for the degree of

Doctor of Philosophy
in Science

by

Kamalesh Maurya

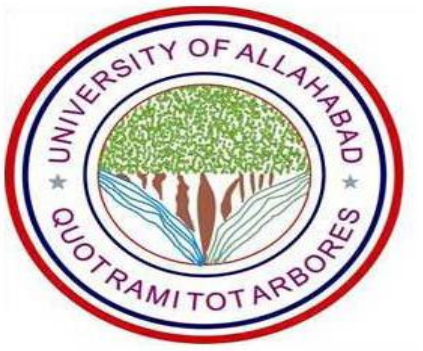

Under the Supervision of
Prof. (Mrs.) Indira Mehrotra
Department of Physics
University of Allahabad
Allahabad -211002
Year 2013

The present thesis has been classified into seven chapters:

Chapter 1-Introduction

Chapter 2- Shell model and Techniques

Chapter 3-Nucleon Nucleon Interaction

Chapter 4-Shell model description of N=51 isotones

Chapter 5-Shell model study of Ca isotopes

Chapter 6- A shell model study of N=50 isotones with $30 \leq Z \leq 46$

Chapter 7- Important and Future prospects

In the **Introduction**, a brief review of nuclear structure has been discussed. In the nuclear shell model progress is made in small steps, by collecting new experimental data and comparing them to theoretical expectations. These advances are based on technical progress, e.g. in cluster computer technology and secondary ion beam technique. The future of nuclear shell model is some how depend on collection of new data from recent experimental data and improving the interactions which is depend on radioactive ion beam facilities and have very bright future. In the introduction the world wide radioactive facilities are also discussed. The four frontiers of the study of exotic nuclei, namely neutron-rich nuclei, proton-rich nuclei, halo and skin phenomena are also discussed in brief. In order to form a stable atomic nucleus, an equilibrium between the number of protons and neutrons has to be maintained, this condition is fulfilled for 259 different combinations of protons and neutrons and these nuclei can be found on

the Earth. In addition, 26 nuclei form a quasi-stable configuration, i.e. they decay with a half-life comparable to or longer than the age of the Earth and therefore still present on the Earth. In addition to these 285 stable or quasi-stable nuclei, some 4000-6000 unstable nuclei are predicted to exist by different model. Close to 2500 nuclei have been observed already and rest are still in terra incognita.

In the **Chapter 2**, shell model and technique of calculation have been discussed. The shell model has always been considered as a fundamental tool for the study of the nuclear structure. The three pillars of the shell model are namely, valence space, effective interaction and shell model code to diaganalize the matrices. Two main problems appear in a shell model description of the nuclear structure. The first one is related to its very foundations, i.e. to the possibility of obtaining a renormalized effective interaction in a given valence space from the bare N-N force. The second problem is technical, with the increases of the size of the valence space or the increases of the number of particles (holes) the dimension of matrices explodes. In the present chapter Nushell code which are used in the calculations are discussed. The Nushell is a shell model code developed by Alex Brown from MSU[2] to tackle dimension up to 105 in the J-T scheme and about 2×106 in the M-scheme. Nushell generates the basis states in m-scheme and then computes the matrix in the j scheme. Therefore, it bypass the complication of the angular momentum algebra in j-j coupled basis and also avoids the huge matrix dimension generated during m-scheme. Nushell consists of seven main programs and some supporting codes. SHELL makes a batch file .*bat that coordinates the program sequence and their inputs. NUBASIS makes a list of all possible M-scheme basis states for a given model space together with a given set of

restrictions. NUPROJ makes linear combinations of the M-scheme basis states that have good J values in p/n formalism or good J and T in isospin formalism. NUMATRIX makes the matrix corresponding to the J (or JT) dimension of the problem. NULANCZOS find the lowest N eigen values for the matrix. MVEC reads the output of Proj and Lanczos to make the eigenvectors in the M-scheme basis. TRAMP calculates overlaps between two wavefunctions. DENS calculates the radial wavefunctions for a given nucleus with oscillator, Woods-Saxon or skyrme Hartree-Fock potentials and reads the .*obd from nushell to calculate B(EL), B(ML) and B(GT) values.

In the **Chapter 3**, different type of interaction are described. The bare nucleon-nucleon interaction is a starting point to derive an effective interaction to be used in nuclear calculations. With the restriction to two-body interactions, the interaction energy in a many particle configuration can be reduced to a weighted sum over TBME only. The value of the matrix elements depends on the residual interaction, the single particle wave functions and on the total spin and isospin of the two particle system. The basic TBME of the residual interaction can be evaluated in three different way.

The most fundamental way to get the two-nucleon interaction to be exploited in the many-body calculations is to derive it from a bare NN potential for free nucleons in a vacuum, by taking into account medium effects, the Pauli principle and truncated model space. This is why such an interaction is called an effective interaction. This approach treats two nucleons in nuclear medium in a way analogous to the scattering of two

nucleons in vacuum . The resulting effective interaction is well-behaved at short distances. At the same time many-body effects are consistently treated when just applying the bare force. To eliminate hard core repulsion the G-matrix has been introduced which is obtained by solving the Bethe-Goldstone equation [3] and NN interaction V is used to calculate the G-matrix [4-6] .

$$G(\omega) = V + V\frac{Q_2 P}{\omega - H_0}G(\omega)$$

Here, ω is the `starting energy' at which G is computed. H_0 is the unperturbed Hamiltonian for the intermediate two-particle state. V is the bare interaction between two nucleons unmodified for the nuclear medium. Q_{2P} is a two-particle projection operator that guarantees that the scattered particle obey the Pauli exclusion principle: the two nucleons can only be scattered to unoccupied states, hence to states that lie above the Fermi energy.

Empirical interactions are extracted from experimental data, in the simplest approach, from the binding energies of CS,$CS \pm 1$ and $CS \pm 2$ nuclei. In the case of a single j shell:

$$\left\langle j^2 J \middle| V \middle| j^2 J \right\rangle = BE\left(CS \pm 2; j^2, I = J\right) - BE\left(CS; g.s.\right) - 2\varepsilon_j$$

Where $\varepsilon_j = BE(CS \pm 1; j^2, I = j) - BE(CS; g.s.)$

Thus the single-particle energies are taken from the spectrum of the nucleus with the some core plus one nucleon and two body matrix elements which are taken as free parameters in a fit for a particular mass region[7]. The energy levels calculated with these parameters are compared to the experimental energy levels and the parameter values are adjusted by means of a least-square fitting procedure.

Departing from the basic properties of the nuclear force, we also use the properties of some of the simple forces such as multiple forces, zero-range or delta-forces and spin exchange component. Such type interaction is Schematic interactions. The earlier interactions are parameterized functions of nucleon coordinates.

Historically, interactions of the Yukawa [8], Gaussian [8], delta [8] and surface delta [9] types, as detailed in various textbooks [10,11,8], have played a significant role in the evolution of shell model calculations. The restrictions and symmetries are imposed on the TBME by a given analytic function and radial dependence introduce deficiencies in the energies (pairing, level density) and electromagnetic transition rates (configuration mixing) calculated in the shell model application. Another type of schematic interaction is widely used in mean field calculations employing the HF method , namely the Skyrme [12,13] and Gogny forces [14]. They have been successfully used to calculate such gross properties as masses, shapes, radii, level densities and single particle energies, but have been scarcely applied to detailed shell model spectroscopy.

In the **Chapter 4**, large scale shell model calculations have been performed for N = 51 isotones nuclide ^{83}Ge, ^{85}Se, ^{87}Kr, ^{89}Sr and ^{91}Zr in valence space $\nu(0g_{7/2}, 1d_{5/2}, 1d_{3/2}, 2s_{1/2}, 0h_{11/2})$ orbitals for neutrons and $\pi(0f_{5/2}, 1p_{3/2}, 1p_{1/2}, 0g_{9/2})$ orbitals for protons with ^{78}Ni core. The effective interaction is based on the renormalization of CD-Bonn nucleon-nucleon potential [15,16] developed by G - matrix theory for nuclei above ^{78}Ni core. Thus simple and pure neutron configurations of $(1d_{5/2})^{1\nu}$ and $(2s_{1/2})^{1\nu}$ above the N=50 shell closure can be assumed to describe the ground state and first excited state of all isotones. Ground state spin $5/2^+$ for all the isotones is associated with the last odd neutron in $d_{5/2}$ state. Similarly $1/2^+$ spin of first excited state can be attributed to the excitation of the last neutron from $1d_{5/2}$ to $2s_{1/2}$ level. The increase in $E(1/2^+)$~$E(5/2^+)$ splitting in going from Z=32 to 40 is direct reflection of the monopole effect wherein the energy of $1/2^+$ state is gradually increasing with the filling of proton orbitals.

The calculated $1/2^+$ levels are consistently lower than the corresponding experimental values. The fitting of higher $3/2^+$,$7/2^+$ and $9/2^+$ states with the corresponding experimental data is not good. Thus, the present interaction in the chosen model space does not give good agreement with the experimental data[17,18]. The reason for this could be manifold. Firstly, all these states have admixtures of coupling of single particle states with core excitation. Secondly, it is well known that the neutron single particle orbital changes with filling of proton number due to the attracting monopole pairing interaction between proton and neutron in spin-orbit partners [19]. So minor adjustment in the monopole part of the

neutron proton interaction and renormalization of the single particle energies of the neutron orbitals can lead to better agreement with the experimental data. Thirdly, recent studies have shown that 3N forces have important effect on the evolution of shell structure in neutron rich nuclei. The three body component of these interactions gives rise to a repulsive contribution to the monopole interaction. These forces when included can give a shift to $1/2^+$ states in the right direction . Lastly, the wave functions of the $7/2^+$ states in ^{85}Se, ^{87}Kr, and ^{91}Zr and $1/2^+$ and $3/2^+$ states of ^{91}Zr have main components in which proton configuration is different than the ground state configuration showing that these states are not pure neutron excitation states.

In the **Chapter 5**, we have performed the shell model calculation using Nushell code for neutron rich even mass Ca isotopes covering N = 22 to N=38. In our calculation ^{40}Ca is chosen as core and valence space comprises of full fp shell $0f_{7/2}$, $1p_{3/2}$, $0f_{5/2}$ and $1p_{1/2}$ for neutrons. Calculations have been carried out with three different interactions, viz. GXFP1A[20], KB3G[21] and FPD6N[22] which are specially developed for fp shell and suitably modified for monopole correction. We have studied the shell structure along the Ca isotopic chain and have observed the subshell closure existence at N=32 with KB3G while GXFP1A and FPD6N interactions predict the subshell closure at N=34. Shell closure at any other neutron number has not been observed. KB3G interaction best suited for lighter pf shell nuclei. FPD6N is based on Kuo-Brown matrix element interaction but the single particle energy are matched with ^{56}Ni.

GXPF1A interaction is modified to reproduce the properties of pf shell nuclei heavier region. From this point of view the results obtained with GXPF1A interaction and to some extent with FPD6N interaction for heavier Ca isotopes should be more reliable. But there is experimental evidence [23,24] for subshell closure at N=32 whereas still now no such evidence has been observed for N=34 subshell closure. Further $B(E2;2^{+}\rightarrow 0^{+})$ transition rate for GXPF1A and FPD6N interactions are much smaller than corresponding experimental values. But shell model calculations suggest that N = 34 may be a magic number in Ca isotopes, depending on the effective interactions used [25]. This is again clearly a region where more experimental data are needed. The availability of experimental data in nuclei with large N/Z ratios may provide a ground to constrain the properties of different components of the interaction, such as the isovector channel of the spin-orbit interaction, which are not well defined but may be responsible for the shell evolution.

In the **Chapter 6**, large scale shell model calculations for even and odd mass N=50 isotones namely ^{80}Zn, ^{82}Ge, ^{84}Se, ^{86}Kr, ^{88}Sr, ^{90}Zr, ^{92}Mo, ^{94}Ru, ^{96}Pd and ^{81}Ga, ^{83}As, ^{85}Br, ^{87}Rb, ^{89}Y, ^{91}Nb, ^{93}Tc, ^{95}Rh have been performed. The calculations have been performed using Nushell code and ^{78}Ni core in the valence space $\pi(0f_{5/2,\ 1}p_{3/2,\ 1}p_{1/2,\ 0}g_{9/2})$ for protons. jj44b Hamiltonian [26] have been used to find the results which has obtained from a fit to experimental data of about 600 binding energies and excitation energies of nuclei with Z=28-30 and N=48-50. The results of our analysis shows that in the chosen configuration space jj44b interaction gives nearly good

agreement with the experimental data[27,28,29] for 0^+ ,2^+ and 4^+ state of even mass N=50 nuclei except some levels of N=50 isotones and all energy levels of ^{92}Mo are reproduced very well. A large separation between 0^+ and 2^+ state in ^{90}Zr is an indication of shell closure at Z=40 which is further supported by corresponding low value of B(E2). For odd mass nuclei results for most of the states are not satisfactory.

The results of our analysis shows that nearly good agreement with experimental levels for both even mass neutron rich nuclei near the drip line and proton rich nuclei near line of stability is obtained indicating suitability of model space and the interaction for these even mass nuclei. However for odd Z, N=50 isotones the poor agreement with experimental results for most of states suggest the need for minor monopole correction in the interaction and more experimental data fitting in this region.

In the **Chapter 7**, importance and future prospects of the presents works have been discussed. Nuclear structure physics and the visible Universe are intimately related since nuclear physics drives many astrophysical processes. These include Big Bang nucleosynthesis and the evolution and final fate of stars. A reliable description of the underlying astrophysical scenarios depends crucially on the knowledge of nuclear properties in the relevant regions of the Segr´e chart involving both nuclei close to stability, in the heavy-ion fusion below the nickel–iron region, which is important for the slow neutron capture (s-process) beyond, as well as exotic nuclei far-off stability in the rapid neutron capture (r-process) on the neutron-rich side and the rapid proton capture (rp-process) close to the proton dripline.

Since the binding energy per nucleon peaks around iron, energy is only released in fusion processes occurring below this point. Since the creation of heavier nuclei by fusion costs energy, nature resorts to the process of neutron capture. Neutrons(due to their lack of charge) are readily absorbed by a nucleus. Thus heavy elements are created by either a *slow* neutron capture process (the so-called *s* process) or by the *rapid*, or *r* process. The *s* process occurs in thermally pulsing stars (called AGB, or asymptotic giant branch stars) and takes hundreds to thousands of years to reach the heaviest elements of lead and bismuth. The *r* process is thought to occur in supernova explosions because the conditions of high temperature, high neutron flux and ejected matter are present. These stellar conditions make the successive neutron captures very fast, involving very neutron-rich species which then beta-decay to heavier elements, especially at the so-called waiting points that correspond to more stable nuclides with closed neutron shells (magic numbers).

N = 51 nuclide are particularly important to understand astrophysical processes since neutron rich nuclei between N = 50 and N = 82 shells cover waiting point in r-processes. Properties of low lying states in these nuclei near closed shell are useful for the description of nuclear structure, quenching of shell gaps and a more uniform spacing of single-particle energy levels [30-32] and influence how heavier nuclei are produced in astrophysical rapid neutron capture (r−) process [33,34]. The astrophysical importance of ^{78}Ni is related to the understanding of the nuclear mechanism of the rapid capture of neutrons by seed nuclei through the r-

process. The path of this reaction network is expected in neutron-rich nuclei for which there is little experimental data, and the precise trajectory is dictated by the details of the shell structure far from stability. Synthesis of heavier elements proceeds by r-process from the seed nucleus Fe following the path among neutron rich nuclei and closing at ^{78}Ni. Since nuclear structure of mostly r process nuclei is not known, the study of these neutron rich nuclei near the ^{78}Ni region will throw light on r-process in nucleosynthesis.

Today research on nuclear physics focuses on exploring nucleonic matter under extreme conditions such as those that can be created in modern accelerator laboratories. The opportunities offered by beams of exotic nuclei for research in the areas of nuclear structure physics and nuclear astrophysics are exciting and world-wide activity in the construction of different types of radioactive beam facilities bears witness to the strong scientific interest in the physics that can be probed with such beams.

Nuclei far from stability allow us to amplify and isolate particular aspects of the nuclear interaction and dynamics. Future work will involve, for example, mapping the neutron drip line further up, investigating neutron halo systems, learning about the astrophysical rp- and r-process paths, exploring the evolution of shell structure and neutron skins, creating further super heavy nuclei, studying super-allowed beta-decay in very light proton rich nuclei, developing a deeper understanding of proton-neutron pairing and studying the exotic phenomenon of proton radioactivity.

The actual mechanism which causes the changes in nuclear structure as neutron/proton number increases in a nuclear system is still an open

question. The present work can be extended to the study of following aspects:

(i) the role of 3N forces in interaction in explaining the structure of N= 50 and 51 isotones and Ca isotopes.

(ii) minor adjustment in the monopole part of the neutron proton interaction and renormalization of the single particle energies of the neutron orbitals to find better agreement with the experimental data for N=50 and 51 isotones.

(iii) study of N = 50 and 51 isotones with ^{100}Sn and ^{132}Sn core as particle-hole pair .

(iv) experimentally unknown Ca isotopes give a base to the future experiment.

(v) shell closure at N=34 is still a question, needs a experimental verification.

(vi) some predicted levels which are experimentally not known, have motivation for the further experiment.

References:

[1] K. Brueckner, Phys. Rev. 97 (1955), 1353.

[2] Nushell@MSU, B. A. Brown and W. D. M. Rae (unpublished).

[3] H. Bethe et al., Proc. Roy. Soc. (London) A 238 (1957), 551

[4] T.T.S. Kuo, G.E. Brown, Nucl. Phys. A **114**, 241 (1968)

[5] T.T.S. Kuo, E. Osnes, Springer Lecture Notes of Physics **364**, 1 (190)

[6] M. Hjorth-Jensen et al., Phys. Rep. **261**, 125 (1995)

[7] P. Brussaard, Shell-Model Applications in Nuclear Spectroscopy, North- Holland, Amsterdam, 1977

[8] K. Heyde, The Nuclear Shell Model, Springer, Berlin, 1994

[9] S. Arvieu, S.A. Moszkowski, Phys. Rev. **145**, 830 (1966)

[10] A. de Shalit, I. Talmi, Nuclear Shell Theory, Academic Press, New York, 1963

[11] P.J. Brussaard, P.W.M. Glaudemans, Shell model applications in nuclear spectroscopy, North-Holland, Amsterdam, 1977

[12] T.R.H. Skyrme, Nucl. Phys. **9**, 615 and 635 (1959)

[13] D. Vautherin and D.M. Brink, Phys. Rev. C **5**, 626 (1972)

[14] D. Gogny, Nucl. Phys. A **237**, 399 (1975)

[15]R. Machleidt, Adv. Nucl. Phys. 19, 189 (1989).

[16] R. Machleidt, K. Holinde, and Ch. Elster, Phys. Rep. **149**, 1(1987).

[17]J.S. Thomas *et al.*, Eur. Phys. J. A **25**, s01, 371 (2005).

[18] O. Perru *et al.*, Eur. Phys. J. A **28**, 307 (2006).

[19] P. Federman and S. Pittel Phys. Lett. B **69**, 385 (1977).

[20] Honma M, Otsuka T, Brown B A and Mizusaki T

Eur. Phys. J. A 25, s01 (2005) 499

[21]A. Poves et. al. Nucl. Phys. A 694 (2001) 157-198.

[22] Richter et al., Nucl. Phys. A523, 325 (1991)

[23] A. Huck et. al., Phys. Rev. C 31 (1985) 2226

[24] M. Honma et. al., Phys. Rev. C 65 (2002) 061301.

[25] J.D. Holt, T. Otsuka, A. Schwenk, and T. Suzuki, J. Phys. G 39, 085111 (2012)..

[26] Lisetskiy and Brown (unpublished)

[27]D. Verney *et. al*. **Phys. Rev. C 76**, 054312(2007)

[28] M. Gorska *et al*. **Phys. Rev. Lett. 79**, No. 13(1997)

[29] ***www.nndc.bnl.gov***

[30] D. Verney *et al.*, Phys. Rev. C **76**, 054312 (2007).

[31] M. Lebois *et al.*, Phys. Rev. C **80**, 044308 (2009).

[32] K. Sieja and F. Nowacki, Phys. Rev. C **81**, 061303(R) (2010).

[33] J.A. Cizewski *et al.*, Nucl. Instum. Methods Phys. Res., Sect. B **241**, 200 (2005).

[34] J.S. Thomas *et al.*, Phys. Rev. C **71**, 021302 (2005).

(i) the role of 3N forces in interaction in explaining the structure of N= 50 and 51 isotones and Ca isotopes

(ii) the role of minor adjustment in the monopole part of the neutron proton interaction and renormalization of the single particle energies of the neutron orbitals to find better agreement with the experimental data for N=50 and 51 isotones

(iii) study of N = 50 and 51 isotones with ^{100}Sn and ^{132}Sn core as particle-hole pair

(iv) experimentally unknown Ca isotopes give a base to the future experiment

(v) shell closure at N=34 is still a question, needs a experimental verification

(vi) some predicted levels which are experimentally not known, have motivation for the further experiment.

References:

[1] D. Verney *et al.*, Phys. Rev. C **76**, 054312 (2007).

[2] M. Lebois *et al.*, Phys. Rev. C **80**, 044308 (2009).

[3] K. Sieja and F. Nowacki, Phys. Rev. C **81**, 061303(R) (2010).

[4] J.A. Cizewski *et al.*, Nucl. Instum. Methods Phys. Res., Sect. B **241**, 200 (2005).

[5] J.S. Thomas *et al.*, Phys. Rev. C **71**, 021302 (2005).